**In Vitro and In Vivo Studies on Antibodies -
N-terminally Truncated Abeta in the 5XFAD Mouse Model**

Dissertation
for the award of the degree
"Doctor rerum naturalium"
of the Georg-August-Universität Göttingen

within the doctoral program *Molecular Physiology of the Brain*

of the Georg-August University School of Science (GAUSS)

submitted by
Bernhard Clemens Richard

from *Münster (Westfalen), Germany*
Göttingen, 2015

Thesis Committee

Prof. Dr. Thomas A. Bayer
Department of Molecular Psychiatry, University Medical Center Göttingen

Prof. Dr. Tiago F. Outeiro
Department of Neurodegeneration and Restaurative Research, University Medical Center Göttingen

Prof. Dr. Holger Reichardt
Department of Cellular and Molecular Immunology, University Medical Center Göttingen

Members of the Examination Board

Referee: Prof. Dr. Thomas A. Bayer
Division of Molecular Psychiatry, University Medical Center Göttingen

2nd Referee: Prof. Dr. Tiago F. Outeiro
Department of Neurodegeneration and Restaurative Research, University Medical Center Göttingen

Further members of the Examination Board

Prof. Dr. Holger Reichardt
Department of Cellular and Molecular Immunology, University Medical Center Göttingen

Prof. Dr. Hubertus Jarry
Department of Endocrinology, University Medical Center Göttingen

Prof. Dr. Thomas Dresbach
Department of Anatomy and Embryology, University Medical Center Göttingen

Prof. Dr. Ralf Heinrich
Department of Cellular Neurobiology, Schwann-Schleiden Research Centre, Göttingen

Date of oral examination: May 7th, 2015

AFFIDAVIT

I hereby declare that my doctoral thesis entitled "In Vitro and In Vivo Studies on Antibodies - N-terminally Truncated Abeta in the 5XFAD Mouse Model" has been written independently with no other sources and aids than quoted.

Bernhard Clemens Richard
Göttingen, March 2015

Vägen, du skall följa den.
Kalken, du skall tömma den.
Svaret, du skall lära det.

inspirerad av
Dag Hammarskjöld
(1905 — 1961)

Publications related to this thesis:

Original Articles:

B. C. Richard, A. Kurdakova, S. Baches, T. A. Bayer, S. Weggen, and O. Wirths. Gene Dosage Dependent Aggravation of the Neurological Phenotype in the 5XFAD Mouse Model of Alzheimer's Disease. *J. Alzheimers Dis.*, 45(4):1223–1236, Jan 2015

E. A. Guzman, Y. Bouter, **B. C. Richard**, L. Lannfelt, M. Ingelsson, A. Paetau, A. Verkkoniemi-Ahola, O. Wirths, and T. A. Bayer. Abundance of Abeta5-X like immunoreactivity in transgenic 5XFAD, APP/PS1KI and 3xTG mice, sporadic and familial Alzheimer's disease. *Mol Neurodegener*, 9:13, 2014

G. Antonios, N. Saiepour, Y. Bouter, **B. C. Richard**, A. Paetau, A. Verkkoniemi-Ahola, L. Lannfelt, M. Ingelsson, G. G. Kovacs, T. Pillot, O. Wirths, and T. A. Bayer. N-truncated Abeta starting with position four: early intraneuronal accumulation and rescue of toxicity using NT4X-167, a novel monoclonal antibody. *Acta Neuropathol Commun*, 1(1):56, 2013   *Equal contribution of **BCR**, GA, NS and YB*

Abstracts:

B. C. Richard, S. Baches, S. Weggen, and T. A. Bayer. The impact of passive immunization against n-terminally truncated abeta species: A comparative study in the 5xfad alzheimers model. *Poster Presentation, The Alzheimers Association International Conference, Copenhagen*, 2014

Publications not included in the Thesis:

Original Articles:

S. Musunuri, K. Kultima, **B. C. Richard**, M. Ingelsson, L. Lannfelt, J. Bergquist, and G. Shevchenko. Micellar extraction possesses a new advantage for the analysis of Alzheimer's disease brain proteome. *Anal Bioanal Chem*, 407(4):1041–1057, Feb 2015

CONTENTS

ABSTRACT

ABSTRACT

Commonly used transgenic mouse models mimic Alzheimer´s disease (AD) to some extent but do as well display differences compared to the human AD phenotype. Growing evidence indicates that N-terminally truncated Aβ isoforms, which are underrepresented in common murine models, represent a key player in AD. These peptides are abundant in AD brains and have increasingly gained attention during the past years. It has been suggested that the equilibrium of aggregation is shifted towards the more toxic low-molecular weight oligomeric assemblies due to N-terminal truncation of Aβ, thereby triggering neurodegenerative processes. In this study, characterization of a recently developed monoclonal antibody, NT4X-167, revealed its engagement with N-terminally truncated $A\beta_{pE3-X}$ and $A\beta_{4-X}$. We also showed the propensity of $A\beta_{4-X}$ to adopt a distinct oligomeric conformation. Analysis of a newly created homozygous 5XFAD mouse strain with NT4X-167 revealed early intracellular accumulation of $A\beta_{4-X}$ in this model, preceding other N-truncated isoforms, $A\beta_{pE3-X}$ and $A\beta_{5-X}$. Investigation of homozygous 5XFAD mice revealed a gene-dose dependence of the neuropathological and behavioral phenotype. Homozygous 5XFAD might especially facilitate the analysis of intracellular Aβ, truncated isoforms in particular. Considering the consensus that Aβ is a key player on one hand, and the failure of recent anti-Aβ immunotherapeutic trials in AD on the other hand, there is an urgent need to find new therapeutic targets and strategies. In the course of this, it has been proposed that targeting N-truncated Aβ might offer therapeutic advantage. In order to explore the therapeutic potential of passive anti-N-truncated Aβ immunization, a comparative study with three monoclonal antibodies (NT4X-167, 9D5, 1-57) in 5XFAD was conducted in this study. As NT4X-167 showed a significant effect, it can be concluded that this antibody might offer therapeutic advantage over antibodies specific for $A\beta_{pE3-X}$.

Part I

INTRODUCTION

INTRODUCTION

1.1 ALZHEIMER'S DISEASE

Auguste Deter, whose case was reported by Alois Alzheimer in the year 1906 at the 37th meeting of the Society of Southwest German Psychiatrists (Tübingen, Germany) was the first patient described with a characteristic combination of symptoms. She displayed character and mood changes as well as progressive memory and language deficits and loss of orientation. After her death, A. Alzheimer found the brain to be atrophic, with intracellularly accumulated neurofibrils and extracellular miliary bodies (plaques) (Alzheimer, 1907). After A. Alzheimer, the disease he had described was named Alzheimer´s Disease later on.

1.2 CLINICAL ASPECTS OF ALZHEIMER'S DISEASE

1.2.1 *Epidemiology*

The World Health Organization estimates the number of people that suffered from dementia in the year 2010 to be 36 million people. This number is believed to increase to 66 million by the year 2030 and 115 million by 2050. The global cost of dementia in 2010 is estimated to $ 604 billion. This amounts to 1 % of the global gross domestic product, a number underlining the impact demential diseases have on society and economy. AD is the most common form of dementia, accounting for 60 - 70 % of these numbers

(World Health Organzation, 2012). According to the German Alzheimer´s Association (Deutsche Alzheimer Gesellschaft), in 2014 1.4 million people were suffering from AD in Germany.

1.2.2   Risk Factors for Alzheimer´s Disease

Two forms of AD are described: An inherited (familial) form which accounts for approximately 1 % of the disease cases (Zetterberg and Mattsson, 2014), and a majority of sporadic cases. The major risk factor to develop AD is age (Blennow et al., 2006). One out of eight people older than 65 years and 45 % of the people older than 85 suffer from AD, but despite this high prevalence of the disease in the elderly it is not part of the normal aging process. Besides aging, epidemiological studies have suggested a variety of risk factors for sporadic AD. Carrying at least one copy of the ApoE4 allel increases the risk of developing AD (Corder et al., 1993). Other risk factors include vascular diseases such as atherosclerosis, hypercholesterolemia, coronary heart disease and heart failure (Kivipelto et al., 2001, 2005; Qiu et al., 2006), obesity, smoking, type II diabetes (Kivipelto et al., 2005; Leibson et al., 1997; Prince et al., 1994). In addition, head injury and traumatic brain injuries could be risk factors for AD (McCullagh et al., 2001; Plassman et al., 2000; Sivanandam and Thakur, 2012). On the other hand, there are studies connecting a healthy, cognitively and physically active lifestyle as well as certain dietary habits with a reduced risk of AD (Fratiglioni et al., 2004; Gu et al., 2010; Hall et al., 2009).

1.2.3   Progression of the Disease

The progression of AD is slow and results in progressive cognitive decline with memory deficits, often in combination with personality or mood changes (Alzheimer´s Association 2012). According to Holtzman et al. (2011), the average development from mild/ moderate AD to a severe clinical phenotype occurs within 7-10 years.
In 2011, the Alzheimer´s Association together with the National Institute of Aging

(NIH) proposed new guidelines for the classification of AD. A division into three stages was suggested: Preclinical AD, mild cognitive impairment due to AD and dementia due to AD (Albert et al., 2011; Jack et al., 2011; McKhann et al., 2011; Sperling et al., 2011). In preclinical AD, no symptoms are observed, whereas patients with mild cognitive impairment display a beginning cognitive decline. The conversion of these patients into the dementia phenotype occurs with a rate of 10-15 % per year. This conversion defines the mild cognitive impairment as an early stage of AD for this patients (Petersen, 2004; Visser et al., 2005). AD leads to severe cognitive decline, motor impairment and loss of visio-spatial abilities. This accumulation and progressive severity of symptoms is ultimately fatal and leads to death subsequently (Holtzman et al., 2011; Wada et al., 2001).

1.3 PATHOLOGICAL HALLMARKS OF ALZHEIMER'S DISEASE

1.3.1 *Amyloid Plaques*

One of the major pathological hallmarks of AD is the formation of extracellular deposits (plaques) composed of the Amyloid-beta peptide (Aβ) that is derived from cleavage of Amyloid-Precursor-Protein (APP) (Holtzman et al., 2011; Serrano-Pozo et al., 2011). The particular isoforms are termed in regard to the amino acid sequence: $Aβ_{X1-X2}$, Amyloid-beta peptide ranging from N-terminal amino acid $X1$ to C-teminal amino acid $X2$. Two distinguishable types of plaques are found in human AD brain: Diffuse plaques and neuritic plaques. Of these types only neuritic plaques are strongly stained by Thioflavin S or Congo Red, dyes that interact with β-sheeted protein assemblies, indicating a fibrillar and more dense structure (Serrano-Pozo et al., 2011). The amyloid deposition typically starts in the neocortex and affects hippocamus and amygdala later. In the end stage of AD, neuritic plaques are additionally found in subcortical structures such as the brain stem (Arnold et al., 1991; Serrano-Pozo et al., 2011; Thal et al., 2002). In the vicinity of neuritic plaques, a range of pathological alterations is observed, such as neuron and synapse loss, astro- and microgliosis and neuritic dystrophies (Holtzman et al., 2011; Lenders et al., 1989; Masliah et al., 1990; Pike et al., 1995a; Selkoe,

2011; Urbanc et al., 2002). The observation that plaques, mainly of the diffuse subtype and with almost no detectable neuritic dystrophy, are also present in healthy older individuals led to the hypothesis that an increase of the plaque load is associated with preclinical AD (Dickson et al., 1992; Knopman et al., 2003; Vlassenko et al., 2011). However, although plaques are a diagnostic hallmark of AD, the absolute plaque burden correlates with cognitive decline and disease stage poorly (Arriagada et al., 1992; Giannakopoulos et al., 2003; Villemagne et al., 2011). In addition, roughly 80 % of the AD patients show the symptom of amyloid deposition in blood vessels, called Cerebral Amyloid Angiopathy (CAA).

1.3.2 *Neurofibrillary Tangles*

Already the initial report of A. Alzheimer (Alzheimer, 1907) mentioned the second neuropathological hallmark of AD, intracellular Neuro-fibrillary Tangles (NFT) consisting of hyper-phosphorylated Tau protein organized in paired helical filaments (Grundke-Iqbal et al., 1986; Kidd, 1963; Lee et al., 1991). Tau is a protein ubiquitously expressed in all nucleated cells and highly abundant in neurons. In its physiological function, Tau is involved in the organization of microtubules (Drechsel et al., 1992; Gustke et al., 1994; Weingarten et al., 1975; Witman et al., 1976). Its hyper-phosphorylation results in reduced tubulin binding and a higher propensity to form paired helical filaments (Alonso et al., 1996; Holtzman et al., 2011). It has been reported that the NFT formation in AD brain is a better correlate for the clinical phenotype than plaque formation (Holtzman et al., 2011). For diagnosis and staging of AD, Tau is crucial (Arnold et al., 1991; Braak and Braak, 1991), but Tau aggregation and NFT formation appear later than amyloid deposition in the development of AD (Galimberti and Scarpini, 2012).

1.3.3 *Inflammation*

Another pathological feature of AD are inflammatory reactions in the brain. In the vicinity of neuritic plaques, activated microglia and astrocytes are found, which suggests

that Aβ acts as a trigger for inflammation (Itagaki et al., 1989; Krause and Muller, 2010; Pike et al., 1995a). In response to activation, microglia and astrocytes release proinflammatory signal molecules, complement factors, chemokines and cytokines (Rubio-Perez and Morillas-Ruiz, 2012; Tuppo and Arias, 2005). Several studies suggest that glial cells surrounding neuritic plaques engulf and process Aβ (Koenigsknecht-Talboo et al., 2008; Meyer-Luehmann et al., 2008). It was in consequence proposed that activated glial cells contribute to Aβ clearance and that this might be beneficial for treatment of AD (Bard et al., 2000; DeMattos et al., 2012). For instance, DeMattos et al. (2012) have reported that treatment with antibodies exhibiting maximal phagocytosis effector function is most efficient in removing deposited Aβ from murine brain. However, it has been questioned if microglia are capable of efficient Aβ degradation (Majumdar et al., 2007; Paresce et al., 1997). It is unclear whether inflammatory responses are generally detrimental in AD or if some aspects of inflammation might be beneficial (Weninger and Yankner, 2001).

1.3.4 *Brain Atrophy and Neuron Loss*

Brain atrophy is a prominent feature of an AD brain, but also of other demential diseases such as frontotemporal dementia or vascular dementia (Blennow et al., 2006). The regions in which atrophy is observed in AD include the medial temporal lobe, hippocampus and amygdala, the inferior temporal as well as the superior and middle frontal gyri, but not the inferior frontal and orbifrontal gyri (Blennow et al., 2006; Duyckaerts et al., 2009; Halliday et al., 2003). Along with others, Kril et al. (2004) have found a strong correlation of neuron number and hippocampal/brain volume, indicating that these are somehow connected. It has further been reported that MRI brain imaging in order to assess hippocampal atrophy can give good indication of the progression from mild cognitive impairment to AD (Jack et al., 2005; Jagust, 2006). What causes the atrophy/neuron loss observed in AD is subject to an ongoing discussion. Some research groups reported a correlation of brain atrophy with NFTs, whereas others suggested that intracellular accumulation of aggregated Aβ plays an important role (Bayer and Wirths, 2010; Gomez-Isla et al., 1997; Haass and Selkoe, 2007).

As it is challenging to confirm neuron loss, it is unclear whether it is essential in AD (Duyckaerts et al., 2008). However, brain neuronal loss is observed in some transgenic murine models of AD (Bouter et al., 2014; Casas et al., 2004; Christensen et al., 2008, 2010a; Jawhar et al., 2012; Meissner et al., 2014; Oakley et al., 2006; Saul et al., 2013; Schmitz et al., 2004; Wirths and Bayer, 2010).

1.4 DIAGNOSIS OF ALZHEIMER'S DISEASE

Currently, an exact diagnosis of AD ist only possible *post mortem*. This diagnosis is essentially based on the analysis of the neuropathological hallmarks mentioned above, i.e. amyloid plaques and NFTs in the brain (Braak and Braak, 1991; McKhann et al., 1984).

Therefore, cognitive impairment and behavioral alterations are assessed to make an assumption whether a person will eventually be diagnosed with AD. To this end, patients presenting with mild cognitive impairment undergo physical and cognitive assessement by various testing procedures such as the Mini-Mental Stage Examination (Folstein et al., 1975), the Clock-Drawing Test (Aprahamian et al., 2010; Sunderland et al., 1989) or the Cambridge Cognitive Examination (Martinelli et al., 2014; Schmand et al., 2000). For a probable diagnosis of AD, deficits that affect the patient in daily activities are crucial (American Psychiatric Association, 1995). Besides memory impairment symptoms such as agnosia, aphasia, apraxia or deficits in executive functions are required (Waldemar et al., 2007). This diagnosis can be supported by neuroimaging employing Magnetic Resonance Tomography, Computer Tomography, or Positron-Emission Tomography (Ballard et al., 2011; Blennow et al., 2006; Perrin et al., 2009; Schroeter et al., 2009). Furthermore, analysis of biomarkers in the cerebrospinal fluid has been established for diagnosis of mild cognitive impairment and AD. Reduced levels of $A\beta_{X-42}$ and increased levels of Tau and phospho-Tau support a diagnosis of AD (Fiandaca et al., 2014; Mattsson et al., 2009; Perrin et al., 2009).

Aβ is derived from sequential cleavage of APP (Korenberg et al., 1989), a type-1 trans-membrane glycoprotein (Puzzo et al., 2014) belonging to the amyloid-precursor-like protein family. Although in general the members of this family are structurally highly conserved, they exhibit large hetrogeneity in the Aβ region (Selkoe, 2001). At least four different mRNAs encoding APP that result from alternative splicing are known. Together with different post-translational modifications, these result in a variety of isoforms expressed in different types of tissues. These isoforms are named by the number of amino acids: The three major forms APP770, -751, and -695 are expressed in neuronal cells, with the latter being most frequently expressed (Selkoe, 2001).

1.5.1   *Processing*

APP is physiologically processed by proteases, resulting in a variety of released peptides. Two alternative pathways of this processing have been described (De-Paula et al., 2012). In the non-amyloidogenic pathway, APP is cleaved within the Aβ region by several α-secretases relasing the so-called sAPPα fragment which has been suggested to have neuroprotective activity to the extracellular space (Chow et al., 2010; Esch et al., 1990; Furukawa et al., 1996; Mattson, 1997; Sisodia et al., 1990). Various enzymes have been proposed to function as α-secretase, including ADAM9, ADAM10, ADAM17, ADAM19 or TACE (Haass, 2004; Haass et al., 2012). Within the cell membrane, a C-terminal fragment, C83, remains and is further cleaved by γ-secretase, releasing the so-called p3 peptide and the APP intracellular domain (AICD) (Carrillo-Mora et al., 2014; Querfurth and LaFerla, 2010).

Amyloidogenic Pathway

The mechanism resulting in release of Aβ is the so-called amyloidogenic pathway (De-Paula et al., 2012). Here, APP is first cleaved at the N-terminus of the Aβ sequence by the aspartyl protease site APP cleaving enzyme 1 which liberates the N-terminal
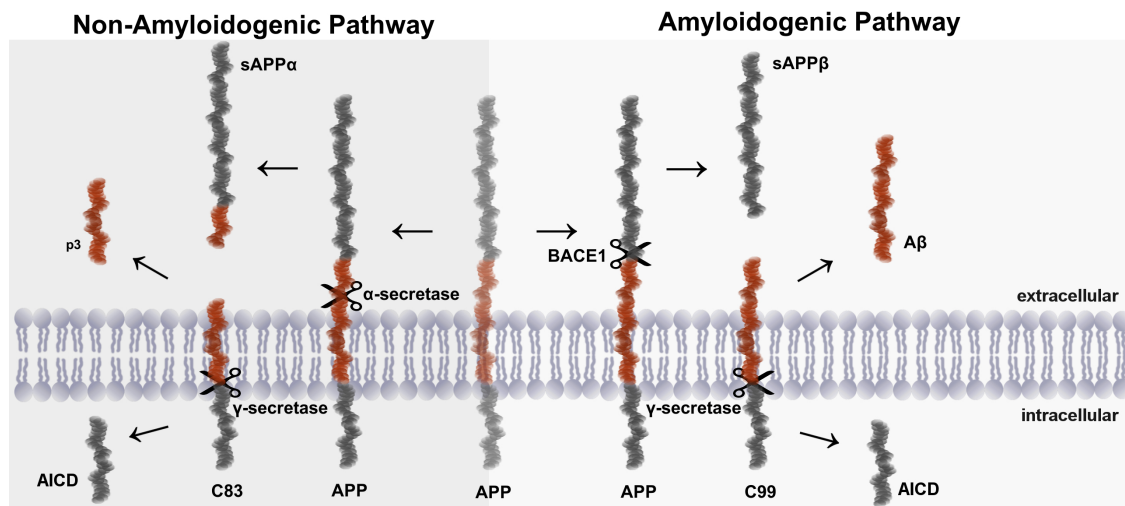
Figure 1.1
APP Processing. In the non-amyloidogenic pathway, APP is first cleaved by α-secretase within the Aβ domain and then further by γ-secretase. Peptides released are sAPPα, the APP intracellular domain (AICD) and the p3 fragment. No Aβ is produced. In the amyloidogenic pathway, APP is processed by aspartyl protease site APP cleaving enzyme 1 (BACE1) in the first step and then by γ-secretase in the second step. The amyloidogenic cleavage of APP results in the release of Aβ, sAPPβ and AICD.

domain sAPPβ (Vassar et al., 1999). The membrane-bound fragment remaining (C99) is further processed by γ-secretase. In consequence, Aβ and the intracellular domain of APP are released (Annaert and De Strooper, 2002).

The γ-secretase, essentially involved in the amyloidogenic pathway, is a complex protease composed of several membrane-bound proteins, presenilin-1 or presenilin-2, nicastrin, anterior pharynx defective-1, presenilin enhancer protein-2 and cluster of differentiation 147 (Kaether et al., 2006; Zhou et al., 2006). The non-amyloidogenic pathway is located to the cell surface, whereas the amyloidogenic cleavage mainly takes place in endocytic organelles (Thinakaran and Koo, 2008). It has further been shown that up-regulation of α-secretase activity results in lower production of Aβ in subcellular compartments (Nitsch et al., 1992; Postina et al., 2004). This indicates that the regulation of APP processing is of importance for the development and progression of AD.

Several hypotheses have been proposed to explain AD. A main step of AD research was the identification of APP, made possible by investigation of Aβ-containing blood vessels in CAA and amyloid plaques (Glenner and Wong, 1984; Kang et al., 1987; Masters et al., 1985). The dominant view since 1991 has been that Aβ deposition in plaques is the main event in AD, triggering the neurodegenerative processes (Duyckaerts et al., 2009; Hardy and Allsop, 1991; Selkoe, 1991) (Figure 1.2, page 16). However, since amyloid plaque burden and cognitive deficits correlate poorly in humans (Price and Morris, 1999) and even animal models (Moechars et al., 1999; Schmitz et al., 2004), this *Amyloid Hypothesis* was controversely discussed.

Genetic studies on familial AD lead to the identification of numerous mutations in the APP, presenilin-1 and presenilin-2 genes as underlying cause of the inherited form of AD. All of these mutations cause an early-onset AD with 100 % prevalence and share the common effects of altering Aβ levels and increasing plaque deposition (Bertram et al., 2010; Pimplikar, 2009). Down syndrome patients, who carry an additional chromosome 21 where the APP gene is located, exhibit abundant plaque and intracellular NFT pathology (Rumble et al., 1989; Schupf and Sergievsky, 2002). Recently, a rare genetic variant of the APP gene that leads to reduced Aβ levels and risk of AD was discovered (Jonsson et al., 2012). The most important genetic risk factor for sporadic AD, apolipoprotein E ε4, is furthermore connected with increased Aβ deposition and reduced clearance from the brain (Bickeboller et al., 1997; Castellano et al., 2011). All these observations support the amyloid cascade hypothesis.

Unlike mutations in the APP and Presenilin (PS) genes, mutations in the Tau gene lead to other neurodegenerative diseases like frontotemporal dementia whose clinical phenotypes are different from these of AD. It has therefore been suggested that the formation of NFTs is not the initial event in AD but likely occurs in response to Aβ aggregation (Goedert and Jakes, 2005; Hutton et al., 1998; Iqbal et al., 2005).

Classic Amyloid Cascade Hypothesis

Modified Amyloid Cascade Hypothesis

Extracellular Aβ

Aβ Re-Uptake

Intraneuronal Aβ

Amyloid Plaque Formation

Amyloid Plaque Formation

Extracellular Soluble Aβ

Neuronal Dysfunction
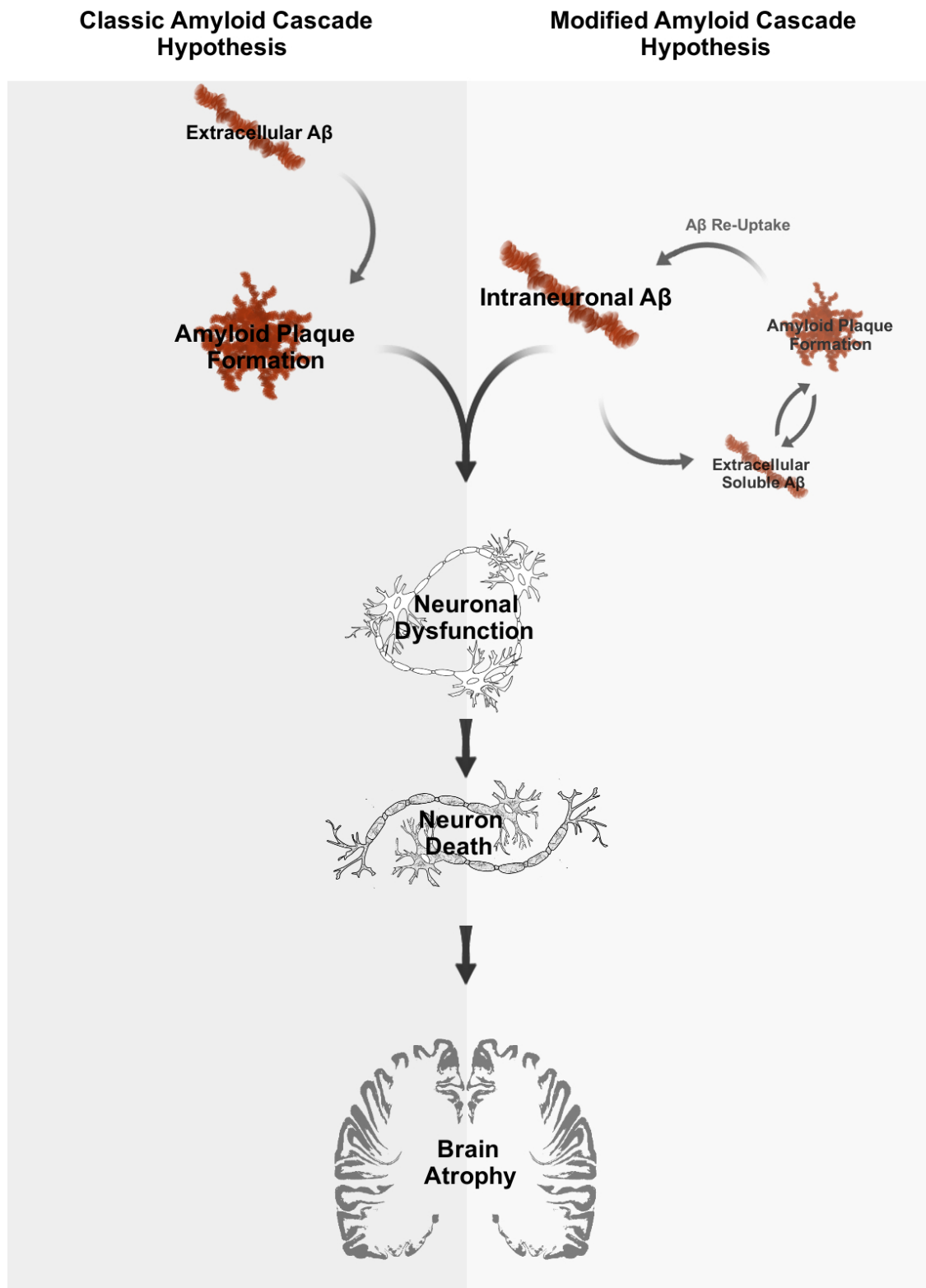
Neuron Death

Brain Atrophy

Figure 1.2

Classic and modified amyloid cascade hypothesis. The classic amyloid cascade hypothesis regards the extracellular formation of amyloid plaques as the main event in AD. In contrast, according to the modified amyloid cascade hypothesis the intracellular accumulation of Aβ is considered the key event triggering the pathologic cascade in AD.

As early as in Masters et al. (1985), the first report on intracellular Aβ was published, and it has been shown later that, prior to formation of plaques and NFTs, Aβ is found intracellularly in brain regions that degenerate in AD (Fernandez-Vizarra et al., 2004; Gouras et al., 2010). Along these lines, it has been found that Down syndrome patients lacking amyloid plaques show intracellular Aβ in the brain (Gyure et al., 2001; Mori et al., 2002). Haass and Selkoe (2007) suggested intracellular Aβ accumulation as the triggering event of neurodenerative alterations in the brain.

The authors proposed that amyloid plaques might serve as a source or reservoir for neurotoxic Aβ-oligomers, which might affect synaptic structure and plasticity. Besides intracellular cleavage of APP, another possible source of intracellular Aβ is re-uptake from the extracellular space (Wirths et al., 2004). The fact that plaques possibly represent a major source of toxic Aβ oligomers has later been plausibly demonstrated by Martins et al. (2008). Within this *modified* or *intracellular amyloid hypothesis* (Figure 1.2, page 16), it has been furthermore suggested that intracellular Aβ aggregation precedes the formation of plaques and other pathologic symptoms of AD (Wirths et al., 2004). The pathologic relevance of intracellular Aβ has been demonstrated in mouse models that show little or no extracellular amyloid deposition but behavioral deficits (Bouter et al., 2013; Wittnam et al., 2012) and models with plaques that develop a substantial neuron loss in regions where Aβ accumulates intracellularly (Christensen et al., 2010a; Jawhar et al., 2012; Oakley et al., 2006). It has been shown that plaques are present some ten years before the first memory complaints in patients and that plaque deposition is virtually at maximal levels by the time of diagnosis (Jack et al., 2010; Morris and Price, 2001; Price et al., 2009). This finding indicates that further plaque deposition is not connected to the progression of the disease. In summary, all mentioned studies suggest a key role of intracellular Aβ rather than extracellular plaques in the etiology of AD.

The Aβ peptides observed in human brain are a heterogenous mixture of various isoforms. The major forms found are $Aβ_{1-42}$ and $Aβ_{1-40}$, the previous representing the major constituent of amyloid plaques, the latter is most abundant in amyloid deposits in blood vessels CAA (Iwatsubo et al., 1994; Suzuki et al., 1994). Besides these major species, commonly termed full-length Aβ, numerous C- and N-terminally divergent variants have been described. These include $Aβ_{1-37/38/39}$ (Portelius et al., 2012; Reinert et al., 2014; Wiltfang et al., 2002) as well as Aβ C-terminally exceeding amino acid 42 (Esh et al., 2005; Van Vickle et al., 2008; Welander et al., 2009). Of these, $Aβ_{X-43}$ was detected in plaques of both mouse models and human AD, for the latter in considerable amount (Welander et al., 2009). Recently, Kaneko et al. (2014) reported eight novel Aβ-like peptides that start and end before the β- and γ-secretase cleavage site, the longest of which consisting of amino acids 663-711 of the APP sequence. Aβ variants with varying terminal end lengths have been described with different aggregation propensity, oligomer stability and structure, resistance to proteolytic degradation and neurotoxic activity (e.g. in Bouter et al. (2013); Jan et al. (2008); Jarrett et al. (1993); Pike et al. (1995b); Russo et al. (2002); Wirths et al. (2010c)).

1.7.1 *N-terminally Truncated Amyloid-beta*

In addition to C-terminally truncated Aβ, a variety of N-terminally deviant isoforms has been described (Bayer and Wirths, 2014; Masters et al., 1985; Mori et al., 1992; Selkoe et al., 1986; Sergeant et al., 2003). These ragged N-termini are believed to result from differential cleavage and/or proteolytic activity after secretion. Besides aspartyl protease site APP cleaving enzyme 1 which has been shown to cleave between Tyr-10/Glu-11 in addition to cleavage before Asp-1 (Vassar et al., 1999), several other peptidases have been proposed to be involved in the generation of N-truncated Aβ. This includes the enzymes meprin-β, producing Aβ starting at residue 2 (Bien et al., 2012), and neprilysin

(neutral endopeptidase, a zinc-metalloprotease) that cleaves between Arg-2/Glu-3, Glu-3/Phe-4, Arg-5/His-6 of the Aβ sequence and myelin basic protein cleaving between Phe-4/Arg-5 (Howell et al., 1995; Iwata et al., 2001; Liao et al., 2009) as well as plasmin which is involved in formation of Aβ starting at His-6 (Tucker et al., 2000; Van Nostrand and Porter, 1999). N-terminal truncation makes the resulting Aβ peptides more prone to aggregate (Pike et al., 1995b), which probably promotes plaque formation *in vivo* (Soto et al., 1995). Aβ with ragged N-termini is highly abundant in human AD brain (Kawarabayashi et al., 2001; Portelius et al., 2010; Saido et al., 1995).

Amyloid-beta Starting with a Pyroglutamate-Modified Residue three (Glu-3)

During the past years, it was in particular Aβ starting with a pyroglutamate-modified residue 3 ($A\beta_{pE3-x}$) that has gained considerable attention. Mori et al. (1992) reported that roughly 15-20 % of Aβ peptides are N-terminally pyroglutamate-modified. This isoform combines characteristic properties deviant from N-terminally intact Aβ: It readily aggregates to oligomeric assemblies, exerts higher neurotoxicity than $A\beta_{1-40/42}$ and is highly resistant to degradation (Kuo et al., 1997; Russo et al., 2002; Wirths et al., 2010c). Its high abundance in AD and Down syndrome patients suggests that it may play an important role in the disease, and it has been found to be a main constituent of highly condensed amyloid plaque cores (Frost et al., 2013; Miller et al., 1993). However, the role of $A\beta_{pE3-x}$ in AD and the possible mechanism of action are subject to ongoing discussion: It has been proposed that $A\beta_{pE3-x}$ oligomers act as a seed in AD and thereby promote plaque formation (Schlenzig et al., 2009) and it has been suggested that $A\beta_{pE3-x}$ might act in a prion-like matter, promoting toxicity by imprinting its conformation onto other Aβ assemblies (Nussbaum et al., 2012). Others see pyroglutamate-modified Aβ as restricted to plaques (DeMattos et al., 2012). $A\beta_{pE3-x}$ has been suggested as a therapeutic target in AD and anti-$A\beta_{pE3-x}$-antibodies have been reported to be capable of influencing the progression of pathological alterations in mouse models of AD (DeMattos et al. (2012); Frost et al. (2012); Wirths et al. (2010c) see also 1.9.3, page 27).

Amyloid-beta Starting at Residue Four (Phe-4)

Another species of N-terminally truncated Aβ that is abundant in human AD brain is Aβ$_{4-X}$. As early as in 1985 it was discovered that these isoforms are a component of patients brain amyloid deposits (Masters et al., 1985). In 2006, Lewis et al. (2006) reported that Aβ$_{4-42}$ is relatively abundant in AD, aged controls and vascular dementia. On the whole, Aβ$_{4-X}$ has not gained much attention and therefore less is known about its function and properties. Aβ$_{4-42}$ is less abundant according to Miller et al. (1993) and Näslund et al. (1994), whereas the results from Portelius et al. (2010) support the findings of Masters et al. (1985) concluding that it is a major component in human AD. Miravalle et al. (2005) found Aβ$_{4-42}$ to be a major constituent of cotton wool plaques in familial AD patients with the V261I mutation in the presenilin-1 gene. A recent study showed that Aβ$_{4-42}$ rapidly assembles to oligomers and is as toxic as Aβ$_{1-42}$ and Aβ$_{pE3-42}$ (Bouter et al., 2013). These studies indicate that Aβ$_{4-42}$ is important for AD, although the precise amount of Aβ starting at Phe-4 in AD remains unclear.

Amyloid-beta Starting at Residue Five (Arg-5)

The knowledge about another isoform with ragged N-terminus, Aβ$_{5-X}$, is even scarcer. It is present in AD and was suggested to be the result of alternative cleavage of APP involving caspase activity (Murayama et al., 2007). The role of Aβ$_{5-X}$ and its toxicity remain unclear (Bayer and Wirths, 2014).

1.8 MOUSE MODELS OF ALZHEIMER'S DISEASE

A variety of transgenic murine models was described after the discovery of mutations that lead to familial AD. The alterations in these models resemble pathologic features of AD such as amyloid deposition, neuron loss, aggregation of phosphorylated Tau and behavioral and/or memory deficits. All these models rely on overexpression of human APP and/or presenilin-1/2 with at least one familial AD mutation. They differ noticeably regarding their phenotype, which is likely to reflect different promotors

used, the genetic background (mouse line), the transgene doses and differring effects of mutations introduced with the transgene(s) (Elder et al., 2010).

1.8.1 *APP-based Models*

The first successful generation of a transgenic AD model was reported by Games et al. (1995) who created the PDAPP model, in which a Platelet-derived groth factor-β (PGDF) promotor-driven human APP transgene with the mutation V717F was introduced. PDAPP exhibits an age-dependent deposition of Thioflavin S-positive amyloid plaques starting at the age of 6 months. Furthermore, the model develops dystrophic neurites, astro-/microgliosis in proximity to the amyloid plaques, age-related learning impairment and synapse loss (Chen et al., 2000; Dodart et al., 2000; Games et al., 1995; Reilly et al., 2003). In a similar approach, a transgenic line overexpressing human APP with the K670N/M671L (Swedish) mutation under a hamster Prion Protein (PrP) promotor was described by Hsiao et al. (1996): The Tg2576 model develops age-dependent amyloid Thioflavin S-postive deposits between 9 and 10 months of age, gliosis and learning deficits and has been widely used for research (Elder et al., 2010). In addition to the PDAPP and Tg2576 models, several other APP-based models have been developed and characterized subsequently. They all show elevated production of Aβ, gliosis and dystrophic neurites. Other features such as behavioral deficits have been frequently described (Elder et al., 2010). Most recently, a human APP Knock-in mouse model has been described. This model develops amyloidosis and memory deficits without expressing the mutant APP beyond endogenous levels (Nilsson et al., 2014).

1.8.2 *Models with Presenilin Mutations*

As mutations in the APP gene cause familial AD, so do mutation in the PS genes 1 and 2. These proteins are constituents of the γ-secretase complex involved in amyloidogenic cleavage of APP. Consequently, human mutant PSs have been overexpressed in

transgenic mice to study their effects. Mouse models harboring only these transgenes do not develop any plaques but show elevated levels of $A\beta_{X-42}$. When crossed to APP overexpressing lines, the PS mutations cause an earlier onset of pathology and more abundant plaque deposition (Elder et al., 2010). Well-characterized lines combining effects of both mutant APP and PS are the APP/PS1ΔE9 model (Borchelt et al., 1997), the APP/PS1KI model (Casas et al., 2004) and the 5XFAD model (see 1.8.2, page 22). Research on these lines contributed considerably to the better understanding of intracellular Aβ, neuron loss and behavioral phenotype (Casas et al., 2004; Christensen et al., 2010a; Jawhar et al., 2012; Oddo et al., 2003; Wirths and Bayer, 2012; Wirths et al., 2009). It is not understood why the mere expression of PS transgenes only poorly resembles the AD features (Elder et al., 2010).

The 5XFAD Mouse Model

Transgenic mice (Tg6799) expressing five familial AD mutations (5XFAD) were first described by Oakley et al. (2006). This strain expresses human Amyloid-Precursor-Protein (isoform APP695) and PS-1 with a total number of five familial mutations known to cause familial AD in humans under a murine Thy-1 promoter (Moechars et al., 1996; Oakley et al., 2006; Vidal et al., 1990): three mutations in the human APP locus, Swedish (K670N, M671L), Florida (I716V) and London (V717I) mutation, as well as two PS-1 mutations, M146L and L286V. When hemizygous, these mice display intraneuronal Aβ accumulation and extracellular plaque pathology at the age of 6-8 weeks (Oakley et al., 2006). At the age of approximately 6 months, female mice show behavioral impairment and working memory deficits. At the age of 12 months, neuron loss in cortical layer V and robust reference memory impairment are found. The neuron loss in cortical layer V has been linked to the accumulation of intracelluar Aβ (Jawhar et al., 2012; Oakley et al., 2006). The 5XFAD model develops its phenotype rapidly and displays important major features of AD. 5XFAD has been widely used and has been employed for several preclinical studies investigating treatment effects on the behavior phenotype (Aytan et al., 2013; Bhattacharya et al., 2014; Cho et al., 2014; Fiol-deRoque et al., 2013; Hillmann et al., 2012; Wirths et al., 2010c).

Other Models

Besides APP and APP/PS transgenic models, several other models have been developed for AD research. Of particular importance are models investigating the effects of N-truncated isoforms expressed exclusively without relying on APP overexpression and processing: The TBA42 and the Tg4-42 model (Bouter et al., 2013; Meissner et al., 2014; Wittnam et al., 2012), develop neuron loss and behavioral/memory deficits despite lacking abundant amyloid deposition in the brain. Therefore, they support the hypothesis that intracellular soluble aggregates of Aβ play a key role in AD (see also 1.8.3, page 24). Another, non-transgenic model addressing the risk factor diabetes mellitus type II is the icv-STZ model that was described with some important pathological features of AD including memory impairment (Chen et al., 2012, 2013; de la Monte and Wands, 2008; Salkovic-Petrisic et al., 2006). Although the relevance of murine, mutant APP/PS transgenic models is sometimes questioned since these are clearly associated with the minor fraction of approximately 1 % familial AD cases, they are widely employed. This is due to the fact that rodent species do not develop any amyloid-related pathology spontaneously, but offer important time and cost advantages over other mammal models such as canines or non-human primates. Besides the icv-STZ model mentioned above, it was recently proposed that the Tg4-42 mouse represents a better model for sporadic AD rather than APP/PS-based models because it does not rely on any mutation (Bouter et al., 2014). However, both the icv-STZ and the Tg4-42 model, do share certain pathologic alterations with various mutation-based models (Bouter et al., 2014; Chen et al., 2013). Furthermore, as do all other models currently available, they do not fully resemble the complex pathological alterations ongoing in human sporadic or familial AD. Thus, due to the convincing resemblance of major AD features, abundant plaque deposition and expression of a heterogenous Aβ peptide pool, mutation-based transgene models must still be considered relevant for sporadic AD.

N-terminally ragged Aβ has not only been observed in brains of AD patients but also in murine models of AD: $A\beta_{pE3-X}$, $A\beta_{4-X}$ and $A\beta_{5-X}$ have been shown to be produced in the 5XFAD model (Jawhar et al., 2012; Wittnam et al., 2012). Also, several N-truncated isoforms of Aβ have been reported in the APP/PS1KI model, including $A\beta_{4-X}/A\beta_{5-X}$ detectable from the age of 2.5 months and $A\beta_{pE3-X}$ from 6 months (Casas et al., 2004) and in the Tg2576 model (Kawarabayashi et al., 2001). These studies have been further supported by a comparative study by Frost et al. (2013) who assessed $A\beta_{pE3-X}$-immunoreactivity semi-quantitatively in 11 different mouse models of AD, including 5XFAD, APP/PS1ΔE9, and Tg2576. Within an approach of passive immunization, an antibody raised against $A\beta_{pE3-X}$ was further reported to strongly label amyloid plaques in the PDAPP model (DeMattos et al., 2012). Several studies have demonstrated that $A\beta_{pE3-X}$ is most abundant in the amyloid plaque cores (Frost et al., 2013; Härtig et al., 2010; Jawhar et al., 2012; Maeda et al., 2007).

Recently generated mouse models support further *in-vivo* toxicity of N-truncated Aβ: In TBA42 (expressing $A\beta_{pE3-42}$) and Tg4-42 (expressing $A\beta_{4-42}$) mice, the mere expression of the respective ragged isoform led to intracellular accumulation of the peptides and subsequently to behavior/memory deficits and massive loss of neurons (Bouter et al., 2013; Meissner et al., 2014; Wittnam et al., 2012).

In addition to the APP/PS1KI model (Casas et al., 2004), $A\beta_{5-42}$ was very recently reported for the 5XFAD and another (3xTg) model (Guzman et al., 2014), but without any evidence of intracellular accumulation.

However, the relative amounts of N-terminally truncated Aβ in mouse models and human AD differ considerably as their levels are much lower in mice (Rüfenacht et al., 2005; Schieb et al., 2011). For instance, in aged Tg2576 mice, Kawarabayashi et al. (2001) reported that only 5 % of the deposited (insoluble) Aβ is N-terminally ragged whereas the relative abundance of N-truncated Aβ in human AD brain is approximately 70-85 %. It was further suggested that the lower percentage of N-truncated Aβ in murine models is connected to the strikingly different solubility observed for amyloid plaques from AD and murine brains (Kalback et al., 2002).

Although there are drugs to treat the symptoms of AD, there is currently no cure. The availabe medication targets the cholinergic system or glutamate-mediated excitotoxicity in the brain and has been shown to have moderate effects, but does not prevent the progression of the clinical symptoms (Bullock and Dengiz, 2005; Bullock et al., 2005; Rogers et al., 1998; Wallin et al., 2011).

The modified amyloid cascade hypothesis suggests that modulating the production or improving the clearance of Aβ could be promising for therapy. Thus, the idea of inhibitors or modulators targeting enzymes that are involved in amyloidogenic cleavage of APP (see 1.5.1, page 13) was followed by several studies. However, this approach has some major flaws: It has not been achieved to date to develop γ-secretase inhibitors that are specific for the substrates but non-toxic. β-secretase inihibitors are at a very early developmental stage. Thus, the focus of research is currently on active and passive immunization approaches (Lannfelt et al. (2014).

1.9.1 *Active Immunization*

Schenk et al. (1999) have demonstrated that active immunization against Aβ can prevent plaque deposition in the PDAPP mouse model. Similar approaches were able to support these results and even show a rescue of behavioral symptoms in transgenic mice (Dodart et al., 2002; Janus et al., 2000; Kotilinek et al., 2002; Morgan et al., 2000). These remarkable effects led to the initiation of clinical trials of active immunization with Aβ preparations in AD patients. In the first clinical phase I safety study, about 60 patients were treated. Although several individuals failed to develop detectable antibody titers, no adverse events were observed (Schenk, 2002). However, clinical phase 2a trials were halted due to the observation that a subset of patients developed symptoms of CNS inflammation and the fact that some even died from pulmonary embolism afterwards (Ferrer et al., 2004; Nicoll et al., 2003).

It was concluded that active immunization led to an autoimmune response, thereby causing severe side effects (Orgogozo et al., 2003). Although a more complete follow-up of these studies suggested slight beneficial effects in a fraction of patients later, many researchers shifted their interest towards passive immunization strategies (Hock et al., 2002).

1.9.2 *Passive Immunization*

Antibodies against Aβ are widely employed as research tools. Monoclonal antibodies have been raised to engage with various epitopes within the Aβ sequence. Besides their potential for detection of Aβ in, or purification of, Aβ from biological samples, several antibodies with specific properties have been proposed for passive immunization. Antibodies evaluated positively in preclinical trials were then humanized to avoid species-specific immune-responses in human patients. The humanized antibodies used in clinical trials recognize N-terminal, C-terminal or central epitopes within the Aβ sequence or neo-epitopes of aggregated Aβ, soluble oligomers, protofibrils, plaques or a subset of them.

Passive immunization strategies against Aβ have been successfully tested in murine models during the past years. These studies demonstrated the capability of peripherally administered antibodies to successfully clear Aβ from murine brain (Bard et al., 2000; DeMattos et al., 2001; Frost et al., 2012; Wilcock et al., 2003, 2004b,c, 2006). However, it was found that passive immunization can also cause side effects, e.g. microhemorhages (DeMattos et al., 2012; Pfeifer et al., 2002; Racke et al., 2005; Schroeter et al., 2008; Wilcock et al., 2004c, 2006). Subsequently it was proposed that these side effects are induced by the effector function of the antibody on microglial activation: It was shown that reducing the effector function, for instance by de-glycosylation of the antibody, can be one way of addressing this issue (Karlnoski et al., 2008; Wilcock et al., 2006).

The clinical trials beyond phase I mostly employed humanized monoclonal antibodies against various Aβ epitopes and neo-epitopes. Some of them have been terminated

due to lack of efficiency or adverse side effects and the overall outcomes are much less promising than preclinical studies have suggested (Lannfelt et al., 2014).

The humanized antibody bapineuzumab (Janssen Alzheimer Immunotherapy and Pfizer) targets fibrillar forms of Aβ preferentially, recognizing the N-terminal domain of the peptide (Miles et al., 2013). In two clinical phase III studies, some evidence of target engagement was reported, as well as a statistically significant reduction of Tau in the cerebrospinal fluid of patients. However, the administration of the antibody was accompanied by a significant number of vasogenic edema and microhemorrhages. Thus the development of bapineuzumab was terminated (Lannfelt et al., 2014).

Solanezumab (Eli Lilly and Co), is a humanized antibody directed against soluble monomeric Aβ, recognizing a mid-sequence epitope. Pooled data from two phase III studies indicated a reduction in rate of conitive decline by 34 %, but without statistical significance. The clinical trials have been extended and solanezumab is further being tested for the prevention of familial AD (Lannfelt et al., 2014).

Other antibodies such as the conformation-specific gantenerumab (targeting amyloid plaques), crenezumab (against monomeric and oligomeric Aβ) and BAN2401 (recognizing soluble Aβ-protofibrils) are currently under clinical investigation, too (Lannfelt et al., 2014). However, none of these antibodies have been proven to substantially influence the progression of symptoms in AD. Additionally, Watt et al. (2014) recently raised doubts whether antibodies used in some of the clinical studies sufficiently engage with the target after administration. Passive immunotherapy is still ongoing in clinical trials and remains a promising option to develop an efficient treatment of AD.

1.9.3 *Most Recent Developments*

During the past years, rapid progression has been achieved in the field of AD research. In particular, the role of soluble toxic assemblies of Aβ and some of its N-truncated isoforms have increasingly gained attention. It has become widely accepted that $A\beta_{pE3-X}$ may play an important role in AD and this isoform has been shown to exhibit deviant biochemical properties compared with N-terminally intact Aβ (see 1.8.3, page 24). The interest in Aβ starting at residue 4 as another abundant N-truncated species is

increasing as well (Bouter et al., 2013, 2014). Most of the immunization approaches against Aβ have been shown to have important disadvantages such as negative side effects or a lack of efficacy in humans (see 1.9.1, page 25 and 1.9.2, page 26). These difficulties further underline the need for a more specific drug that is safe and efficacious at the same time. Therefore, interest in N-truncated Aβ as a possible therapeutic target has increased. Marcello et al. (2011) showed that patients with AD have reduced levels of autoantibodies against N-truncated Aβ. A first pilot study of anti-$Aβ_{pE3-X}$ immunotherapy in mice had promising outcomes (Wirths et al., 2010c). During the time that the studies described here were conducted two other studies supported the importance of $Aβ_{pE3-X}$ as a possible target for treatment, describing altered Aβ levels after passive immunization with anti-$Aβ_{pE3-X}$ antibodies in two different mouse models without induction of microhemorrhage, a commonly seen side effect (DeMattos et al., 2012; Frost et al., 2012). McLaurin et al. (2002) reported that therapeutic benefits observed in mice after active immunization with protofibrillar Aβ are due to antibodies recognizing residues 4-10 of the Aβ sequence. However, the question if and how $Aβ_{4-X}$ can be employed for therapeutic strategies remains unanswered.

Among others, the group of Prof. T.A. Bayer (Göttingen) has developed several monoclonal antibodies specifically targeting N-terminally truncated Aβ with different binding preferences that could have therapeutic potential: NT4X-167 was raised against an $Aβ_{4-X}$ epitope; 1-57 is a non-conformation-specific antibody against $Aβ_{pE3-X}$ (Wirths et al., 2010a) and 9D5 is an oligomer-specific antibody against $Aβ_{pE3-X}$ (Wirths et al., 2010c). The experimental work carried out in this doctoral thesis aims to extend and broaden the investigations of N-terminally truncated Aβ as a possible target for AD therapy. To this end, a comparative pilot study with three monoclonal antibodies (NT4X-167, 1-57, 9D5) engaging with different fractions of N-truncated Aβ was designed. This comparative approach aims to give insight into the contribution of the two major fractions of N-terminally truncated peptide isoforms, $Aβ_{pE3-X}$ and $Aβ_{4-X}$. Since discrepancies regarding the abundance of N-terminally truncated Aβ between murine models and human AD have been described (see 1.8.3, page 24), it was of particular importance to thoroughly investigate the model that should be employed (5XFAD) regarding its suitability for the purpose of the study. A homozygous 5XFAD strain was created to elevate transgene expression and Aβ production. This was intended to improve detection and analysis of the less abundant N-truncated peptide species. The aims of the study can be summarized in main objectives/main questions as follows:

- Characterization of the newly developed monoclonal antibody NT4X-167

- Generation and Characterization of a homozygous 5XFAD strain

- Is the 5XFAD model suitabe to study the effects of N-terminally truncated Aβ?

- Does targeting N-truncated Aβ, in particular $Aβ_{4-X}$, offer any therapeutic advantages for AD?

Part II

MATERIAL AND METHODS

<div style="text-align: right">

2

</div>

MATERIAL AND METHODS

2.1 MATERIAL

2.1.1 *Chemicals, Reagents, Kits and Technical Devices*

The chemicals used within this study are listed in table 2.1, reagents and formulations used are listed in table 2.2. Kits used are listed in table 2.3 and the technical devices used are listed in table 2.4.

2.1.2 *Antibodies*

The primary antibodies used for Western Blot and/or Immunohistochemistry are listed in Table 2.5. Secondary antibodies employed in western blotting or immunohistochemistry are listed in Table 2.6.

Table 2.1
Chemicals

Chemical	Manufacturer
4´6-Diamidin-2-Phenylindol	Roth, Karlsruhe, Germany
Acetonitrile	Merck, Darmstadt, Germany
Agarose	Lonza, Basel, Switzerland
Ammoniumbicarbonate	Sigma, St. Louis, MO, USA
Boric Acid	Sigma, St. Louis, MO, USA
Bovine serum albumin	Roth, Karlsruhe, Germany
Citric Acid	Roth, Karlsruhe, Germany
Molecular Grade Water	Braun, Melsungen, Germany
Diaminobenzidin	Roth, Karlsruhe, Germany
Ethylenediaminetetraacetic Acid	Roth, Karlsruhe, Germany
Ethanol	Merck, Darmstadt, Germany
Ethidiumbromide	Roth, Karlsruhe, Germany
Formic Acid 98 %	Roth, Karlsruhe, Germany
Hydrochloric Acid	Merck, Darmstadt, Germany
Hydrogenperoxide	Roth, Karlsruhe, Germany
Isopropanole	Roth, Karlsruhe, Germany
Liquid Nitrogen	Air Liquide
Methanol	Roth, Karlsruhe, Germany
Sodium Chloride (NaCl)	Roth, Karlsruhe, Germany
Sodium dodecyl sulfate	Roth, Karlsruhe, Germany
Sodium hydrogen phosphate	Merck, Darmstadt, Germany
Sodium hydroxide	AppliChem
Sinapinic Acid	Bruker Daltonics
Thioflavin S	Sigma, St. Louis, MO, USA
Tris(hydroxymethyl)-aminomethane	Roth, Karlsruhe, Germany
Triton X-100	Roth, Karlsruhe, Germany
Tween-20	Roth, Karlsruhe, Germany
Xylene	Roth, Karlsruhe, Germany

Table 2.2
Reagents and Formulations

Reagent	Manufacturer
10X Reaction Buffer for PCR	Axon, Kaiserslautern, Germany
100 bp Ladder	Bioron, Ludwigshafen, Germany
Agarose Sample Buffer (Blue Juice)	Life Technologies, Carlsbad, CA, USA
Amyloid-beta Peptides, Synthetic	Peptide Specialty Laboratories, Heidelberg, Germany
Cømplete Proteinase Inhibitor tablets	Roche, Basel, Switzerland
Taq DNA-Polymerase	Axon, Kaiserslautern, Germany
Desoxyribonukleoside-triphosphates	Axon, Kaiserslautern, Germany
Dynabeads M-280 sheep anti-mouse	Life Technologies, Stockholm, Sweden
Dynabeads M-280 sheep anti-rabbit	Life Technologies, Stockholm, Sweden
Fetal Cow Serum	Thermo Fisher Scientific, Waltham, MA, USA
Fluorescence Mounting Medium	DAKO, Glostrup, Danmark
Hematoxylin Solution	Roth, Karlsruhe, Germany
Ketamine 10 %	Medistar, Ascheberg, Germany
Luminata crescendo Western HRP Substrate	Merck, Darmstadt, Germany
Magnesium chloride (MgCl$_2$) for PCR	Axon, Kaiserslautern, Germany
Native Anode Buffer for BN/CN	SERVA, Heidelberg, Germany
Native Kathode Buffer for BN/CN	SERVA, Heidelberg, Germany
Native Marker, Liquid Mix for BN/CN	SERVA, Heidelberg, Germany
Nitrocellulose Membranes, Hyobond ECL	GE Healthcare, Chalfont St. Giles, GB
Non-Fat Dry Milk	Roth, Karlsruhe, Germany

Table 2.2 (continued)
Reagents and Formulations

Reagent	Manufacturer
Paraffin for Tissue Embedding	Roth, Karlsruhe, Germany
PBS pH 7.4	Sigma, St. Louis, MO, USA
PBS pH 7.4	Merck, Darmstadt, Germany
4-16% Serva*Gel*^{TM} N 4-16	SERVA, Heidelberg, Germany
Primers for genotyping	Eurofins, Ebersberg, Germany
Proteinase K	Peqlab, Erlangen, Germany
Roti-Histokitt	Roth, Karlsruhe, Germany
Sample Buffer for Blue Native (2x)	SERVA, Heidelberg, Germany
SERVA Blue G Solution for Blue Native, 1 %	SERVA, Heidelberg, Germany
Superfrost glass slides	Thermo Fisher Scientific, Waltham, MA, USA
Xylazine (Xylariem)	Ecuphar, N.V. Oostkamp, Belgium

Table 2.3
Kits

Kit	Manufacturer
DC Protein Assay Kit	Biorad Laboratories, Hercules, CA, USA
DyNAmo Flash SYBR Green qPCR Kit	Thermo Fisher Scientific, Waltham, MA, USA
RotiQuant Protein Assay	Roth, Karlsruhe, Germany
Vectastain ABC Kit	Vector Laboratories, Burlingame, CA, USA

Table 2.4
Technical Devices

Device	Manufacturer
Biophotometer	Eppendorf, Hamburg, Germany
Centrifuge (Stratos Biofuge Heraeus)	Thermo Fisher Scientific, Waltham, MA, USA
EG1140 H Embedding Station	Leica, Wetzlar, Germany
Electrophoresis Chamber BlueVertical PRiME	Serva, Heidelberg, Germany
Embedding Casettes	Simport, Beloeil, QC, Canada
Eppendorf LoBind reaction tubes	Eppendorf, Hamburg, Germany
Heating block (UNO-Thermoblock)	Biometra, Göttingen, Germany
HM 335E Microtome	Thermo Fisher Scientific, Waltham, MA, USA
Individually Ventilated Cages	Tecniplast, Hohenpleissberg, Germany
Odyssey FC	Li-Cor, Bad Homburg, Germany
BX-51 Microscope	Olympus, Shinjuku, Japan
0.2 ml PCR Tubes	Greiner Bio-One, Kremsmuenster, Austria
Semi-Dry Blotting Chamber	Biorad Laboratories, Hercules, CA, USA
Lab Cycler for PCR	SensoQuest, Göttingen, Germany
Savant SPD131DDA Speed Vac Concentrator	Thermo Fisher Scientific, Waltham, MA, USA
Nutating Shaker	Gesellschaft für Labortechnik (GFL), Burgwedel, Germany
MX3000P Real-Time Cycler	Stratagene, Santa Clara, CA, USA
Pap Pen Lipid Pen	Kisker Biotech, Steinfurt, Germany
Ultraflextreme Mass Spectrometer	Bruker Daltonics, Billerica, MA, USA
Uvette 220-1600 nm Cuvettes	Eppendorf, Hamburg, Germany
Sonics Vibra-Cell VCX-130 Sonifier 150	Sonics & Materials, Newtown, USA
ThermoMixer compact	Eppendorf, Hamburg, Germany
TP 1020 Automatic Tissue Processor	Leica, Wetzlar, Germany
Vortexer, Vortex Genie 2	Scientific Industries, Bohemia, NY, USA
Water Bath for mounting of paraffin tissue	Medax, Olching, Germany
Water Bath Sonorex RK 100H	Bandelin electronic, Berlin, Germany

Table 2.5
Primary Antibodies

Antibody	Manufacturer/Reference
1-57	Synaptic Systems, Göttingen, Germany Wirths et al. (2010a)
24311	Bouter et al. (2013)
4G8	Covance, Princeton, NJ, USA
6E10	Covance, Princeton, NJ, USA
82E1	Immuno-Biological Laboratories, Minneapolis, MN, USA
9D5	Synaptic Systems, Göttingen, Germany Wirths et al. (2010a)
Abeta42	Synaptic Systems, Göttingen, Germany
G2-10	Merck Millipore, Darmstadt, Germany
IC16	Gift of Prof. Dr. Sascha Weggen, Heinrich-Heine University Düsseldorf, Germany
NT4X-167	Antonios et al. (2013)

Table 2.6
Secondary Antibodies

Antibody	Manufacturer
Goat-anti-rabbit HRP conjugated	Dianova, Hamburg, Germany
Rabbit-anti-mouse HRP-conjugated	Dianova, Hamburg, Germany
Rabbit-anti-mouse IgG biotinylated	DAKO, Glostrup, Danmark
Swine-anti-rabbit IgG biotinylated	DAKO, Glostrup, Danmark

2.2.1 *Electrophoresis and Western Blotting of Synthetic Peptides*

Synthetic Aβ peptides were dissolved at 1 mg/ml in 10 mM Sodium hydroxide (NaOH) and sonicated for 5 minutes in an ice-cold sonication water bath. Aliquots of 10 µl were flash frozen in liquid nitrogen and stored at -80 °C prior to use. 2 µg peptide per well (mixed with an equal volume of sample buffer for blue native (2x)) were loaded on Vertical Native Gels and run at a constant current of 120 V in the BlueVertical PRiME electrophoresis chamber containing Native Kathode Buffer for BN/CN supplemented with SERVA Blue G Solution for Blue Native, 1 % and Native Anode Buffer for BN/CN. After electrophoresis, the peptides were transferred onto 0.45 µm nitrocellulose membranes for 30 minutes per membrane at constant 25 mA in a semi-dry transfer chamber. Free binding sites were blocked with 4 % (w/v) non-fat dry milk dissolved in Tris-buffered saline supplemented with Tween-20 (TBS-T) (50 mM Tris(hydroxymethyl)-aminomethane (Tris) pH 8.0 supplemented with 0.05 % (v/v) Tween-20) for one hour at acRT. For detection, the primary antibodies NT4X-167 (0.5 µg/ml), 1-57 (0.5 µg/ml), IC16 (0.25 µg/ml) and 24311 (0.5 µg/ml) were dissolved in TBS-T and incubated on a shaker over night at 4 °C. After three washing steps (5 minutes each) with TBS-T, secondary antibodies rabbit-anti-mouse HRP-conjugated or goat-anti-rabbit HRP conjugated were diluted 10000-fold in TBS-T and incubated with the membrane for 2 hours at Room Temperature (RT). Exposure was facilitated with 1 ml of Luminata crescendo Western HRP Substrate in an Odyssey Fc.

2.2.2 *Immunohistochemistry on Paraffin Sections*

Mouse tissue samples were prepared and processed similar to the way described previously (Wirths et al., 2001). Paraffin sections of 4 µm mounted on superfrost slides were de-parrafinized in two steps (5 minutes each) by the use of 100 % Xylene. Then, sections were re-hydrated in aqueous ethanol solutions with descending ethanol con-

centrations (100 % ethanol for 10 minutes, 95 % (v/v) for 5 minutes, 70 % for 5 minutes) and subsequently immersed for 5 minutes in deionized water. In the next step, sections then were pretreated with 0.3 % (v/v) H_2O_2 in Phosphate-buffered saline (PBS) for blocking of endogenous peroxidases and then washed for 5 minutes in deionized water. For antigene retrieval, the tissue was treated with citrate buffer (0.01 M citric acid, pH adjusted to 6.0 with NaOH) at 95 °C and washed again in PBS for 5 minutes. A second antigene retrieval step of a 3-minute incubation in 88 % (v/v) formic acid was performed and the slides were washed again twice in PBS. In sections treated this way, unspecific binding sites were blocked for 1 hour at RT in blocking solution (PBS supplemented with 10 % (v/v) fetal cow serum and 4 % (w/v) fat free milk powder). The slices were indivdually circled with a Lipid Pen and primary antibodies were applied in PBS supplemented with 10 % (v/v) fetal cow serum for 16 hours at RT. The slides were washed in PBS supplemented with 0.5 % (v/v) Triton X-100. This was followed by incubation (1 hour at 37 °C) with biotinylated secondary antibody rabbit-anti-mouse or swine-anti-rabbit in PBS supplemented with 10 % (v/v) fetal cow serum, before staining was visualized using the ABC method (Vectastain ABC kit). To this end, a 1:100 dilution of both Solution A and B in PBS supplemented with 10 % (v/v) fetal cow serum was prepared and incubated with the slices for 30-60 minutes at 37 °C. Visualization was then facilitated after 15 minutes washing in PBS by exposure of the slices to 25 μg/ml diaminobenzidin and 0.0025 % (v/v) H_2O_2 dissolved in an aqueous solution of 50 mM Tris pH 7.4. The sections were washed twice in PBS for 5 minutes and, except for the case of immunohistochemistry for plaque load quantification, counterstained in hematoxylin solution for 45 seconds. After washing in deionized water for five minutes under constant exchange (running tab), sections were de-hydrated in a reversed aqueous ethanolic solution chain (as for re-hydration, see above), followed by two five-minutes steps of washing in xylene. The so treated sections were then embedded with Roti-Histokitt and left to dry for at least 48 hours prior to examination. Primary antibodies used were: Mouse monoclonal antibodies NT4X-167 reacting with $A\beta_{pE3-X}$ and $A\beta_{4-X}$ (1 μg/ml, visualization in diaminobenzidine solution for 4 minutes), 1-57 reacting with $A\beta_{pE3-X}$ (1 μg/ml, visualization for 1 minute), G2-10 reacting with $A\beta_{X-40}$ (3 μg/ml, visualization for 3 minutes), 82E1 reacting with $A\beta_{1-X}$

(1μg/ml, visualization for 1 minute), and rabbit polyclonal antibody Abeta42 reacting with $A\beta_{X-42}$ (0.5 μg/ml, visualization for 30 seconds) as well as 24311 (0.5 μg/μl, visualization for 2 minutes).

2.2.3   *Thioflavin S Staining of Paraffin Sections*

For Thioflavin S fluorescent staining as in Christensen (2009), paraffin tissue was de-paraffinized and rehydrated as in 2.2.2, washed twice (1 minute) in deionized water and then treated with 1 % (w/v) ThioflavinS in aqueous solution for 8 minutes. Sections were washed twice again for 1 minute in water and immersed in the Thioflavin S solution for another 4minute, washed twice in 80% (v/v) ethanol and three times in water (1minute each), counterstained in a 1 % (w/v) aqueous solution of 4´6-diamidin-2-phenylindol, washed again in water for five minutes and embedded in Aqueous Fluorescent Mounting Medium.

2.2.4   *Lysis of Murine Brain Tissue*

Brains were homogenized in 8-fold amount of Tris-buffered saline (TBS) Lysis Buffer (50 mM Tris, pH 8.0 supplemented with 1 tablet/10 ml of Cømplete Protease Inhibitor cocktail (Roche)) and homogenates were spun down for 20 minutes at 17.000 x g, 4 °C in a stratos Biofuge. Supernatant (termed TBS fraction) was separated. The pellet was resuspended in 1 ml TBS lysis buffer and spun down again. The supernatant was discarded and the pellet dissolved in Sodium dodecyl sulfate (SDS) lysis buffer (2 % SDS, supplemented with 1tablet/10ml Cømplete Protease inhibitor cocktail) using the Vibra-Cell sonifier 150 at power '2' with 10 single pulses. The lysate was spun down again as described above and the supernatant (termed SDS-Fraction) was separated. Total protein concentrations of both fractions were determined using the RotiQuant Protein Assay with Bovine serum albumin (BSA) as a standard.

2.2.5 *Isolation of Genomic DNA and Genotyping of Animals*

Genomic DNA was isolated from tail biopsies. Per sample, 500 µl of lysis buffer (100 mM Tris/hydrochloric acid pH 8.5, 5 mM ethylenediaminetetraacetic acid, 0.2 % (w/v) SDS, 200 mM NaCl, 10 µl/ml proteinase K) were added and left overnight at 55 °C in a Thermomixer Compact under gentle agitation. Solutions were centrifuged at 13000 rpm in the stratos centrifuge for a duration of 10 minutes and the pellet was discarded. The lysates were diluted into 500 µl of isopropanole. Samples were then vortexed and centrifuged again for 10 minutes at 13000 rpm. Pellets were washed in 500 µl of 70 % (v/v) ice-cold ethanol and spun down for 10 minutes at 13000 rpm. After the supernatant was discarded, the pellets were left do dry at RT and further dissolved in 50 µl H_2O. The DNA concentration was then measured using the Bio-photometer (DNA preparations with A260/A230 and A260/A280 ratios > 1.8 were considered sufficiently pure) and diluted in molecular grade water to reach a concentration of 20 ng/µl. 5XFAD mice carrying the transgene were identified using conventional Polymerase-chain-reaction (PCR) as follows:

A reaction mix for the polymerase chain reaction was set up according to table 2.7 without the DNA. DNA was then given into a PCR reaction tube and the prepared reaction mix (18 µl) was added. The cycling protocol is listed in table 2.8. After this, the samples were subjected to agarose gel electrophoresis to identify transgene animals. 100 ml of TBE buffer (89 mM Tris, 89 mM boric acid, 2 mM ethylenediaminetetraacetic acid) were added to 2 g agarose and heated in a microwave until the agarose was completely dissolved. 3 µl ethidumbromide (10 mg/ml) were added and the gel was casted in a casting tray with a comb to form wells. After the gel was cooled down, the comb was removed and the samples (10 µl mixed with 1 µl of 10X agarose sample buffer) were loaded into the wells. The gel was run in a horizontal electrophoresis chamber (Biorad Laboratories, Hercules, CA, USA).For size indication, one well was filled with 5 µl of 100 bp DNA ladder and run in TBE buffer for approximately 45 minutes at 120 V constant current. The DNA in the gel was visualized under a UV lamp. Animals that showed the expected amplicon band of approximately 250 base pairs were considered transgenic.

Table 2.7
Master Mix for 5XFAD Genotyping

Reagent	Volume [µl]
DNA (20 ng/µl)	2.0
Primer hAPP-for (table 2.9)	0.5
Primer hAPP-rev (table 2.9)	0.5
dNTPs (2 mM)	2
$MgCl_2$ (25 mM)	3.2
10X reaction buffer	2
Molecular grade water	9.6
Taq polymerase (5 U/ul)	0.2

Table 2.8
Cycling Programm for 5XFAD Genotyping

Step	Temperature [°C]	Duration [s]
1	94	180
2	94	45
3	58	60
4	72	60
5	Repetition of steps 2 - 4	(35 times)
6	72	300
7	4	for storage

2.2.6 *Quantitative Real-Time PCR Genotyping*

To identify homozygous animals, quantitative Real-Time PCR was performed using a Stratagene MX3000P Real-Time Cycler with 10 ng of genomic DNA per reaction. For quantification of the PCR product, the SYBR-green based DyNAmo Flash SYBR Green qPCR Kit containing ROX as an internal reference dye was used, adopting the conventional APP genotyping protocol for 5XFAD mice. The reaction mix and cycling protocol are given in tables 2.10 and 2.11. The reaction was performed in duplicates and separate tubes for each pair of primers.

Table 2.9
Primer used for genoyping of 5XFAD mice

Primer	Sequence
hAPP-for	5´ - GTA GCA GAG GAG GAA GAA GTG - 3´
hAPP-rev	5´ - CAT GAC CTG GGA CAT TCT C – 3´
mAPP-for	5´- TCT TGT CTT TCT CGC CAC TGG C – 3´
mAPP-rev	5´ - GCA GTC AGA AGT TCC TAG G – 3´

Table 2.10
Reaction Mix for 5XFAD Quantitative Real-Time Genotyping

Reagent	Volume [µl]
DNA (20 ng/µl)	2.0
Primer mAPP-for or hAPP-for (table 2.9)	0.5
Primer mAPP-rev or hAPP-rev (table 2.9)	0.5
Master Mix	10
ROX	0.2
Molecular grade water	6.3

Average CT values were determined from the duplicates, and relative quantification was performed using murine APP as a reference gene for normalization. The transgene levels of human APP were normalized to those of murine APP and calibrated to a selected heterozygous 5XFAD animal using the ΔΔCT method (Schmittgen and Livak, 2008) (i):

$$\text{(i)} \qquad \text{Amount}_{Gene} = 2^{-\Delta\Delta CT}$$

Table 2.11
Cycling Programm for 5XFAD Quantitative Real-Time Genotyping

Step	Temperature [°C]	Duration [s]
1	95	600
2	95	15
3	64	20
4	72	30
5	Repetition of steps 2 - 4	(40 times)
6	95	60
7	55	30
8	95	30
9	4	for storage

For an animal (q), the level of human APP (hAPP) gene expression normalized to the expression of murine APP (mAPP) as a reference gene and calibrated to a confirmed hemizygous animal (cb), $\Delta\Delta CT$ is calculated as follows (ii) and (iii):

$$\text{(ii)} \qquad \Delta C_T = C_{T,hAPP} - C_{T,mAPP}$$

$$\text{(iii)} \qquad -\Delta\Delta C_T = -_{T,q} - \Delta C_{T,cb}$$

Figure 2.1 gives a typical example, with animals A and C being identified as potentially homozygous 5XFAD ($5XFAD^{hom}$) animals.

2.2.7 *Immuno-precipitation of Amyloid-beta*

Frozen murine brain samples (three left hemibrains from 7-month-old hemizygous 5XFAD mice) were homogenized to powder in liquid nitrogen using mortar and pistil and aliquoted at 50 mg in 1.5 ml Eppendorf LoBind reaction tubes (LoBind tubes were used for all subsequent steps). One aliquot of brain powder was dissolved in 330 μl 0.01 M PBS and sonicated with the Sonics Vibra-Cell VCX-130 sonifier for one minute
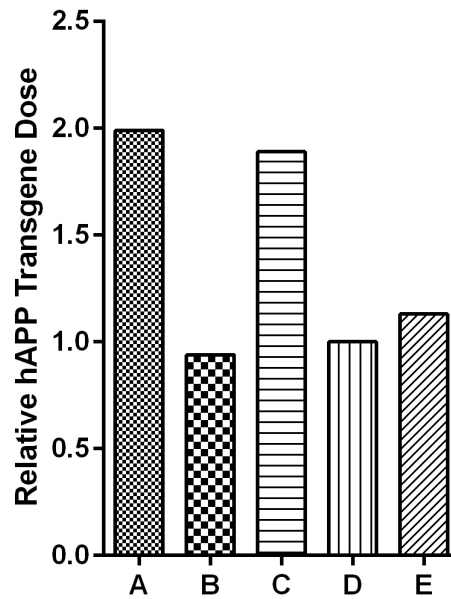
Figure 2.1
A typical example for Real-Time-PCR genoyping of 5XFAD mice. Here the animals A and C whose human APP gene dose was appromately twice as high in comparison to a confirmed hemizygous animal (D) were identified as potential homozygous 5XFAD. Animals B and E were considered hemizygous.

applying pulses of 2 s at an amplitude of 30 %. Formic acid was added to a final concentration of 70 % (v/v) and the sample was sonicated again, the insoluble fraction spun down for 20 minutes at 17.000 g. The pellet was discarded and concentrations were determined using a DC Protein Assay Kit, based on the modified Lowry method with BSA as standard (Lowry et al., 1951). The extract was aliquoted at 200 µl and finally dried down in the SpeedVac at 45 °C and stored at –80 °C. For Immuno-Precipitation (IP), the extract was re-dissolved in 100 % FA to a concentration of 4 mg total protein/ml and neutralized diluting it by 21-fold (50 µl sample + 1100 l of 1 M Tris, 0.5 M Na_2HPO_4). For IP of Aβ from murine brain lysates, a 1:1 mixture of the antibodies 6E10 (Epitope 4–9) and 4G8 (Epitope 17–24) was used. Paramagnetic Dynabeads M-280 sheep-anti-mouse/rabbit were concentrated using a magnetic rack and washed twice in 1 ml PBS supplemented with 0.1 % (w/v) BSA and coupled with the capture antibody mixture (8µg/50 µl bead suspension) over night under gentle agitation. After coupling, beads were washed three times in PBS/BSA and incubated with 1 ml of neutralized sample for 6 hours. Following incubation, beads were washed twice

with PBS/BSA and twice with 50 mM ammoniumbicarbonate and eventually eluation was facilitated using 100 µl 0.5 % (v/v) FA. After transfer to a new LoBind vial, the eluate was dried down at 45 °C in the SpeedVac and stored at -80 °C prior to use.

2.2.8 *MALDI-TOF detection of Amyloid-beta*

For Matrix-Assisted Laser Desoption/Ionisation - Time of Flight (MALDI-TOF), the dried eluate obtained from IP was re-dissolved in 20 µl of 20 % (v/v) acetonitrile, 0.1 % (v/v) formic acid and sonicated in the water bath for 10 minutes. Sample was plated at 1-2 µl + equal volume of sinapinic acid as matrix (20 mg/ml in a 1/1 (v/v) mixture of acetonitrile/water). For MALDI-TOF, samples were re-dissolved in 20 µl of 20 % (v/v) acetonitrile with 0.1 % (v/v) FA, sonicated in the ultrasound waterbath for 10 minutes, spun down briefly and subjected to the steel target plate at 1 µl. Matrix solution was added in equal amounts directly onto the target and the mixture was allowed to crystallize at room temperature until found dry. Desorption and time-of-flight mass spectrometry was carried out in a Ultraflextreme mass spectrometer in reflection mode at a laser intensity of 80-90 % collecting accumulated spectra of a total number of 10000 single laser shots. For calibration, 1 µl of a synthetic Aβ peptides mixture (Aβ$_{pE3-40/42}$ and Aβ$_{4-40/42}$, 0.01 mg/ml each in 10 mM NaOH) was plated with an equal amount of matrix. Baseline was substracted from the obtained spectra.

2.3 ANIMALS AND ANIMAL EXPERIMENTS

2.3.1 *General Considerations*

All animals used in this study were of the species *Mus musculus*. All animals used for these studies were housed under specific pathogen-free (SPF) conditions in individually ventilated cages at the central animal facility of the Göttingen University Medical Center. Mice were kept with a constant 12 h/12 h inverted dark/light daily cycle (light from 8.00 p.m. to 8.00 a.m.) and had *ad libitum*-access to food and water.

All experimental procedures were performed during the night cycle (8.00 a.m. to 8.00 p.m.) Mice were handled according to the guidelines of the 'Society for Laboratory Animals Science' (GV-SOLAS) and the guidelines of the 'Federation of European Laboratory Animal Science Association' (FELASA). All animal experiments were approved by the "Landesamt für Verbraucherschutz und Lebensmittelsicherheit" (LAVES) Niedersachsen. Individuals that displayed conditions such as blind eyes or massive loss of weight (> 20 %) at any time before or during the experiments were sacrificed immediately and excluded from all analyses.

2.3.2 *Transgenic Mice*

In this work, the 5XFAD model, initially described by Oakley et al. (2006) has been used (see also 1.8.2, page 22). Mice were maintained on a C57Bl6/J genetic background (Jackson Laboratories, Bar-Harbor, ME, USA) (Jawhar et al., 2012).

2.3.3 *Tissue Collection and Preservation*

Mice were deeply anesthetized by intraperitoneal injection with a mixture of ketamine (100 mg/kg) and xylazine (10 mg/kg) and transcardially perfused with ice-cold PBS. Brains and spinal cords were dissected, spinal cords and right brain hemispheres including olfactory bulb and cerebellum were placed into embedding casettes and postfixed in phosphate-buffered formaldehyde solution Roti Histofix for five to seven days. The tissue was treated according to Wirths et al. (2010a): Using a TP 1020 Automatic Tissue Processor, the tissue was first submerged in Histofix for 5 minutes and the carried over to deionized water (30 minutes), dehydrated with aqueous solutions of ascending ethanol content (50 % (v/v), 60 %, 70 %, 80 %, 90 % for one hour each) followed by two times xylene (one hour each), and further two steps in melted paraffin (one hour each) and finally embedded in paraffin. Spinal cords and left hemispheres (olfactory bulb and cerebellum removed) were flash frozen on dry ice and stored at -80 °C prior to use. Paraffin-embedded tissue was sliced to 4 µm sections with a

microtome, mounted on superfrost slides in a water bath at RT and further fixed on the slides in a second water bath at approximately 52 °C. Before using the sections for immunohistochemistry, the slices were dried over night at 37 °C.

2.3.4 *Passive Immunization of 5XFAD Mice*

All monoclonal antibodies used for passive immunization consisted of a murine IgG2b backbone: NT4X-167, 1-57, 9D5 dissolved in PBS (c = 1 mg/ml) were obtained from Synaptic Systems, Göttingen (Germany), aliquoted, flash frozen in liquid nitrogen and thawed at RT right before injection.

Female hemizygous 5XFAD ($5XFAD^{hem}$) mice were immunized in a chronic parenteral approach; animal received weekly intraperitoneal injections, over a course of ten weeks, starting at the age of 4.5 months. The dosage of antibodies was 10 mg/kg body weight. Two days after the 9th administration, the mice were subjected to behavioral testing, starting with the cross maze test (see 2.3.6, page 52) at day one followed by the elevated plus maze (see 2.3.6, page 51). After a one-day pause, morris water maze training started (see 2.3.6, page 53). The last treatment was administered approximately six hours prior to the first trial of morris water maze acquisition training stage.

2.3.5 *Motorical Testing*

Clasping Test

The clasping phenotype of mice was performed as determined as previously described in Miller et al. (2008). Mice were suspended by the tail and given a score from 0-3, with 0 representing no clasping, 1 for forepaw clasping only, 2 for forepaws and one hindpaw clasping, and 3 for all paws clasping.

Balance Beam Task

The balance beam test (Hau and Schapiro, 2002; Luong et al., 2011) was performed as follows: A 50 cm long wooden round beam (1 cm in diameter) with a 9 x 15 cm escape platform at either end was used to assess balance and general motor function. The beam was elevated by 40 centimeters and the ground below was padded to prevent mice from injury. Mice were gently released in the middle of the beam and given 60 s to escape to one of the platform. Time on the beam was recorded as latency to fall. Escape to one of the platforms was recorded as full time (Jawhar et al., 2012). For statistics, the average of three trials per mouse, with an interval of at least 20 minutes between the trials was analyzed. Between the single trials, the apparatus was cleaned with 70 % ethanol to remove any olfactory cues and marks left by the animals during testing.

String Suspension Task

The string suspension task allows to assess animals for motor coordination and grip strength (Arendash et al., 2001b; Hullmann, 2012). Similar to the balance beam, animals were placed on a string connecting two escape platforms of 9 x 15 cm. String and platforms were approximately 40 cm above the padded ground. The performance was rated according to the following system: 0 = unable to remain on string; 1 = mouse hangs on platform by paws only; 2 = as 2, but with attempts to climb up; 3 = mouse sits on the string and keeps balance; 4 = mouse is able to move laterally on the string; 5 = escape to one of the platforms (Jawhar et al., 2012; Moran et al., 1995). For analysis, the average ranking out of three independent trials (60 s each) per mouse was taken. Between the single trials, the apparatus was cleaned with 70 % ethanol to remove any olfactory cues and marks left by the animals during testing.

2.3.6 Behavioral Testing

Elevated Plus Maze

This paradigm based on the tendency of a mouse to avoid open spaces was originally described in Karl et al. (2003). The mice were introduced into an elevated, cross-shaped
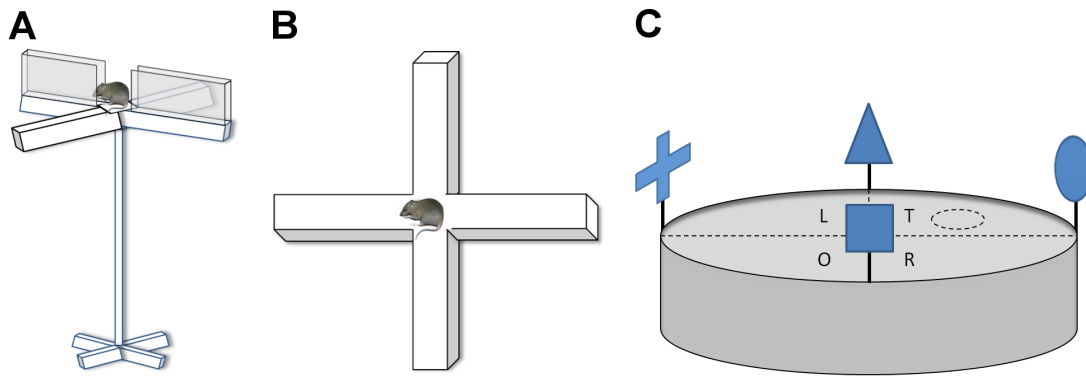
Figure 2.2
Behavioral testing paradigms. A Elevated plus maze **B** Cross Maze **C** Morris water maze. Reprinted with kind permission of Dr. Anika Saul, Göttingen

apparatus (length 15 cm x width 5 cm) with two enclosed arms opposing each other and two opposing wall-free arms (See Figure 2.2). The apparatus was elevated by 75 cm above ground level. Mice were allowed to freely explore the apparatus for 5 minutes. For analysis, the percentage of time spent in the open/closed arms was displayed. The total distance travelled and average speed in the mice were measured as control parameters to judge the locomotion abilities of the mice. Between the single trials, the apparatus was cleaned with 70 % ethanol to remove any olfactory cues and marks left by the animals during testing.

Cross Maze

The cross maze task was performed similar to the way described in Jawhar et al. (2012). In brief, the mice were subjected to a cross-shaped symmetrical maze with 4 arms (length 30 cm x width 8 cm x height 15 cm) (See Figure 2.2). To start the test, mice were placed in the center area of the apparatus and allowed to freely explore the setup for 10 minutes. Sequential visits of all four arms (e.g. arm 1, arm 3, arm 2, arm 4) were counted as correct alternations, with overlap of sequences being allowed (Arendash

et al., 2001b). The percentage of alternations was expressed in regard to the number of total possible alternations (n(arm antries)-3). Total distance travelled and average speed in the maze were measured as control parameters. This test is based on the natural tendency of mice to explore the least visited arm rather than a recently visited one (Wietrzych et al., 2005). Between the single trials, the apparatus was cleaned with 70 % ethanol to remove any olfactory cues and marks left by the animals during testing.

Morris Water Maze

The morris water maze paradigm (originally described in Morris (1984)) was performed as follows, similar to the way described in Bouter et al. (2013). The apparatus consisted of a round steel pool with a diameter of 120 cm filled with water (made opaque by adding non-toxic white paint) up to approximately 20 cm and virtually divided into four quadrants (see Figure 2.2). For acclimatization and testing of motoric/visual abilities, an animal was released at the border of the pool and trained over three days (cued training stage) to find a visible (cued) platform (15 cm in diameter) slightly reaching over the water level. A blue plastic cylinder (5 cm in diameter) with white vertical stripes served as the platform cue. Each training day consisted of four independent trials. Between trials, the platform position and release point were semi-randomly shifted between four different positions excluding the quadrant being the target quadrant in later stages (Vorhees and Williams, 2006). The duration of a single trial was 60 s. In case a mouse did not find the platform, it was gently directed to reach the platform and allowed to rest for five seconds. No external cues were used during the cued training stage. Having finished the cued training stage, water was filled up to a level of 0.5 cm above the platform, the platform cue was removed and proximal/distal cues placed at the pool borders in the middle of each virtual quadrant. Mice were then trained during a five-day period (acquisition training stage) with four trials a day to localize the hidden platform in the target quadrant. Again, mice were released from four different positions at the pool border, allowed to freely search for the platform for 60 s and given five seconds to rest on the platform. Mice that did not localize the platform within the given time were again gently directed towards the

platform and allowed to familiarize. At all stages, the animals were allowed to rest and dry between two trials for at least 15 min. After the acquisition training stage, the mice were subjected to a single probe test trial where the platform was removed and the mice were allowed to search freely for 30 s. Parameters taken into analysis were average swimming speed and time to reach the platform position (escape latency) for the cued and acquisition training stages. For the probe trial, swimming speed was measured as a control parameter and further, the percentage of time in the four quadrants as well as the average proximity to the memorized target platform position was calculated. Between the single trials, the apparatus was cleaned with 70 % ethanol to remove any olfactory cues and marks left by the animals during testing.

2.4 COMPUTATIONAL METHODS

2.4.1 *Quantification of Plaque Load*

Extracellular Aβ load was evaluated in sagittal brain sections of 4 μm for anterior motor cortex (stereotactic coordinates from the bregma: AP 3 – 2 mm, D 0.75 – 1.75 mm) and thalamus (AP -1 - 2 mm,D2.25–3.25 mm). Five to six sections per mouse and per antibody were analyzed by immunohistochemistry with diaminobenzidine as a chromogene and Thioflavin S fluorescent staining. Sections starting from the lateral cutting plane of approximately 0.36 mm from the bregma were assessed for plaque load quantification, and pairs of parallel sections were stained in three independent experiments for each animal and antibody/dye. Therefore, the sections for the three experimental turns using the same antibody/dye were 80 μm apart from each other. Images were taken at 100-fold magnification using an Olympus BX-51 microscope equipped with an Olympus DP-50 camera. Using ImageJ the images (Thioflavin S images were inverted) were binarized to 8-bit black and white images and a fixed intensity threshold was applied defining the stained area. For the subiculum, an ellipsoid area of constant size approaching the desired brain region was selected before quantification, and the outside of this ellipsoid was cleared. The single measurements (% area fraction) for each section were normalized to the average of the PBS injected control group, giving a

relative plaque load level expressed in percent for each individual experimental turn. For statistical analysis, the average of the three experimental turns was used.

2.4.2 *Software and Statistics*

For all behavioral testing, AnyMaze Software combined with a camera (Computar, Commack, NY, USA) for tracking was used. Statistical analysis was performed using GraphPad PRISM 6 (GraphPad Software, San Diego, CA, USA). Quantitative Real-Time PCR Data were collected and processed with the MxPro MX3000P Software (Stratagene, Santa Clara, USA). Images were processed with ImageJ V1.41, NIH, USA and/or Adobe Photoshop CS2 (Adobe Systems, San Jose, CA, USA). Figures were composed with Adobe Photoshop CS2 and/or Adobe Illustrator CS 2 (Adobe Systems, San Jose, CA, USA). The mass-spectrometric data was processed with the flexAnalysis software Version 3.0.54.0 (Bruker Daltonics, Bremen, Germany).

Statistical tests performed were students-two-tailed t-test, one-way-Analysis of Variance (ANOVA) and repeated-measures ANOVA for grouped analysis, followed by Dunnet´s or Tukey´s post-hoc tests for mutiple comparison. Data were expressed as mean $\pm$ SEM and a 0.5 % general significance niveau was defined, with significance levels as follows: *: $p < 0.05$; **: $p < 0.01$; ***: $p < 0.001$.

Part III

RESULTS

RESULTS

3.1 CHARACTERIZATION OF THE ANTIBODY NT4X-167

Peptide-binding Properties of NT4X under Native Conditions

Freshly dissolved Aβ peptides were probed on a nitrocellulose membrane under blue native conditions, where peptides migrate approximately proportional to their molecular weight. All peptide species tested, though freshly dissolved, formed higher molecular weight oligomers of different sizes immediately. NT4X-167 detected both $A\beta_{pE3-40/42}$ and $A\beta_{4-40/42}$. Interestingly, the latter migrated in a distinct band of approximately 50 kDa, though the other peptides probed were present in different distinct bands of approximately 20, 30 and 50 kDa for $A\beta_{pE3-40}$ and approximately 30, 50, 55 and > 70 kDa for $A\beta_{pE3-42}$. Probing with N-terminal specific antibody IC16 revealed bands at approximately 20 and 30 kDa for $A\beta_{1-40}$, approximately 20, 30, 55 kDa, as well as larger aggregates > 70 kDa for $A\beta_{1-42}$. Furthermore, stronger signals indicated that NT4X-167, though recognizing both $A\beta_{pE3-40/42}$ and $A\beta_{4-40/42}$, shows a preference for the latter. Probing of a duplicate membrane with antibody 24311 revealed that in fact $A\beta_{4-40/42}$ migrated in a distinct single band of 50 kDa and do not readily form oligomers of different molecular weight (Figure 3.1).
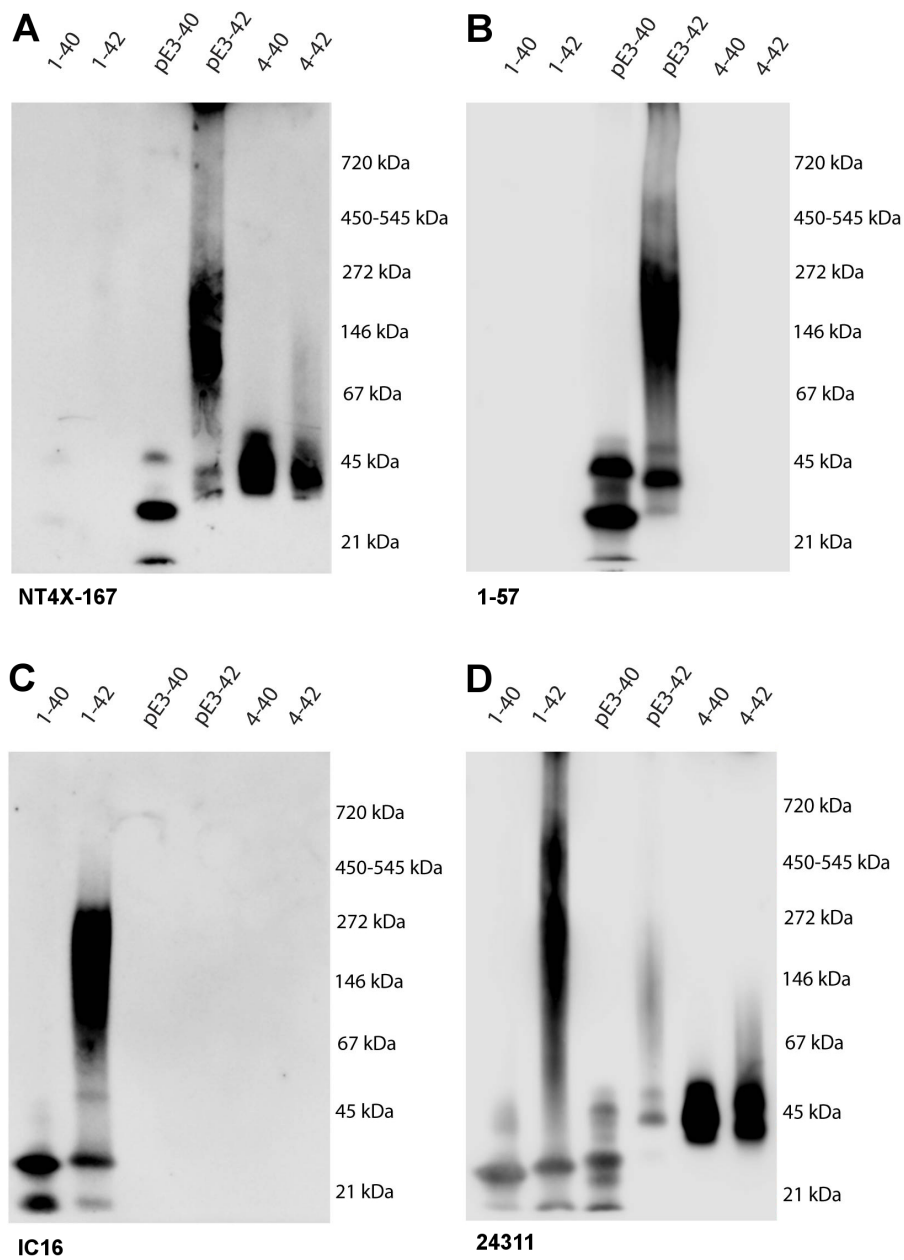
Figure 3.1

Blue Native Western Blot of synthetic Aβ Peptides. Freshly dissolved synthetic $A\beta_{1-40/42}$, $A\beta_{pE3-40/42}$ and $A\beta_{4-40/42}$ were probed onto a nitrcellulose membrane. **A** Antibody NT4X-167 recognized both $A\beta_{pE3-40/42}$ and $A\beta_{4-40/42}$, with the latter migrating in distinct bands at approximately 50 kDa. **B** Antibody 1-57 showed strong recognition of $A\beta_{pE3-40/42}$ exclusively. **C** Antibody IC16 recognized only $A\beta_{1-40/42}$ **D** The polyclonal antibody 24311 recognized all probed peptides, revealing that $A\beta_{4-40/42}$ indeed migrated as single distinct bands of approximately 50 kDa without any higher or lower molecular weight bands.

3.2.1 *Generation of Homozygous 5XFAD*

Confirmed transgenic 5XFAD^{hem} males and females were set up as breeding pairs to generate 5XFAD^{hom} animals. All animals of the resulting litters were screened for the transgenes by conventional APP genotyping and animals found positive were further analyzed by quantitative Real-Time PCR of genomic DNA as described. Homozygosity was then verified by backcrossing with wild-type C57B6/J (WT). Confirmed 5XFAD^{hom} individuals were then taken for further breeding. When breeding the 5XFAD^{hom} strain, female mice were well propagating up to the age of approximately 4.5 months, male animals up to the age of 8 months, with regular litter sizes between 5-8 pups. Female 5XFAD^{hom} mice had to be sacrificed due to ethical considerations at an age between 6-7 months and male 5XFAD^{hom} animals at the age of 9-10 months, because they displayed massive motor impairment and a generally poor condition at later stages.

3.2.2 *Transgene Expression in young 5XFAD*

Immunohistochemical analysis of young 5XFAD^{hem} and 5XFAD^{hom} revealed elevated human APP expression in subiculum and cortex already at the age of 16 days for the homo-zygous animals. This increased APP expression was persisting at the age of 6 weeks (Figure 3.2). In order to compare the Aβ-distribution in cortex between 6 weeks old 5XFAD^{hem} and 5XFAD^{hom} mice, sagittal brain paraffin sections were treated with the monoclonal antibody Aβ[N] (against N-terminal Aβ). In cortical layer V cells, abundant punctate intracellular immunoreactivity was found (Figure 3.3), which revealed a vesicular staining pattern at higher magnification (Figure 3.4).
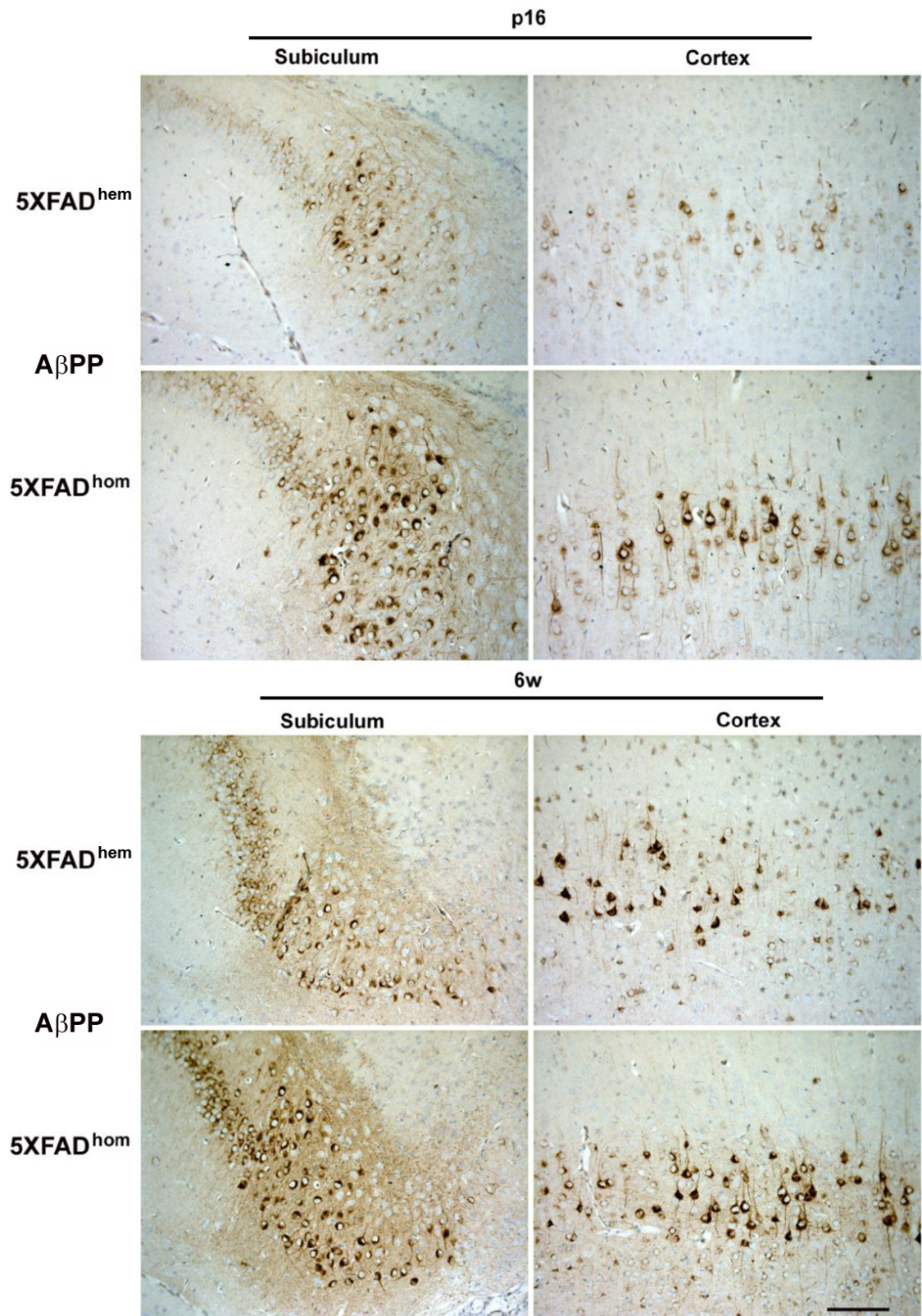
Figure 3.2
Early age APP-expression in 5XFAD mice. Both 5XFAD^{hem} and 5XFAD^{hom} mice displayed detecteable APP expression already at then age of 16 days (p16) in both subiculum and cortex, with a more abundant APP-positive signal in the 5XFAD^{hom}. This finding persisted at 6 weeks (6w) of age in both genotypes. Scalebar represents 50 µm for all images.
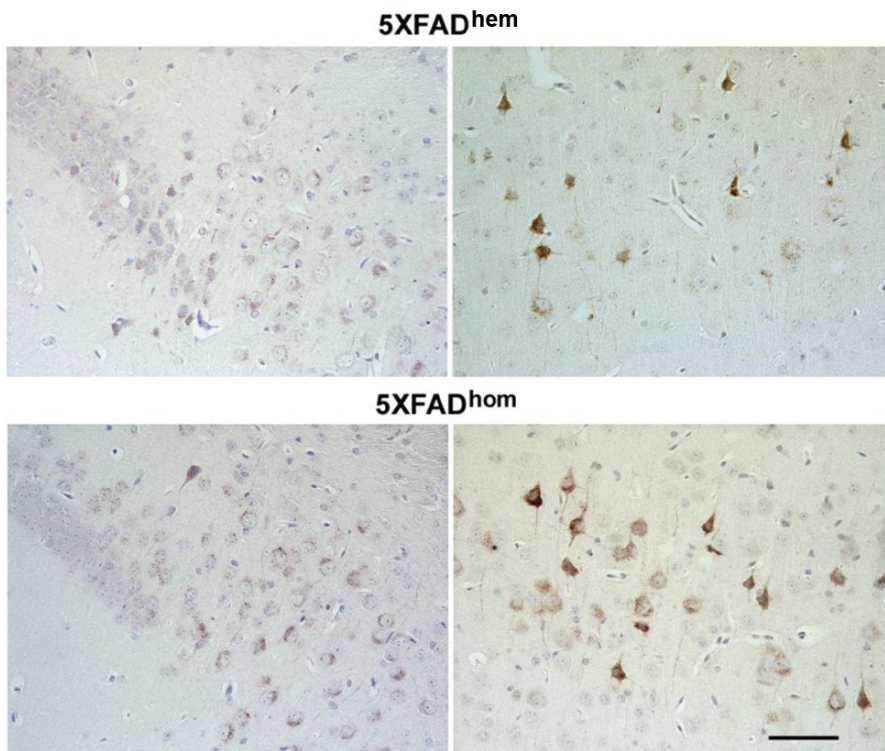
5XFAD^hem

5XFAD^hom

Figure 3.3
Early age intracellular Aβ accumulation in 5XFAD mice. In 6-week old 5XFAD, intracellular accumulation of Aβ was detected with the antibody Aβ[N] in the cortex (Right), with the 5XFAD^hom displaying a stronger Aβ immunoreactivity than 5XFAD^hem. In the subiculum (Left), at this age no intracellular Aβ was detected. Scalebar represents 50 μm for all images.
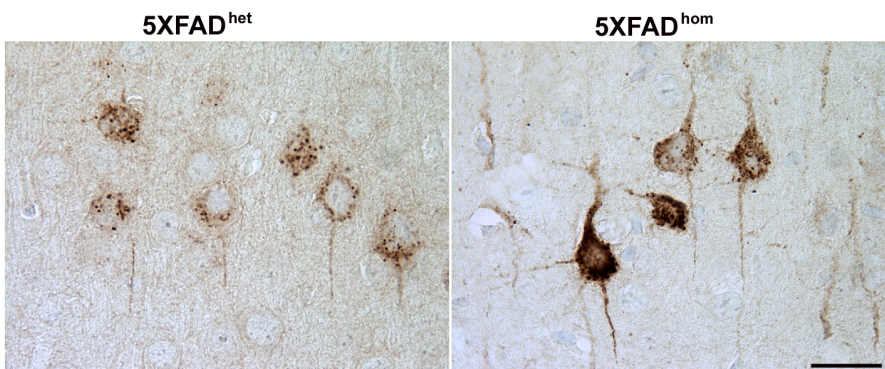

5XFAD^het   **5XFAD^hom**

Figure 3.4
High magnification revealed a vesicular pattern of intracellular Aβ accumulation in young 5XFAD mice. Scalebar represents 20 μm for both images.

To further verify the presence of N-terminally truncated Aβ and estimate relative abundance of minor peptide isoforms in the 5XFAD model, a pooled sample of three 7-month-old female 5XFAD^{hem} individuals was subjected to IP followed by MALDI-TOF. Besides Aβ$_{1-40/42}$, several C-terminally and N-terminally truncated Aβ isoforms were detected as described previously by Wittnam et al. (2012): Aβ$_{pE3-42}$, Aβ$_{4-42}$ and Aβ$_{5-42}$. Here, Aβ$_{1-43}$, Aβ$_{1-37}$, Aβ$_{1-38}$, Aβ$_{1-39}$ and Aβ$_{4-40}$ were detected in addition to the previously reported ones as shown in figure 3.2.3.
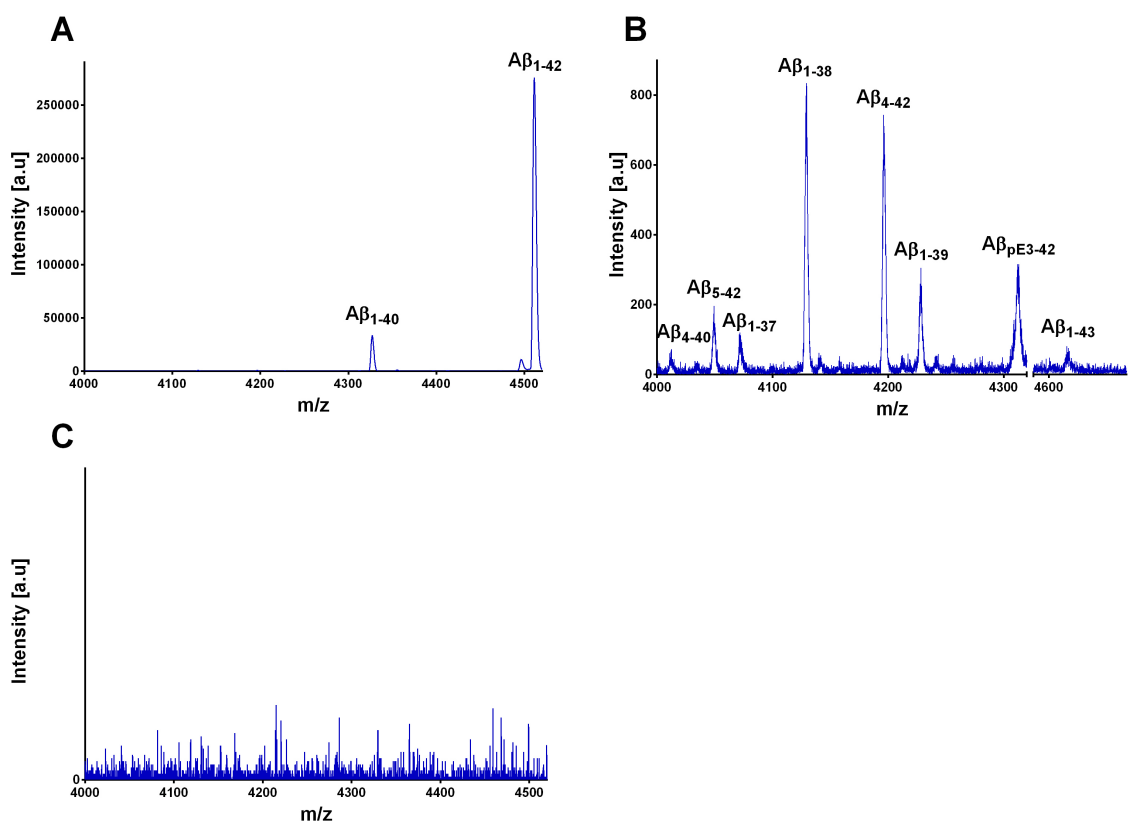

Figure 3.5
Aβ isoforms in 5XFAD brain.
  A Major species detected were Aβ$_{1-40/42}$. **B** (Zoomed view of A) Less abundant species detected in 5XFAD brains were Aβ$_{1-43}$, Aβ$_{1-37/38/39}$, Aβ$_{4-40/42}$, and Aβ$_{5-42}$. **C** No peaks corresponding to Aβ were detected in the WT control.

Table 3.1
Amyloid-beta Peptides detected between in 5XFAD brain by IP/MALDI-TOF

Peptide	Monoisotopic Weight	m/z	Intensity	Signal/ Noise
$A\beta_{4-40}$	4012.04	4012.42	72.00	6.14
$A\beta_{5-42}$	4049.09	4049.40	196.00	16.71
$A\beta_{1-37}$	4071.99	4071.63	120.00	10.23
$A\beta_{1-38}$	4129.01	4129.11	799.00	68.12
$A\beta_{4-42}$	4196.16	4196.16	744.00	63.43
$A\beta_{1-39}$	4228.08	4228.36	305.00	26.00
$A\beta_{pE3-42}$	4307.21	4312.09	298.00	25.41
$A\beta_{1-40}$	4327.15	4327.15	33683.00	2871.83
$A\beta_{1-42}$	4511.27	4511.27	275605.00	23498.24
$A\beta_{1-43}$	4612.32	4612.59	75.00	6.39

3.2.4 *Phenotypical Characterization of Homozygous 5XFAD*

The newly generated $5XFAD^{hom}$ strain was characterized regarding transgene expression pattern, Aβ expression, physical condition parameters and behavior phenotype in comparison to both age-matched WT and age-matched $5XFAD^{hem}$. The following numbers of animals were used for the motor testing and behavior analysis: WT: n = 10 (2 months), n = 7 (5 months); $5XFAD^{hem}$: n = 8-10 (2 months), n = 6-7 (5 months); $5XFAD^{hom}$: n = 8-9 (2 months), n = 5-7 (5 months).

3.2.5 *Physical Condition and Motor Abilities of Homozygous 5XFAD*

At the age of two months, both $5XFAD^{hem}$ and $5XFAD^{hom}$ had a significantly reduced body weight as compared to WT animals (both p < 0.001). At the age of 5 months, $5XFAD^{hom}$ again showed a significantly lower body weight as compared to both, WT and $5XFAD^{hem}$ animals (both p < 0.01). However, no weight differences were observed comparing $5XFAD^{hem}$ mice to WT animals (Figure 3.6).

As previously described (Jawhar et al., 2012), 5XFAD mice displayed a characteristic

so-called clasping phenotype, an unusual retraction of fore- and hindlimbs when the animal is suspended by the tail. Applying a clasping score scale ranging from 0-3 revealed that in both genotypes revealed that this symptom is already present at the age of 2 months, whereas WT mice showed no such motor impairment (both $p < 0.05$). The clasping phenotype revealed progressing moto-neuronal impairment at the age of 5 months with significantly higher scores in 5XFAD^{hem} mice ($p < 0.01$) compared to WT, and yet more aggravated impairment in 5XFAD^{hom} than in WT and 5XFAD^{hem} ($p < 0.001$ and $p < 0.05$ respectively; Figure 3.7).
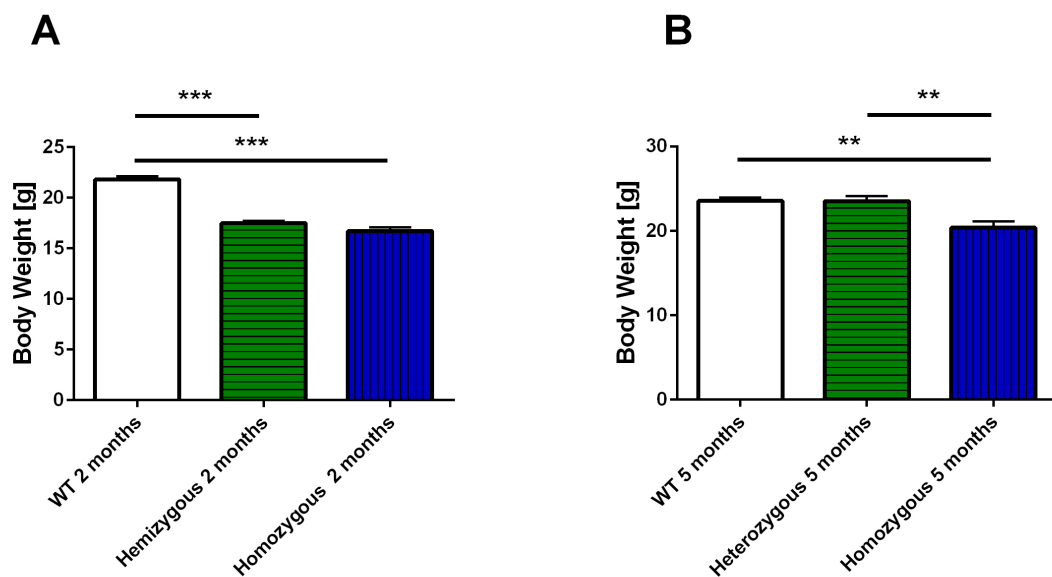
Figure 3.6
Body weight of 5XFAD mice at the age of 2 and 5 months. A At 2 months of age, both 5XFAD^{hem} and 5XFAD^{hom} displayed a significantly reduced body weight as compared to WT control animals. **B** At 5 months, only 5XFAD^{hom} animals showed a reduced body weight compared to both WT and 5XFAD^{hem} mice. (One-way ANOVA followed by Tukey´s post-hoc test; *: $p < 0.05$; **: $p < 0.01$; ***: $p < 0.001$)

To analyze the sensory-motor performance, mice were subjected to the balance beam and the string suspension task (Figures 3.8 and 3.9). In the balance beam task, 5XFAD^{hom} mice performed significantly poorer at the age of 5 months as compared to age-matched WT and 5XFAD^{hem} animals ($p < 0.001$ and $p < 0.05$). In the string suspension test 5XFAD^{hom} performed worse than WT ($p < 0.001$) and 5XFAD^{hem} ($p < 0.05$).
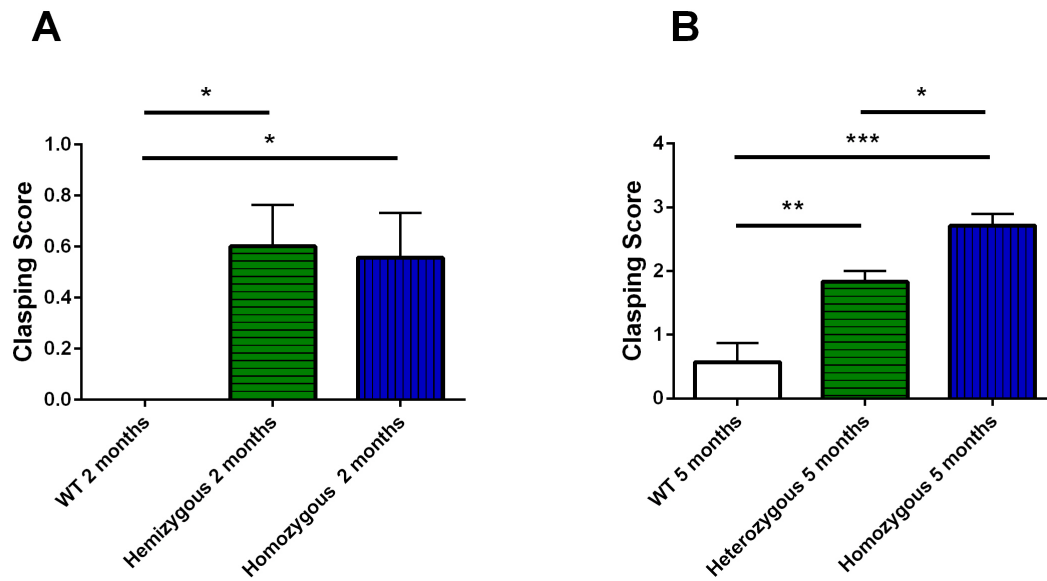
Figure 3.7
Clasping phenotype of 5XFAD mice. A Whereas no clasping phenotype was observed for 2 month old WT animals, both 5XFAD^{hem} and 5XFAD^{hom} showed a characteristic retraction of paws. **B** At 5 months of age, 5XFAD^{hem} showed a significantly aggravated clasping phenotype compared to WT controls that was even more pronounced in 5XFAD^{hom}, showing a significantly higher clasping score than both WT and 5XFAD^{hem} animals. (One-way ANOVA followed by Tukey´s post-hoc test; *: $p < 0.05$; **: $p < 0.01$; ***: $p < 0.001$)

3.2.6 *Anxiety in Homozygous 5XFAD*

Already at the age of two months, anxiety levels in 5XFAD^{hom} animals were significantly lower compared to the age-matched 5XFAD^{hem}, as indicated by an increased ratio of open versus total arm entries ($p < 0.05$). The average number of arm entries remained unaltered (Figure 3.10, page 67). At 5 months, both 5XFAD^{hem} ($p < 0.05$) and 5XFAD^{hom} ($p < 0.001$) displayed altered anxiety behavior compared to WT controls, with a more pronounced phenotype in the 5XFAD^{hom} group ($p < 0.05$ compared to 5XFAD^{hem}). The control parameter, i.e.the total number of arm entries was not significantly different between all three groups (Figure 3.11, page 68).
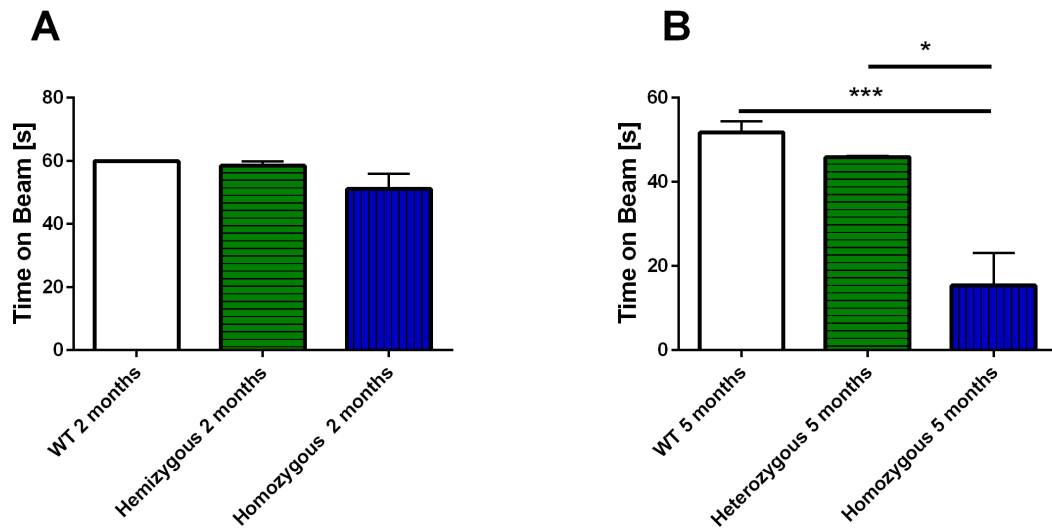
Figure 3.8
Sensory-motor performance of 5XFAD in the balance beam task. A No significant differences were observed between the 2-month old groups. **B** 5-month old 5XFAD^{hom} animals performed significantly worse than age-matched WT or 5XFAD^{hem} mice. (One-way ANOVA followed by Tukey´s post-hoc test; *: $p < 0.05$; **: $p < 0.01$; ***: $p < 0.001$)

3.2.7 *Working Memory Performance of Homozygous 5XFAD*

No differences between all tested groups were found for the alternation rate, total number of arm entries, average speed in the maze and distance travelled in the cross maze task, indicating that both 2 and 5 month old 5XFAD animals have no working memory impairment independent of the genotype (One-way ANOVA followed by Tukey´s post-hoc test; data not shown).
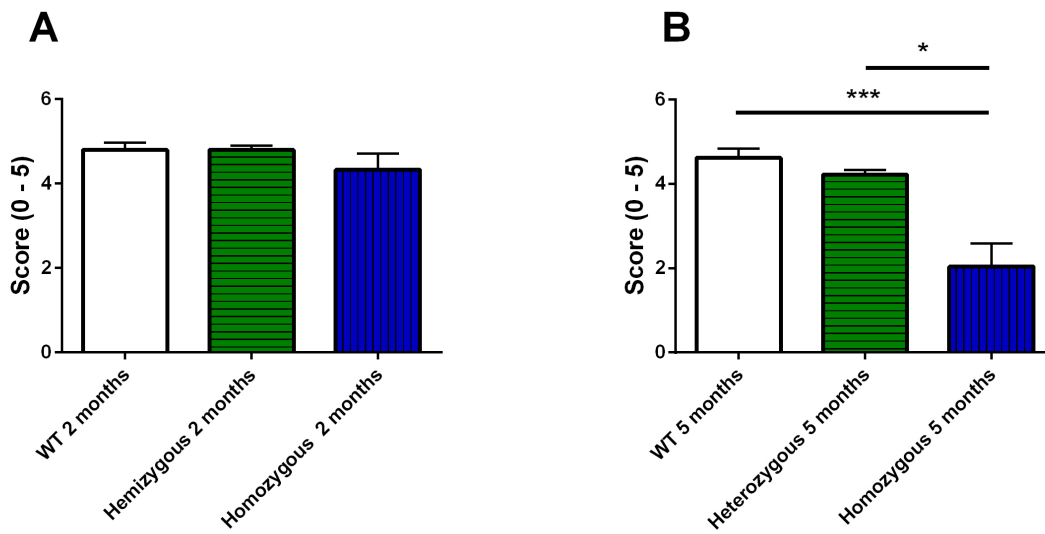
Figure 3.9
Sensory-motor performance of 5XFAD in the string suspension task. A No significant differences were observed between the 2-month old groups. **B** 5-month old 5XFAD^{hom} animals performed significantly worse than age-matched WT or 5XFAD^{hem} mice. (One-way ANOVA followed by Tukey´s post-hoc test; *: p < 0.05; **: p < 0.01; ***: p < 0.001)
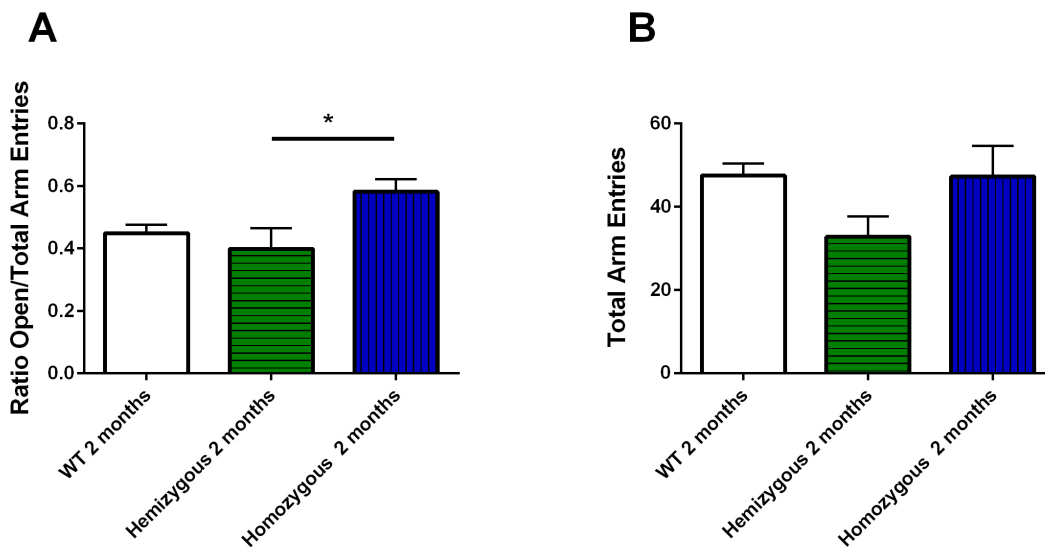

Figure 3.10
Anxiety levels in the 5XFAD model. A At 2 months of age, the 5XFAD^{hom} animals showed significantly reduced anxiety compared to the 5XFAD^{hom} group. **B** The number of total arm entries was not significantly different between the groups (One-way ANOVA followed by Tukey´s post hoc test, *: p < 0.05; **: p < 0.01; ***: p < 0.001)
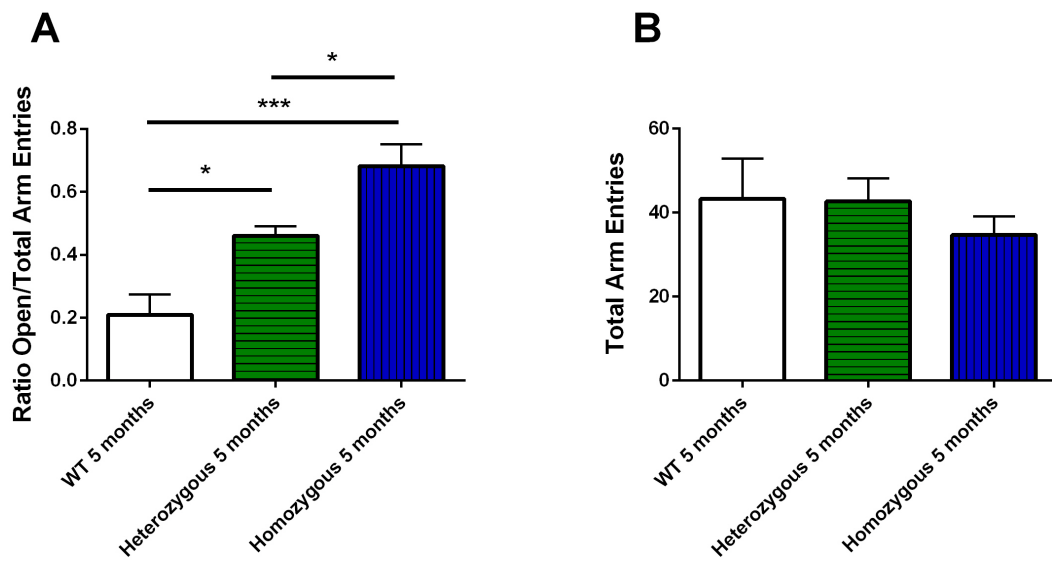
Figure 3.11
Anxiety levels in the 5XFAD model A At 5 months of age, the 5XFAD^{hem} animals showed significantly altered anxiety compared to the WT group. The 5XFAD^{hom} animals showed significantly reduced anxiety compared to the WT- as well as the 5XFAD^{hom} group. **B** The number of total arm entries were not different between the groups (One-way ANOVA followed by Tukey´s post hoc test, *: p < 0.05; **: p < 0.01; ***: p < 0.001)

3.2.8 *Spatial Reference Memory Impairment of Homozygous 5XFAD*

To assess the spatial reference memory performance, WT, 5XFAD^{hem} and 5XFAD^{hom} mice at 2 and 5 months were subjected to the morris water maze task. The initial cued training phase, serving as a control experiment to exclude that sensory or motor deficits bias the interpretation of the results, revealed that mice of all ages and genotypes showed progressively decreasing escape latencies. 5 month old 5XFAD^{hom} animals showed a significantly lower average swimming speed. However, no significant difference in swimming speed at day 3 of the cued training phase was observed. Therefore, all groups fulfilled the criteria for the task. In the following acquisition training phase, mice were forced to memorize an escape platform hidden below the water surface during five days of training. Already at the age of 2 months, a significant main genotype effect for the escape latency was evident (Repeated measures-ANOVA, F = 7.405, p =0.05) for 5XFAD^{hom}, whereas no significant differences between 2-month old WT and 5XFAD^{hem} mice were observed. However, significant differences over the training days 1-5 were not evident at the age of two months (Figure 3.12). Again, at the age of 5 months, there was a significant main effect for the genotype evident (Repeated measures-ANOVA, F = 25.05, p < 0.001), with 5XFAD^{hom} showing a significantly longer escape latency, although no differences in the swimming speed were detected among the groups (One-way ANOVA, both p < 0.001). Furthermore, the escape latency of 5XFAD^{hom} was significantly higher than that of WT animals at day 1 to day 5, and significantly different compared to the 5XFAD^{hem} group at days 2 and 3 of the acquisition training trial (Figure 3.13) On day 6 after start of the acquisition training, mice were given a 30 s probe trial in which they were allowed to freely search for the platform´s positon to assess spatial reference memory. Except for the group of the 5-month-old 5XFAD^{hom} group, all genotypes and ages showed a clear, significant preference for the target quadrant (Figure 3.14). The average proximity to the target platform position did not differ significantly for the groups of 2-month-old animals in the probe trial, whereas, in line with the loss of a target quadrant preference, the average proximity to the target position was significantly lower in the 5 month old 5XFAD^{hom} group (Figure 3.14).
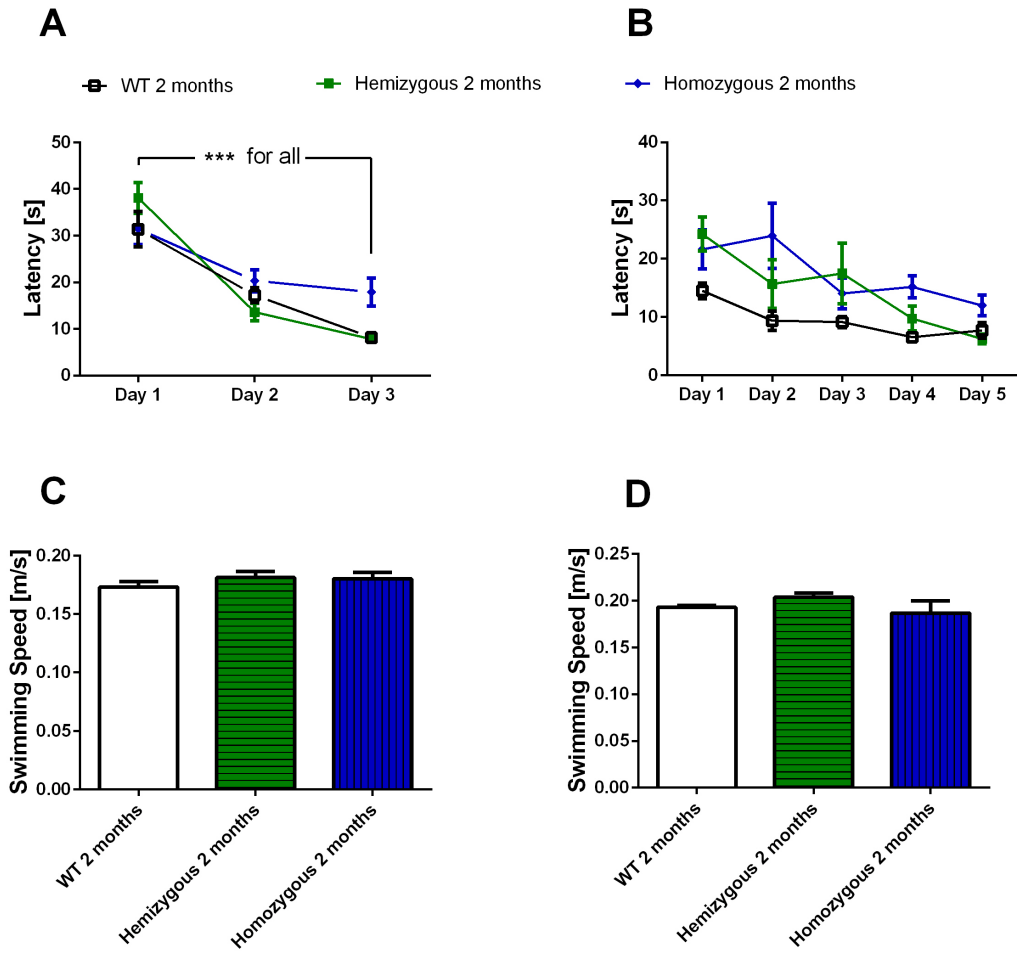
Figure 3.12

Spatial reference learning in 2-month-old 5XFAD mice. A In the cued training phase, all groups displayed significantly reduced escape latencies within a three-day timespan. **B** Similar to A, in the acquisition training stage, all groups showed significantly reduced escape latencies between day 1 and day 5 of the training. **C, D** In both cued training and acquisition training, no differences in the swimming speed were observed. (A, B: Two-way ANOVA followed by Dunnett´s post-hoc test for multiple comparison; C, D: One-way ANOVA followed by Dunnett´s post-hoc test for multiple comparison; *: $p < 0.05$; **: $p < 0.01$; ***: $p < 0.001$)
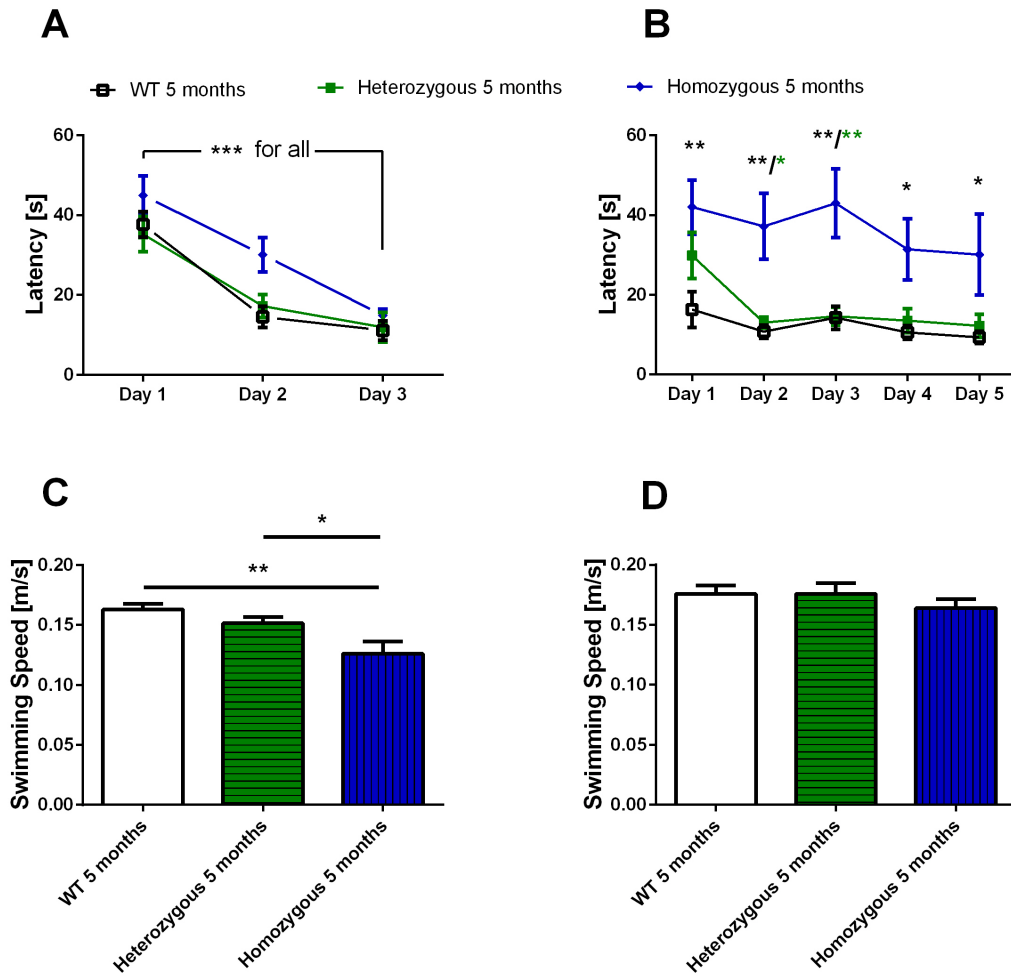
Figure 3.13

Spatial reference learning in 5-month-old 5XFAD mice. A In the cued training phase, all groups displayed significantly reduced escape latencies within a three-day time span. **B** During the entire duration of the acquisition training stage, the 5XFAD$^{\text{hom}}$ group showed a significantly poorer performance in escape latencies than WT and 5XFAD$^{\text{hem}}$ animals. **C** In the cued training stage, 5XFAD$^{\text{hom}}$ swam significantly slower than the WT and 5XFAD$^{\text{hem}}$ group, whereas **D** in the acquisition training, no differences for the swimming speed were observed. (A, B: Two-way ANOVA followed by Dunnett´s post-hoc test for multiple comparison; C, D: One-way ANOVA followed by Dunnett´s post-hoc test for multiple comparison; *: $p < 0.05$; **: $p < 0.01$; ***: $p < 0.001$)
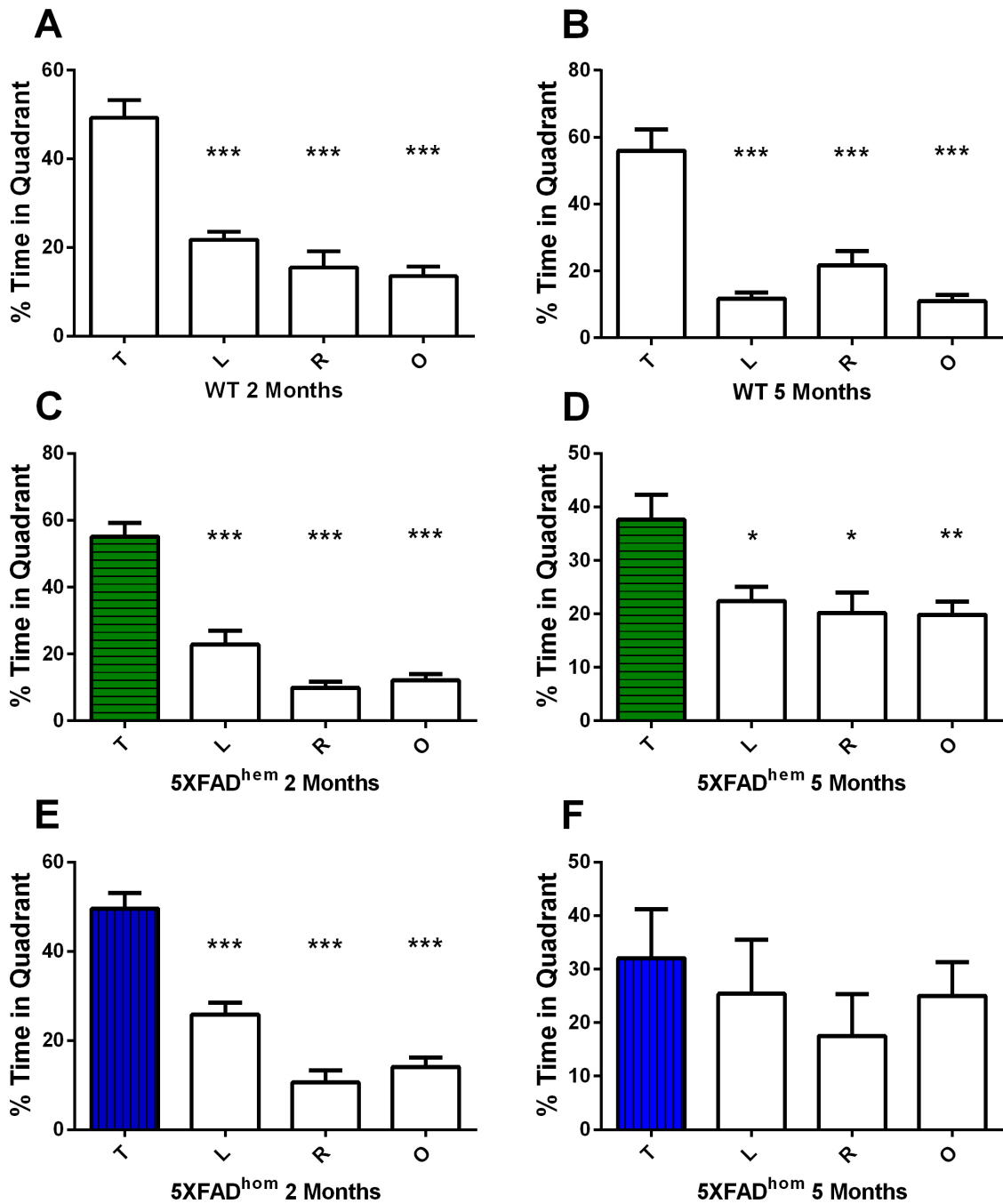
Figure 3.14

Spatial reference memory of 5XFAD mice. A At two months of age, all tested groups showed a significant preference for the target quadrant (T) over the left (L), right (R) and opposite (O) quadrant (**A, C, E**). **B, D** Of the 5 month old groups, the WT and the hemizygous 5XFAD animals showed a clear and significant preference for the target quadrant as well. **F** In the 5 month old homozygous animals, no significant preference was observed for the target quadrant. (One-way ANOVA followed by Dunnett´s post-hoc test for multiple comparison; *: $p < 0.05$; **: $p < 0.01$; ***: $p < 0.001$)

Female 5XFAD^{hem} were immunized for a duration of ten weeks with antibodies NT4X-167 (termed NT4X-167 group), 1-57 (termed 1-57 group) and 9D5 (termed 9D5 group) at a dosage of 10 mg/kg body weight. At the age of 7 months, mice were subjected to behavioral testing and then sacrificed for biochemical analysis. The elevated plus maze was performed first, followed by the cross maze task and then, after a one day pause, mice were trained in the morris water maze paradigm, receiving the last of ten injections approximately 6 hours prior to the the acquisition training trial. The experimental approach compared three antibody-treated groups with a PBS-injected control (termed PBS group). After the behavior testing, mice were sacrificed and further analyzed biochemically regarding plaque load and soluble/insoluble Aβ levels.

3.3.1 *Quantification of Amyloid Plaque Deposits after Passive Immunization*

The numbers of animals used for the passive immunization experiments were: (PBS-group: 7; NT4X-167-group: 9; 1-57-group: 7, 9D5-group: 8). To exclude that the administered antibody would bias the plaque load detection, blind stainings (primary antibody incubation was skipped) were performed for all animals. The so-treated slices were free of any immunoreactivity. Thus, plaque load measurement was not biased by pre-existing immunoreactivity due to chronic passive administration of antibodies.

General Aβ plaque load levels were assessed by fluorescent Thioflavin S staining of amyloid deposits. In the anterior motor cortex of mice immunized with the antibody NT4X-167 there was a significantly ($p < 0.05$) lower plaque load compared to the PBS-injected controls (PBS-group: 100.00 ± 14.10 %; NT4X-group: 61.20 ± 9.85 %). In the thalamus, no significant differences of thioflavin S positive deposits were observed between all groups. However, there was a trend towards a lower plaque burden for the
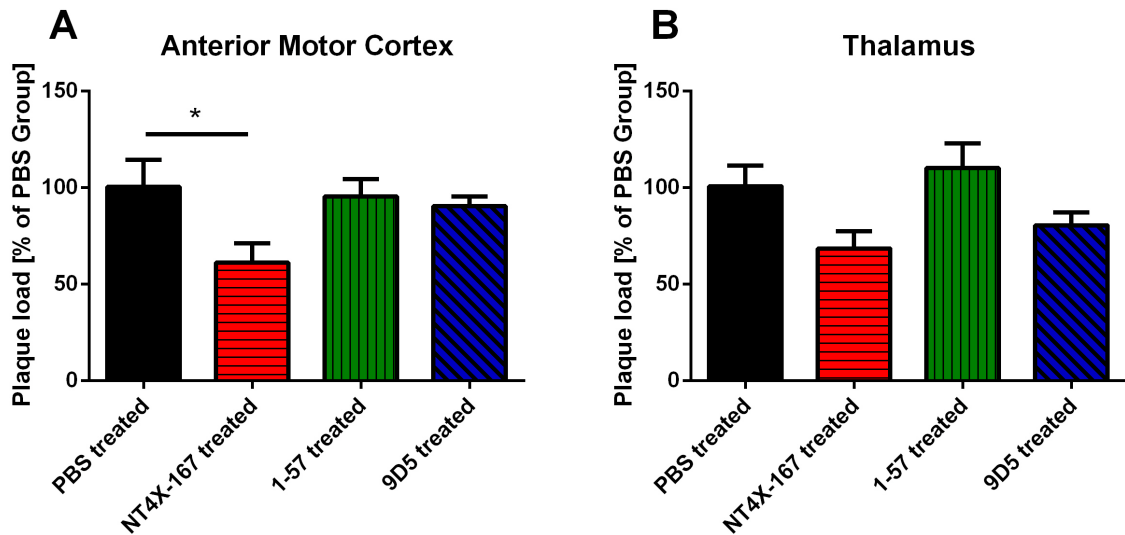
Figure 3.15
Quantitative analysis of Thioflavin S-positive plaques in passively immunized 5XFAD mice.
A The plaque burden in the anterior motor cortex was significantly lowered in the NT4X-167 group compared to the PBS group, whereas no significant differences to the PBS group were observed for the 1-57- and the 9D5 group **B** A trend, but no significant reduction in thioflavin S-positive plaques was observed for the NT4X-167 group and the 9D5 group in the thalamus. (One-way ANOVA followed by Dunnett´s post-hoc test for multiple comparison to the PBS group, *: $p < 0.05$; **: $p < 0.01$; ***: $p < 0.001$)

NT4X-167 group and the 9D5 group with approximately 30 % (NT4X-167 group) and 20 % (9D5 group) lower measures compared to the PBS group (Figure 3.15 page 74).

The amount of $A\beta_{pE3-x}$ was measured by immunohistochemistry using the antibody 1-57. In the NT4X-group, a significantly lower plaque burden (-43.41 %) was observed compared to the PBS group (PBS group: 98.47 ± 11.53 %; NT4X-167 group: 55.05 ± 7.09 %; $p < 0.01$). Similar as in the thioflavin S staining, lower plaque load (-34.10 %) was seen for the NT4X-167 group in the thalamus, but, however, this trend did not reach significance. Between all other groups, no significant differences were found for both brain regions (Figure 3.16, page 75).

The levels of amyloid deposits reacting with the antibody NT4X-167 were not significantly altered for any of the antibody treated groups compared to the PBS group in both anterior motor cortex and thalamus (Figure 3.17, page 76).
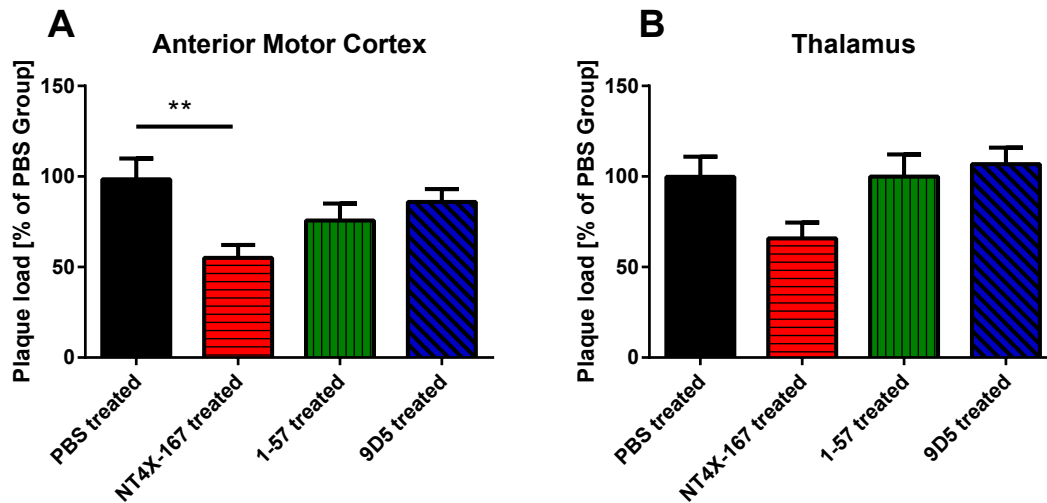
Figure 3.16
Quantitative analysis of $A\beta_{pE3-X}$-positive plaques in passively immunized 5XFAD mice.
A The levels of plaques reacting with antibody 1-57 were significantly lower in the NT4X-167 group compared to the PBS group in the anterior motor cortex, whereas the 1-57 group and the 9D5 group did show a plaque burden that was not significantly altered compared to the PBS group. **B** For the thalamus there was a slightly lower, but not significantly different, plaque load than in the PBS group found for the NT4X-167 group. Again, the 1-57 group and the 9D5 group were not different compared to PBS injected animals. (One-way ANOVA followed by Dunnett's post-hoc test for multiple comparison to the PBS group, *: $p < 0.05$; **: $p < 0.01$; ***: $p < 0.001$)

Plaque load level determination using the antibody G2-10 reacting with $A\beta_{X-40}$ revealed significantly lower plaque load for the NT4X-167 group compared to the PBS group in the anterior motor cortex (PBS group: 100.50 ± 11.05 %; NT4X-167 group: 67.19 ± 7.90 %; $p < 0.05$), whereas the G2-10 reactivity in the 1-57 group and the 9D5 group remained unaltered. As seen before for the thioflavin S- and $A\beta_{pE3-X}$ stainings, a slightly lower plaque load (-28.49 %) for the NT4X-167 group was also found in the thalamus, but this trend did not reach significance. Thus, no significant differences between the four groups were observed in the thalamus regarding $A\beta_{X-40}$ reactivity (Figure 3.18, page 77).

The plaque load levels for $A\beta_{1-X}$ as detected with the antibody 82E1 remained indifferent between all four groups in both anterior motor cortex and thalamus (Figure 3.19, page 78). The same holds true for $A\beta_{X-42}$ (detected with the polyclonal antibody Abeta42) as shown in figure 3.20, page 78.
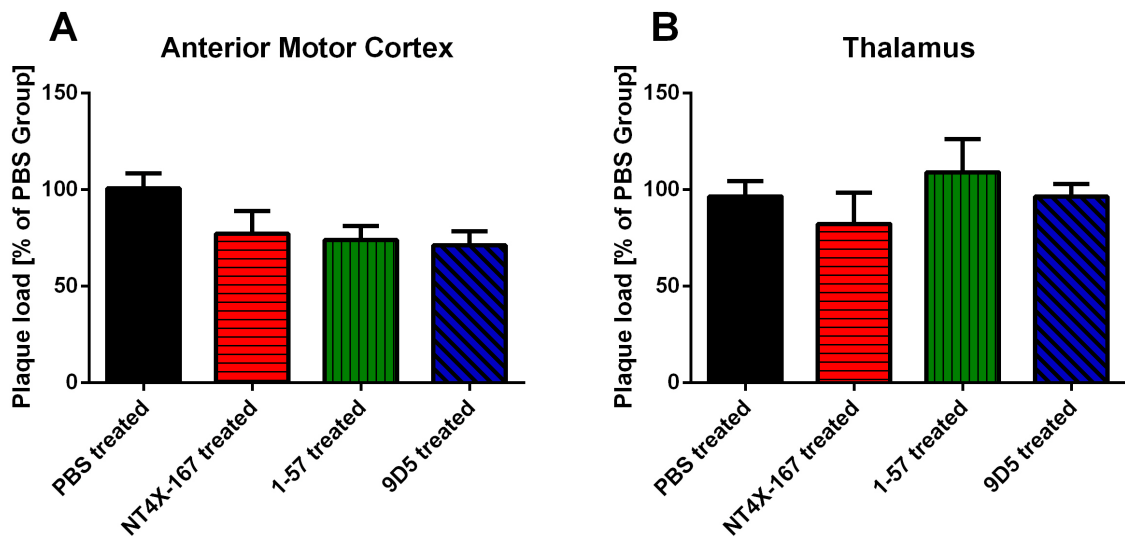
Figure 3.17
Quantitative analysis of $A\beta_{pE3-X}$- and $A\beta_{4-X}$-positive plaques in passively immunized 5XFAD mice. A The average levels of plaques reacting with NT4X-167 was not significantly altered for all three, the NT4X-167-, 1-57- and 9D5 group. **B** The same holds true for the thalamus. (One-way ANOVA followed by Dunnett´s post-hoc test for multiple comparison to the PBS group, *: $p < 0.05$; **: $p < 0.01$; ***: $p < 0.001$)

3.3.2 *Behavioral Phenotype of 5XFAD Mice after Passive Immunization*

Following the plaque load analysis, the same groups were analyzed regarding their behavioral phenotype in the cross maze and the elevated plus maze paradigm. Here, likewise handled, PBS-injected WT (n = 7) animals were taken as an additional control group.

Working Memory Performance of 5XFAD Mice after Passive Immunization

Compared to the PBS-injected WT animals, the PBS group showed significantly impaired working memory indicated by a reduced rate of correct alternations in the maze (WT: 32.36 ± 3.60 %; PBS group: 19.94 ± 1.82 %; $p < 0.05$). None of the treatment groups performed significantly different from the PBS group in this task as shown in figure 3.21, page 79. However, a significant t-test in comparison to the PBS group ($p < 0.05$) indicated a trend towards a rescue of the working memory performance in the NT4X-167 group. No such trend was, however, observed for the 1-57 group (t-test, $p > 0.1$), which displayed higher variability, and the 9D5 group (t-test, $p > 0.1$), which performed
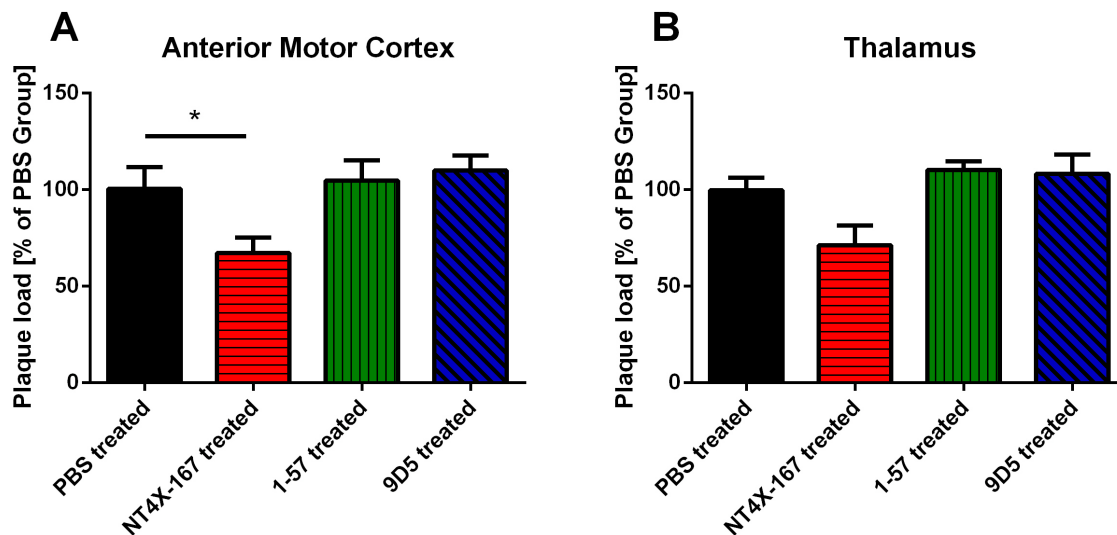
Figure 3.18
Quantitative analysis of $A\beta_{X-40}$-positive plaques in passively immunized 5XFAD mice. A
In the anterior motor cortex, the levels of plaques reacting with the antibody G2-10 was significantly lower in the NT4X-167 group compared to the PBS group, whereas the average amyloid burden of the 1-57 group and the 9D5 group was not different from the plaque load levels observed in PBS-injected animals. **B** In the thalamus, none of the antibody injected groups was significantly different from the PBS controls, though a trend towards lowered plaque load was observed in the NT4X-167 group. (One-way ANOVA followed by Dunnett´s post-hoc test for multiple comparison to the PBS group, *: $p < 0.05$; **: $p < 0.01$; ***: $p < 0.001$)

almost indentical to the PBS group. The control parameters, i.e. average distance travelled and average speed in the maze, were not significantly different for any of the treatment groups compared to the PBS injected animals (data not shown).

Anxiety Phenotype of 5XFAD Mice after Passive Immunization

In the elevated plus maze, importantly, the PBS-group was found to perform almost as described previously in Jawhar et al. (2012), displaying significantly different percentage of time spent in the open arms than the PBS-injected WT control group ($p < 0.05$) (Figure 3.21 B, page 79). No significant alteration in anxiety behavior has been observed for the antibody-treated groups. The ratio of open arm and total arm entries as well as the average speed and distance travelled were not significantly different comparing the treatment groups to the PBS injected 5XFAD controls (data not shown).
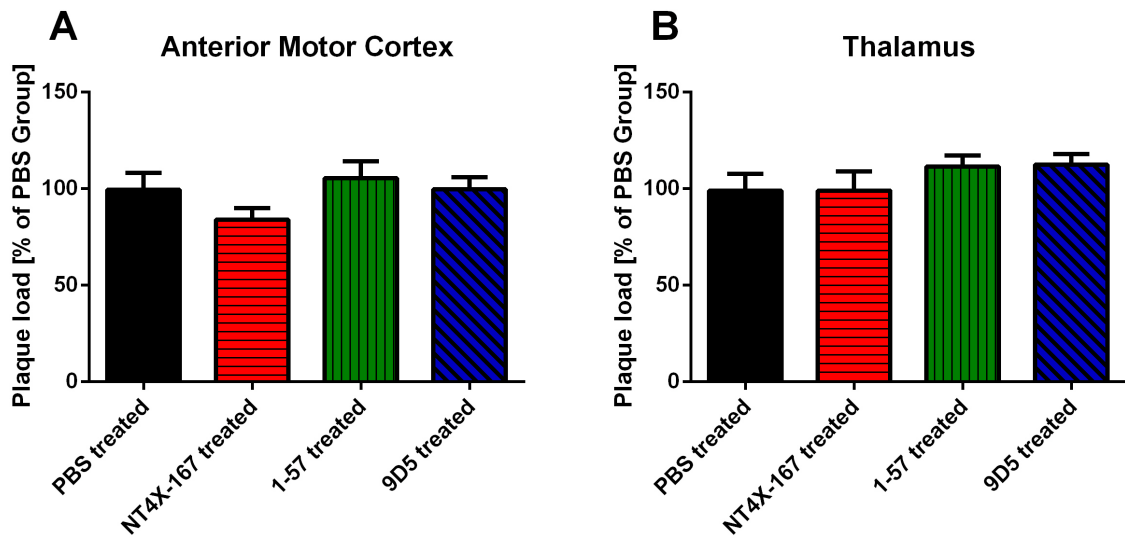
Figure 3.19
Quantitative analysis of $A\beta_{1-X}$-positive plaques in passively immunized 5XFAD mice. A The levels of plaques reacting with antibody 82E1 were not significantly different between all groups compared to the PBS group in the anterior motor cortex. **B** The same holds true for the thalamus. (One-way ANOVA followed by Dunnett´s post-hoc test for multiple comparison to the PBS group, *: $p < 0.05$; **: $p < 0.01$; ***: $p < 0.001$)
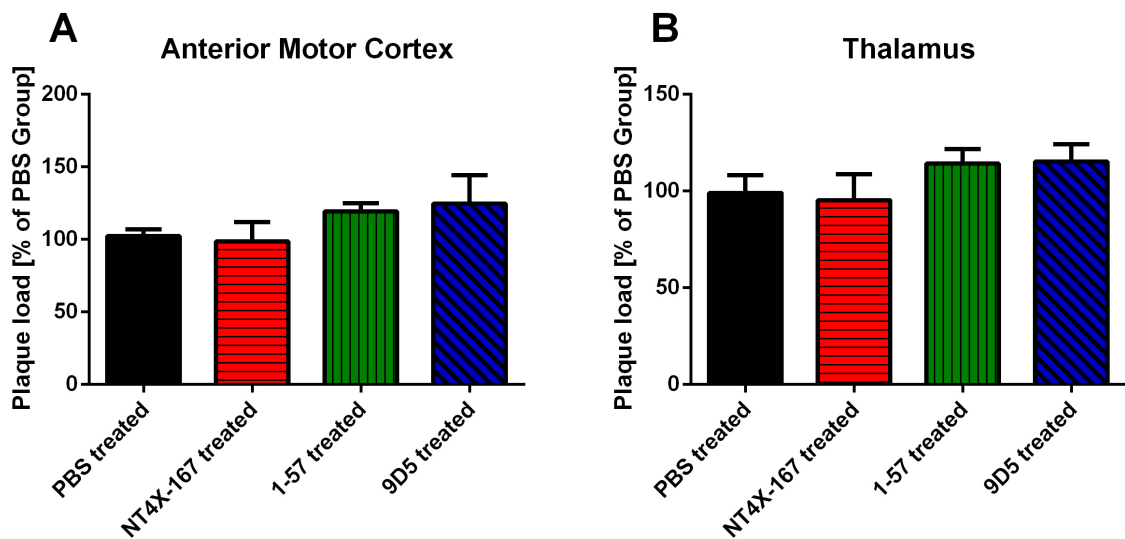
Figure 3.20
Quantitative analysis of $A\beta_{42}$-positive plaques in passively immunized 5XFAD mice. None of the antibody-injected groups showed significantly altered levels of antibody Abeta42-positive amyloid plaques in the anterior motor cortex and **B** the thalamus. (One-way ANOVA followed by Dunnett´s post-hoc test for multiple comparison to the PBS group, *: $p < 0.05$; **: $p < 0.01$; ***: $p < 0.001$)
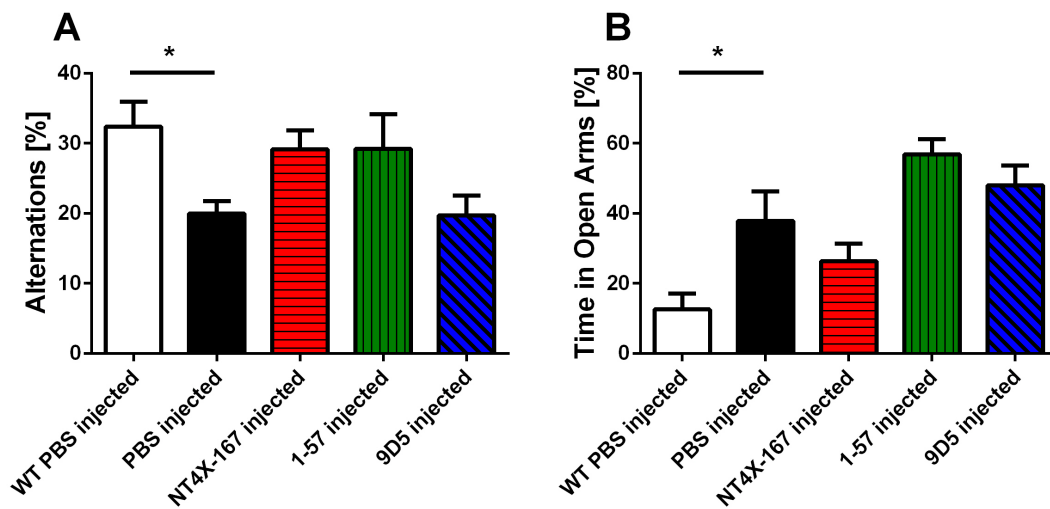
Figure 3.21
Working memory performance and anxiety behavior of passively immunized 5XFAD mice.
A The PBS group showed significantly impared working memory in the cross maze paradigm in comparison to the PBS-injected WT control animals. The performance of the antibody-treated groups was not significantly different from the PBS-injected 5XFAD group, however, a positive trend was observed for the NT4X-167 injected mice. **B** Compared to PBS-injected WT controls, PBS-injected 5XFAD showed a reduced anxiety phenotype as shown by the significantly increased time exploring the open arms of the paradigm, whereas none of the antibody-treated groups was significantly different from the PBS-injected 5XFAD controls. (One-way ANOVA followed by Dunnett´s post-hoc test for multiple comparison to the PBS group, *: $p < 0.05$; **: $p < 0.01$; ***: $p < 0.001$)

Part IV

DISCUSSION

4

DISCUSSION

4.1 CHARACTERIZATION OF THE ANTIBODY NT4X-167

To investigate distinct Aβ species, specific antibodies are a valuable research tool. The monoclonal antibody NT4X-167 (IgG2b; official name of the cell line $Aβ_{4−40}$ NT4X-167; DSM ACC3162) was raised against unconjugated $Aβ_{4−40}$ by immunization of Balb/c mice and antibody-producing cells were fused with the myeloma cell line P3-X63-Ag8 to generate hybridoma cells. The antibody was generated to specifically recognize an N-terminal epitope of oligomeric $Aβ_{4−40}$ and was selected to bind to amino acids 4-10 of the Aβ sequence and with $Aβ_{4−40}$ but not with amino acids 36-40. It was shown subsequently, that the phenylalanine at position four is essential for target engagement by NT4X-167. NT4X-167 is the first antibody reacting with $Aβ_{4−X}$ (Antonios et al., 2013).

Toxic Aβ oligomers have increasingly gained attention during the past years. $Aβ_{pE3−42}$ and $Aβ_{4−42}$ have been shown to rapidly form stable oligomers whereas $Aβ_{1−42}$ rather stays in equilibrium with the monomeric state (Bouter et al., 2013). It has been proposed that the N-terminal truncation of Aβ triggers a disequilibrium of monomers and oligomers leading to increased levels of oligomers, which in turn trigger neuropathologic alterations (Bayer and Wirths, 2014). Varying terminal end lenghts have been reported to alter the aggregation properties of Aβ (Bouter et al., 2013; Jan et al., 2008; Jarrett et al., 1993; Pike et al., 1995b). Thus, combinatory effects of varying terminal ends might determinine the stability and solubility of Aβ oligomeric assemblies.

In fact, this $A\beta_{4-X}$ aggregation pattern observed in Western Blot under blue native conditions was clearly different from that observed for $A\beta_{1-40/42}$ and $A\beta_{pE3-40/42}$. These experiments revealed that NT4X-167 recognizes $A\beta_{pE3-40/42}$ and $A\beta_{4-40/42}$, of which the latter migrated as a single band at approximately 50 kDa (see 3.1, 57). In a different approach, Bouter et al. (2013) reported a high propensity of $A\beta_{4-42}$ to form stable oligomers as well. In contrast, pyroglutamate $A\beta_{pE3-40/42}$ ran as oligomers of different sizes including higher molecular weight oligomers formed by $A\beta_{pE3-42}$ and $A\beta_{1-42}$.

In addition, varying N-terminal length seemed to account somehow for different SDS-resistance of $A\beta_{4-X}$: In Western Blot under reducing conditions we found that $A\beta_{pE3-40}$ and $A\beta_{4-40}$ migrated as monomers and dimers, whereas $A\beta_{pE3-42}$ and $A\beta_{4-42}$ produced trimers and tetramers in addition (Antonios et al., 2013), as it was shown previously (Masters et al., 1985; Wirths et al., 2010c). Solubility/aggregation propensity of N-terminally intact $A\beta$ has previously been reported to depend on the carboxy-terminal of the peptide (Jan et al., 2008; Jarrett et al., 1993). Here, unlike the pattern observed under reducing conditions, $A\beta_{4-42}$ showed aggregation to oligomers of identical size as $A\beta_{4-40}$ under native consitions. In contrast, for $A\beta_{pE3-42}$ and $A\beta_{1-42}$ formation of higher molecular weight oligomers was observed in this approach.

In human AD tissue, NT4X-167 revealed an interesting affinity pattern, staining CAA preferentially but barely reacting with extracellular plaques (Antonios et al., 2013). Similarly, this has been described previously for the anti-$A\beta_{pE3-X}$ conformation-specific antibody 9D5 that reacts with lower molecular weight oligomers exclusively (Wirths et al., 2010c). In murine tissue, NT4X-167 reacted with both intracellular $A\beta$ aggregates and extracellular amyloid deposits (Antonios et al., 2013).

We have further shown that $A\beta_{4-42}$ is cytotoxic and that NT4X-167 rescued $A\beta_{4-42}$- but not $A\beta_{pE3-42}$- and $A\beta_{1-42}$-induced cytotoxity (Antonios et al., 2013) in a cell culture model. This further underlines the importance of toxic oligomers composed of $A\beta$ starting at residue 4.

These experimental findings point to the conclusion that the newly developed monoclonal antibody NT4X-167 is selective for N-truncated Aβ, with a preference for Aβ_{4-X}, and could have potential to investigate its role *in vivo*. Moreover, Western Blotting of synthetic peptides revealed that under native conditions, A$\beta_{4-40/42}$ display an oligomer aggregation pattern that is different from Aβ_{1-40}/ Aβ_{1-42} and A$\beta_{pE3-40/42}$, which further supports structural differences of Aβ_{4-X} asseblies as previously reported in Bouter et al. (2013). The migrating pattern under native conditions indicated that Aβ_{4-X} is more prone to form stable oligomeric assemblies. It has been demonstrated for Aβ_{1-40} and Aβ_{1-42} that presence of the previous interferes with aggregation of the latter (Jan et al., 2008). Interaction of N-truncated Aβ_{pE3-42} with Aβ_{1-42} has been shown to alter conformation and increase toxicity of hetero-oligomers (Nussbaum et al., 2012), and the existence of a distinct oligomeric species of Aβ_{pE3-X}, possibly of particular interest for AD diagnosis and therapy, has been demonstrated by Wirths et al. (2010c). The observation that NT4X-167 barely reacts with densely aggregated plaques in AD Antonios et al. (2013) indicates that, probably due to a similar effect of Aβ_{4-X}, NT4X-167 prefers a more soluble oligomeric conformation of Aβ aggregates. However, if and how Aβ_{4-X} isoforms display similar effects is yet unknown.

NT4X-167 is the first monoclonal antibody reacting with Aβ_{4-X} and therefore represents a valuable tool to investigate the mechanism and consequences of an altered equilibrium between soluble and insoluble Aβ induced by N-terminal truncation of Aβ. It has been shown that *in vitro* NT4X-167 rescues Aβ_{4-42} induced cytotocity (Antonios et al., 2013). In summary, this raises the interest in NT4X-167 as an experimental and possible therapeutic tool.

4.2.1 *Generation of the Mouse Line*

The 5XFAD model is a transgenic mouse line overexpressing human APP and human PS-1 with a total number of five familial AD mutations that are inherited together. This leads to massive and rapid accumulation of amyloid plaques and elevated $A\beta_{X-42}$ levels in the brain. 5XFAD was described previously as one of few models displaying a combination of several major hallmarks of human AD including neuron loss (Eimer and Vassar, 2013; Jawhar et al., 2012; Oakley et al., 2006). Neuronal loss is a feature that has not been reported for some other commonly used APP transgenic models such as the PDAPP (Games et al., 1995), Tg2576 (Hsiao et al., 1996) and the APP/PS1ΔE9 models (Borchelt et al., 1997). The 5XFAD model displays accumulation of intracellular Aβ prior to plaque formation as early as at 6-8 weeks of age in the subiculum and furthermore in cortical layer V, a region where abundant neuron loss is observed at later stages (Jawhar et al., 2012; Oakley et al., 2006). This feature of early intracellular Aβ accumulation has, among others, been described for several AD models including $APP_{SDL}/PS1_{M146L}$ (Wirths et al., 2001), $APP_{SL}/PS1_{M146L}$ (Wirths et al., 2002), Tg2576 (Takahashi et al., 2002), 3xTg (Oddo et al., 2003) or APP/PS1KI (Casas et al., 2004).

The focus of the present study lay on N-terminally truncated Aβ: It was described previously that besides full length Aβ, minor species such as $A\beta_{pE3-X}$ (Frost et al., 2013; Wittnam et al., 2012), $A\beta_{4-X}$ and $A\beta_{5-42}$ (Wittnam et al., 2012) are present in the 5XFAD model . $A\beta_{pE3-X}$ species have also been shown to be present in brains of murine models, canines, non-human primates as well as in human AD brain samples (Frost et al., 2013; Mori et al., 1992). It was further shown that $A\beta_{pE3-X}$ represents a major fraction in human AD brain (Portelius et al., 2010; Saido et al., 1995). N-terminally truncated $A\beta_{pE3-X}$ has gained much attraction since then and it was further described that increased levels of $A\beta_{pE3-X}$ aggravate the behavioral phenotype whereas a knock-out of glutaminyl cyclase, the enzyme responsible for pyroglutamate formation, rescues behavioral deficits (Jawhar et al., 2011; Wittnam et al., 2012).

However, although it was described as early as in 1985 (Masters et al., 1985), and it was shown to be relatively abundant in brains of AD and vascular dementia patients (Lewis et al., 2006), Aβ starting at position four did not received likewise attention. As well, not much is known about Aβ starting at position 5. It has been shown to be deposited in human AD brain and to be produced due to caspase activity (Murayama et al., 2007; Takeda et al., 2004). More recently, a new, $A\beta_{4-42}$-expressing model (Tg4-42) displaying abundant neuron loss and behavioral deficits amyloid deposition was created (Bouter et al., 2013). In contrast to prominent intracellular Aβ-immunoreactivity, no extracellular amyloid deposition was described for Tg4-42 mice (Bouter et al., 2013).

Besides these N-terminally ragged Aβ peptides, several C-terminally truncated species such as $A\beta_{X-38}$ have been also described in mouse models, familial and sporadic AD cases (Karran et al., 2011; Moro et al., 2012). It was shown that $A\beta_{pE3-X}$ correlates better with cognitive decline in human AD than does plaque deposition (Holtzman et al., 2011). In contrast to the findings in AD, N-truncated Aβ represents a minor fraction in 5XFAD (Wittnam et al., 2012). This raised the question if and to what extent 5XFAD represents a suitable model to investigate the pathophysiologic effects of N-truncated Aβ variants. In fact, some APP overexpressing models have not been reported to show neuron loss (e.g. PDAPP, APP/PS1ΔE9, Tg2576; table 4.1, page 95), which is a feature of AD (Blennow et al., 2006). Together with this, the remarkably different Aβ stoichiometry observed somehow questions the validity of commonly used models.

To address this issue, a homozygous 5XFAD line was created to increase the transgene expression and elevate the Aβ levels in the animals brains. Breeding transgenic mouse models of AD to homozygosity is a common procedure to aggravate the extent of the phenotype and accelerate its progression and has been performed previously for models such as PDAPP (German et al., 2003), ARTE10 (Willuweit et al., 2009) and Tg4-42 (Bouter et al., 2013). The consequences of homozygosity and related findings will be discussed in the following subsections.

4.2.2 *Transgene Expression in young 5XFAD*

Immunohistochemistry on parrafin sections of young $5XFAD^{hem}$ and $5XFAD^{hom}$ mice revealed that both APP expression (at postnatal day 16 and persisting at the age of six weeks) and $A\beta$ production (in six weeks old mice) is elevated in the $5XFAD^{hom}$ animals compared to $5XFAD^{hem}$ mice (Figures 3.2, page 60 3.3, page 61 3.4, page 61). To determine the effects of the elevated transgene expression, the $5XFAD^{hom}$ strain was thoroughly characterized at later ages subsequently.

4.2.3 *Prevalence of N-truncated Amyloid-beta in young 5XFAD*

Based on the observation that indeed the levels of $A\beta$ are elevated in $5XFAD^{hom}$ mice, we performed immunohistochemstry on brain sections of six weeks old $5XFAD^{hom}$ animals to investigate whether $A\beta_{pE3-X}$, $A\beta_{4-X}$ and $A\beta_{5-X}$ can be detected at this early time point. Employing the newly developed antibody NT4X-167 recognizing both $A\beta_{pE3-X}$ and $A\beta_{4-X}$ in combination with the antibody 1-57 specifically reacting with $A\beta_{pE3-X}$, we could show abundant intracelluar NT4X-167 reactivity in the $5XFAD^{hom}$ animals in contrast to no detecteable $A\beta_{pE3-X}$-immunoreactivity. This immunohisto-chemical pattern was not found in $5XFAD^{hem}$ animals of the same age, indicating that an high transgene expression levels are crucial for detection of underrepresented $A\beta$ species in young 5XFAD. Immunohistochemistry did not reveal any extracellular $A\beta_{pE3-X}$ in 6 weeks old 5XFAD. This observation led to the conclusion that in the 5XFAD model, $A\beta_{4-X}$ precedes $A\beta_{pE3-X}$ (Antonios et al., 2013). Later Appearance of $A\beta_{pE3-X}$ in this model is further supported by Frost et al. (2013), who found no $A\beta_{pE3-X}$ immunoreactivity in 2.5-month-old 5XFAD. Importantly, $A\beta_{4-X}$ was detected together together with $A\beta_{1-X}$ in the neurons of cortical layer V that are prone to degenerate in 5XFAD mice at the age of 12 months (Jawhar et al., 2012; Oakley et al., 2006). Such transient intraneuronal $A\beta$ correlated with subsequent neuron loss has also been reported for several other APP/$A\beta$ models (Alexandru et al., 2011; Bouter et al., 2013; Casas et al., 2004; Christensen et al., 2008, 2010a; Wirths et al., 2009).

Several reports found intracellular accumulation of Aβ in AD, too (D'Andrea et al., 2001, 2002; Fernandez-Vizarra et al., 2004; Mochizuki et al., 2000). It has been shown that this intracellular accumulation takes place in AD-vulnerable regions (Gouras et al., 2000).

Similarly, we performed stainings for $A\beta_{5-X}$ employing the polyclonal antibody AB5-3 to elucidate whether this N-truncated variant is also present at this time point. In contrast to $A\beta_{4-X}$, $A\beta_{5-X}$ does not appear to be abundantly produced in six weeks old 5XFAD^{hom} mice, since no intracellular aggregates or extracellular amyloid plaques were detected with AB5-3 at six weeks of age (Guzman et al., 2014). The feature of intracellular Aβ accumulation preceeding plaque deposition in this model is well in line with the findings in AD. Assuming that intracellular Aβ accumulation represents a pathologic key event, the finding of early intraneuronal $A\beta_{4-X}$ suggests that this isoform might contribute to neurodegenerative processes, which is in line with observations in the newly generated Tg4-42 model (Bouter et al., 2013).

4.2.4 *Amyloid-beta in 7-month-old 5XFAD*

In order to assess whether minor ragged Aβ variants are also present in older 5XFAD and to further validate the findings from immunohistochemistry, I performed a combined IP/MALDI-TOF approach on brain tissue homogenates from 7-month-old 5XFAD. Using a mixture of the antibodies 4G8 and 6E10 coupled to paramagnetic Dynabeads, Aβ was precipiated from neutralized formic acid extracts of the brain homogenate. The MALDI-TOF detection enabled for identification of peaks corresponding to a total number of ten Aβ peptides. Among these, as described earlier, $A\beta_{1-40}$ and $A\beta_{1-42}$ were detected with the highest intensity peaks (Wittnam et al., 2012), with the latter signal being approximately 10-fold more intense than the peak for $A\beta_{1-40}$. As described in Wittnam et al. (2012) for six month old mice, the less abundant peptides $A\beta_{4-42}$, $A\beta_{pE3-42}$ and $A\beta_{5-42}$ were detected. Beyond the findings from Wittnam et al. (2012), the IP/MALDI-TOF approach with 4G8/6E10 described here revealed the presence of $A\beta_{4-40}$, $A\beta_{1-37}$, $A\beta_{1-38}$, $A\beta_{1-39}$, $A\beta_{pE3-42}$ and $A\beta_{1-43}$.

Since this MALDI-TOF approach can be biased by several factors such as the choice of the antibodies for IP, it is not suitable for an accurate quantification of the single Aβ peptides. However, since the selected antibodies both recognize central linear epitopes within the Aβ sequence (which likely minimizes the bias of preferential binding), the peak intensities allow for a rough estimation of the relative abundance of the peptides. Of the minor species detected, the $A\beta_{4-42}$ and $A\beta_{1-38}$ were most abundant as indicated by peak intensity. This is in line with the previous finding that in 5XFAD mice $A\beta_{4-X}$ is detectable at earlier time points than $A\beta_{pE3-X}$ and further supports the view that the minor species $A\beta_{4-X}$ may play an important role in the progress of pathologic alterations in this model (see also table 3.2.3, page 62; Antonios et al. (2013)).

Taken together, 5XFAD represents a model with early-life expression and intracellular accumulation of $A\beta_{4-X}$, a peptide that is expressed and accumulated continously up to the age of 7 months. In addition, it expresses $A\beta_{pE3-X}$, $A\beta_{5-X}$ and other minor Aβ isoforms. The most abundant peptides produced are, however, $A\beta_{1-40/42}$, which does not resemble the stoichometry of the different Aβ peptides found in human AD, where N-terminally truncated Aβ has been reported to be highly abundant or even the major fraction in brains of AD patients (Kawarabayashi et al., 2001; Portelius et al., 2010; Saido et al., 1995). Nevertheless, 5XFAD produces a heterogenous mixture of Aβ that comprises the major species found in AD patients.

4.2.5 *Gene Dosage-dependent Effects in the 5XFAD Model*

For a detailed investigation of gene-dose effects, 5XFAD[hem] and 5XFAD[hom] mice were compared to WT animals regarding their behavior phenotype (see 3.2.6 ff, page 65 ff) and the course of amyloid pathology in animals. Whereas 5XFAD[hem] mice have been reported previously to show behavior impairment in the elevated plus maze and the cross maze at the age of 6 months (Jawhar et al., 2012) and spatial reference memory deficits when 12 months old (Bouter et al., 2014), the onset of behavior deficits is considerably shifted towards earlier time points in the 5XFAD[hom] strain. Anxiety behavior is significantly altered already at 2 months of age compared to the 5XFAD[hem] group.

This early onset and genotype dependent aggravation of behavior deficits is persisting at the age of 5 months, where 5XFAD[hem], 5XFAD[hom] and WT groups showed clear and significant differences in their tendency to explore the open arms of the maze. In the water maze, an overall effect of the genotype on the escape latency was detecteable already at the age of 2 months, and a robust significant impairment of the spatial reference memory was evident at the age of 5 months for the 5XFAD[hom] group, whereas age-matched 5XFAD[hem] showed no impairment in this task. The shift of behavioral impairment to an earlier onset was accompanied by a likewise aggravation of other alterations typically observed in 5XFAD such as reduced body weight, and faster development of a motor phenotype, indicated by higher clasping scores and poorer performance in the balance beam and the string suspension task for 5XFAD[hom]. Importantly, at an age 2 of months, 5XFAD[hom] animals displayed first behavioral alterations but no significant aggravation of their motor phenotype compared to the 5XFAD[hem] transgene group. Therefore, the accelerated development of impaired behavior precedes the manifestation of aggravated motor deficits.

In Richard et al. (2015), we have further shown that, along with the accelerated development of behavioral impairment, the levels of both extracellularly deposited amyloid, soluble and insoluble Aβ are significantly elevated in the 5XFAD[hom] groups compared to the respective 5XFAD[hem] groups: A significant increase of the amyloid plaque burden was noted in cortex (+ 332 %), hippocampus (+ 715 %) and thalamus (+ 411 %) of 2 month old 5XFAD[hom]. The same holds true for 5 month old animals (+ 328 %, + 564 % and 201 % respectively) as well as for 9 month old male 5XFAD[hom] (+ 32 %, + 52 % and + 75 %) (experiments performed by Anastasiia Kurdakova using the antibody Aβ[N]). Interestingly, the relative plaque load was found to increase slower with aging which might reflect a saturation effect. This is in line with the initial description of the model, which, although not quantified, indicated a slower increase of the amyloid pathology between the analyzed 6- and 9 month old groups (Oakley et al., 2006). Similar observations were also reported for the APP/PS1KI and the PDAPP models which also exhibit an abundant plaque pathology but a plateau in deposition without significant increase in amyloid burden (DeMattos et al., 2012; Wirths et al., 2010a).

A plateau stage has also been described for AD (Jack et al., 2013). Plaque load quantification experiments were performed by my colleague Anastasiia Kurdakova.

In addition, we subjected whole-brain lysates (TBS and SDS-fraction) of 2- and 5 month old animals to quantitative ELISA measurement and found significantly elevated levels of soluble and insoluble $A\beta_{1-42}$ and insoluble $A\beta_{1-40}$ in 5XFAD^{hom} animals (2 and 5 months) compared to age-matched 5XFAD^{hem} (ELISA measurements were performed by Sandra Baches, Dept. of Neuropathology, Heinrich Heine Universität Düsseldorf, Germany). These findings are consistent with the increased plaque burden observed for 5XFAD^{hom} (Richard et al., 2015).

Besides the described acceleration of amyloid plaque deposition and the increased levels of soluble and insoluble $A\beta$ levels, we could also demonstrate that 5XFAD^{hom} at 9 months show significantly increased axonal degeneration. This was assessed by immunohistochemistry on brain and spinal cord sections employing the antibodies against NF200 (a neurofilament subunit) that revealed disclosed marked axonal swellings, mainly large axonal spheroids that were independent from plaques (Experiments performed by my colleague Anastasiia Kurdakova). The number of these dilatations was significantly increased for 5XFAD^{hom} mice compared to 5XFAD^{hem} animals in both pons and spinal cord gray matter (Richard et al., 2015). Such an age-dependent axonopathy in brain and spinal cord of 5XFAD has been reported previously (Jawhar et al., 2012) and spinal cord pathology including formation of amyloid plaques has been reported in other mouse models overexpressing mutant APP (Christensen et al., 2014; Seo et al., 2010; Wirths et al., 2006, 2007; Yuan et al., 2013).

In summary, increasing the transgene dose in 5XFAD leads to increased expression of APP/$A\beta$, a significant aggravation of pathology and a considerably earlier onset of related behavioral alterations. The early onset of spatial memory deficits suggests that 5XFAD^{hom} represents a well-suited model for preclinical studies within short time frames. It might moreover especially facilitate the analysis of intracellular $A\beta$, truncated isoforms in particular, as investigation of young 5XFAD^{hom} was imperative to detect early accumulation of intracellular $A\beta_{4-X}$.

The 5XFAD model represents one of the most thoroughly investigated transgenic models of AD and the knowledge about it has been further broadened here. Together with the APP/PS1KI model, 5XFAD exhibits a very early onset of plaque pathology at the age of two months that is preceeded by intracellular accumulation of intracellular Aβ. N-terminally truncated Aβ has been reported in various other mouse models: Aβ peptides starting at position 2/3 and position 4/5 have been reported for the APP/PS1KI model (Casas et al., 2004). $A\beta_{pE3-X}$ and $A\beta_{2/3-40}$ have been described in the APP23 mouse (Schieb et al., 2011). APP/PS1ΔE9 expresses $A\beta_{pE3-X}$ an the age of 6 months and is accessible as a therapeutic target (Frost et al., 2012, 2013). Less is known about N-terminally truncated Aβ in PDAPP, however, passive immunization of PDAPP with an $A\beta_{pE3-X}$-specific antibody reduced insoluble Aβ, indicating the presence and accessibility of at least $A\beta_{pE3-X}$ (DeMattos et al., 2012). The Tg2576 model has been proven to produce $A\beta_{pE3-X}$, too (Kawarabayashi et al., 2001). An important disadvantage of the APP/PS1KI model, which shows a similar phenotypical progression as that of 5XFAD, is that it has to be maintained with two parental lines because the APP- and PS transgenes do not co-segregate (Casas et al., 2004). Other, more recently developed models are exclusively expressing N-truncated $A\beta_{pE3-42}$ and $A\beta_{4-42}$ which makes them valuable tools to investigate N-truncated Aβ in particular. Both display a strinking phenotype including intracellular Aβ aggregation, behavioral impairment and neuron loss (Bouter et al., 2013, 2014; Meissner et al., 2014; Wittnam et al., 2012). However, in passive immunization studies, analysis of these models showing no plaque deposition would be complicated as plaque load has been a well-accepted and widely used measure in immunotherapeutic approaches (Bard et al., 2000; DeMattos et al., 2001, 2012; Frost et al., 2012; Wirths et al., 2010c). The rapid onset and progression of the phenotype in 5XFAD animals further offers time advantages over other commonly employed models like Tg2576 (Hsiao et al., 1996), PDAPP (Games et al., 1995) and APP/PS1ΔE9 (Borchelt et al., 1997) and APP23 (Sturchler-Pierrat et al., 1997) which show a considerably later onset of plaque deposition and intracellular Aβ.

Moreover the AD feature of neuron loss (Blennow et al., 2006) has not been reported for PDAPP, APP/PS1ΔE9 and Tg2576. An overview of the mentioned APP transgenic models in comparison to 5XFAD is presented in table 4.1, page 95.

Is the 5XFAD Model Suitabe to Study N-truncated Amyloid-beta?

5XFAD meets essential assumtions of the modified amyloid cascade hypothesis with neuron loss in regions that accumulate intracellular (N-truncated) Aβ and offers time-advantage due to its rapid phenotypical progression compared to other models. It is easy to maintain due to co-segregation of the APP and PS-1 transgenes which gives it advantage over another model displaying rapid development of pathology (APP/PS1KI). These facts support the choice of 5XFAD for the passive immunization pilot study presented here.

Table 4.1
The 5XFAD Model in Comparison to other commonly used transgenic models. Abbreviations: m: months; h: human; mu: murine; ha: hamster

Model	Plaque Onset	Intracellular Aβ	Confirmed N-truncated Aβ	Neuron Loss	Behavior Deficits	Promotor & Transgene(s)	References
5XFAD^{hem}	2 m	1.5 m (Ctx,Sub)	$A\beta_{pE3-40/42}$, $A\beta_{4-40/42}$, $A\beta_{5-42}$	12 m (Cortical Layer V)	anxiety, working memory (6m), spatial reference memory (12m), fear learning (12m)	Thy-1 & hAPP770 (K670N/M671L,I716V,V717I) Thy-1 & hPS1 (M146L,L286V)	Oakley et al. (2006), Jawhar et al. (2012), Bouter et al. (2014); Here: 3.2-3, page 62
5XFAD^{hom}	2 m	1.5 m (Ctx,Sub)	$A\beta_{pE3-X}$, $A\beta_{4-X}$, $A\beta_{5-X}$	not assessed	anxiety (2m) spatial learning and reference memory (5m)	Thy-1 & hAPP770 (K670N/M671L,I716V,V717I) Thy-1 & hPS1 (M146L,L286V)	Antonios et al. (2013), Guzman et al. (2014), Richard et al. (2015)
PDAPP	9-12m	8-12m	$A\beta_{pE3-X}$	not reported	spatial learning & memory (2-4m) recognition memory (6m) cued fear conditioning (11m)	PGDF & hAPP (V717F)	Games et al. (1995), Rockenstein et al. (1995), Masliah et al. (1996), Dodart et al. (1999), Nilsson et al. (2004), Hartman et al. (2005)
APP/PS1ΔE9	5-6m		$A\beta_{pE3-X}$	not reported	spatial learning (6m)	mPrP & hAPP695 (K670N/M671L) muPrP & hPS1 (Deletion of Exon 9)	Borchelt et al. (1997), Garcia-Alloza et al. (2006), Xiong et al. (2011)
APP/PS1KI	2m	1.5m (Ctx)	$A\beta_{2/3-42}$, $A\beta_{4/5-42}$	6m (CA1/2)	working memory (6m)	Thy-1 & hAPP (V717I,K760N/M671L) endogenous & hPS1 (M233T,L235P)	Casas et al. (2004), Wirths et al. (2010b), Christensen et al. (2008), Christensen et al. (2010b)
Tg2576	11-13m	6m	$A\beta_{pE3-X}$	not reported	working memory (1-2m) fear learning (1-2m) spatial learning (3-5m)	haPrP & hAPP695 (K670N/M671L)	Hsiao et al. (1996), Chapman et al. (1999), Arendash et al. (2001a), Dineley et al. (2002), Takahashi et al. (2002), Arendash et al. (2004),
APP23	6m	15m	$A\beta_{pE3-X}$, $A\beta_{2/3-40}$	14-18m (CA1)	spatial learning/memory (3m), passive avoidance test (25m)	Thy-1 & hAPP751 (K670N/M671L)	Sturchler-Pierrat et al. (1997), Calhoun et al. (1998), Kelly et al. (2003), Van Dam et al. (2003), Schieb et al. (2011), Rijal Upadhaya et al. (2013)

Passive immunization with various antibodies against Aβ has been widely studied since the first successful approach by Bard et al. (2000) (A representative subset of chronic passive immunization approaches is summarized in appendix table 4.2, pages 115 ff). Some studies suggested a significant reduction of pre-existing plaques in transgenic mice (Frost et al., 2012; Wilcock et al., 2004b,c, 2006), however others discussed that clearance of pre-existing plaques is limited (Tucker et al., 2008) or did not occur after passive immunization (Dodart et al., 2002; Levites et al., 2006). On the contrary, evidence for a plaque-preventative effect of administered anti-Aβ antibodies was frequently reported (Bard et al., 2000, 2003; Bussiere et al., 2004; DeMattos et al., 2001, 2012; Frost et al., 2012; Levites et al., 2006; Lord et al., 2009b). *In vivo* antibody effects were not restricted to alterations in the amyloid plaque burden: In a subset of passive immunization experiments it was shown that antibody-administration led to increased vascular amyloid (DeMattos et al., 2012; Racke et al., 2005; Schroeter et al., 2008; Wilcock et al., 2004c, 2006).

It has been proven difficult to translate the success of preclinical passive immunization trials into clinic. For instance, Bapineuzumab, the humanized equivalent of the 3D6 antibody investigated first in Bard et al. (2000), showed some target engagement but the treatment did not benefit patients. (Lannfelt et al., 2014). Solanezumab, the humanized equivalent to the antibody 266 (DeMattos et al., 2001) was not reported to have significant effects in patients as well. Whereas trials on bapineuzumab were terminated, investigation of solanezumab in clinical trials is driven further currently. Furthermore, side effects such as increased occurence of microhemorrages have been reported after passive immunization of mice against Aβ (DeMattos et al., 2012; Racke et al., 2005; Schroeter et al., 2008; Wilcock et al., 2004c, 2006), even in a subchronic approach with few doses only (Lee et al., 2005). Importantly, the observation of side effects in preclinical studies was somehow predictive of severe adverse events that led to halting of some human clinical trials (Lannfelt et al., 2014). This was despite of some preclinical approaches showing both a significant rescue or amelioration of behavioral and/or memory impairment in transgenic mice and induction of side effects in the

same cohorts (Wilcock et al., 2004c, 2006). However, the overall outcome of clinical passive immunization studies targeting Aβ was much less promising than results from murine trials suggested (Lannfelt et al., 2014). These numerous studies taken together point out a need to find a more specific and safer immunotherapeutic approach for AD. In the course of this it has been proposed that N-terminally truncated Aβ might represent a suitable target for immunotherapy.

Two recent studies addressing this hypothesis (DeMattos et al., 2012; Frost et al., 2012) share the idea of passively immunizing mice against N-truncated Aβ with the current study but differ from previous studies, each other and the present one in a variety of parameters which are 1) the antibodies used for immunization, 2) the animal model employed and 3) the administration in regard of both dosage and time course. These factors are likely to influence the outcome of passive immunization trials: Frequently used animal models display different Aβ stoichiometry and morphology of amyloid deposits, e.g. PDAPP and Tg2576 mice (Fryer et al., 2003; Hsiao et al., 1996; Sasaki et al., 2002). Unlike some other models, the 5XFAD mouse carries several mutations that elevate $A\beta_{X-42}$ levels disproportionally (Oakley et al., 2006), and APP23 mice are notable for abundant vascular amyloid desposition. Different monoclonal antiobodies have been shown to have highly different potential for preventative and therapeutic approaches (DeMattos2012) and the induction of side effects and alterations of plaque load levels has been shown to be dose-dependent (DeMattos et al., 2012; Schroeter et al., 2008). Some studies on passive immunization found diverging results when analyzing extracellular plaque burden and total levels of Aβ peptides in brain lysates (DeMattos et al., 2012; Frost et al., 2012). This complicates inter-experimental comarison and underlines the importance of conducting comparative experiments as in the present study.

To address the questions whether a) $A\beta_{4-X}$ and/or $A\beta_{pE3-X}$ are contributing to the etiology of the disease-like phenotype in the 5XFAD mouse model and b) NT4X-167 might be suitable as a therapeutic tool, a pilot study comparing three different monoclonal antibodies (IgG2b) against N-truncated Aβ was conducted. Female $5XFAD^{hem}$ mice were injected with 10 mg/kg body weight of NT4X-167, antibody 1-57 (recogniz-

ing $A\beta_{pE3-X}$ exclusively, independent of conformation, (Wirths et al., 2010a), see also 3.1, page 57) or antibody 9D5 which reacts with low molecular weight oligomers of $A\beta_{pE3-X}$ exclusively (Wirths et al., 2010c). PBS-injected 5XFAD animals served as a control in this study. The experimental setup chosen here was essentially based the approach of Wirths et al. (2010c), to treat a well-described model (5XFAD) with abundant amyloid pathology, behavioral deficits and fast phenotypical progression in a comparative approach with three different antibodies. The treatment duration was prolonged to assess potential effects on behavior in the animals at a time point were the behavioral impairment is more manifest, somewhat later than the time point where they become visble at first (6 months; Jawhar et al. (2012)).

In contrast to the current study, both therapeutic trials conducted in DeMattos et al. (2012) and Frost et al. (2012) and the preventative trial of DeMattos et al. (2012) were initiated at time points where the behavioral phenotype is already manifest (see 4.1, page 95). The preventative treatment of Frost et al. (2012) started at the age of 5.8 months, only little before first behavioral impairment for APP/PS1ΔE9 model become visible (6 months). In both publications, no behavioral data have been reported which makes it impossible to conclude whether the antibody administration had effects beyond clearance of $A\beta$.

In general has the majority of chronic passive immunization studies investigated either prevention of amyloid deposition at early stages or aimed to remove plaques at very late stages. To date, few studies described a mid-stage approach of anti-$A\beta$ passive immunization (DeMattos et al., 2012; Schroeter et al., 2008; Wirths et al., 2010c). In human AD, plaque deposition starts decades before the onset of clinical symptoms and is virtually at maximal levels by time of diagnosis (Jack et al., 2010; Morris and Price, 2001; Price et al., 2009), patients with mild cognitive impairment due to AD are therefore at a stage well after disease initiation. Thus, the majority of preclinical studies focusing on prevention of amyloid deposition or removal of pre-existing plaques, investigated stages that are reminescent of the disease onset prior to diagnosis or very late symptomatic stages of AD. For a very early intervention in AD by passive immunization, it would be necessary to identify patients that are likely to develop the disease. Unless for the rare cases of familial AD, to date biomarkers that allow for identification of patients

before they develop amyloid deposits/cognitive symptoms are lacking. It is therefore impossible to clearly distinguish individuals that will remain healthy from those that will convert to a cognitively impaired phenotype (Fiandaca et al., 2014). Therefore, even if very early therapeutic invention has significant effects in a preclinical study as in Frost et al. (2012), it is hardly possible to design studies translating this approach into clinical trials. Opposite to the prevention of amyloid deposition, the majority of therapeutic trials in mice does reflect a stage of fully-blown AD with abundant plaques in the brain and advanced cognitive impairment.

In contrast to abundantly undertaken preventative and late-stage therapeutic approaches, such as those performed by DeMattos et al. (2012) and Frost et al. (2012), the 5XFAD mice treated in the present study already had considerable levels of deposited amyloid plaques at the starting point of immunization, but were at an age before onset of behavioral symptoms. The present study therefore likely reflects an approach closer to late preclinical or early symptomatic AD.

4.4.1 *Chronic Passive Immunization of 5XFAD Mice*

In the NT4X-167 group, Thioflavin S staining for fibrillar Aβ aggregates (Bussiere et al., 2004) revealed lowered levels compared to PBS-injected controls. A significantly lower plaque burden was observed as well for Aβ_{pE3-X} and Aβ_{X-40} in the anterior motor cortex of the NT4X-167 group when specific antibodies were employed to further characterize the nature of the amyloid deposits. The 1-57- and 9D5 group showed unaltered plaque levels. In the thalamus, the observed differences in the plaque load were not significant, although the lower average levels of Thioflavin S-positive plaques and Aβ_{X-40}/ Aβ_{pE3-X} immunoreactiviy indicate a trend in line with the finding of reduced plaque burden in the anterior motor cortex. It might be that the thalamus is less accessible to administered antibodies for some reason, or that the plaque deposition follows a different pattern. (Frost et al., 2012), wo reported lesser treatment effects in certain brain regions such as the cerebellum, discussed similarly.

Plaque abundance and plaque deposition in the brain are linked to soluble Aβ (DeMattos et al., 2002; Hong et al., 2011; Koffie et al., 2009), and further soluble protofibrillar Aβ was correlated with spatial learning in an AD mouse model (Lord et al., 2009a). Nevertheless, according to the modified amyloid hypothesis plaques might still function as a source for soluble peptides. Targeting plaques directly can therefore be considered an approach to reduce a potential secondary source or reservoir of soluble/ intracellular Aβ, whereas a direct engagement with the soluble peptide fraction would prevent further plaque deposition.

In mid stage treatment approaches such as the present study, antibody-mediated removal of pre-existing plaques must be sufficient to exceed the amount of newly deposited amyloid or the administered antibody must prevent deposition of soluble Aβ efficiently enough to induce significant differences at the time of analysis or the antibody must be capable to exert activity serving both mechanisms, leading to an overall reduced plaque burden. This probably explains the observed less robust treatment effects compared to previous studies (Bard et al., 2000; DeMattos et al., 2001, 2012; Frost et al., 2012) and might provide further explanation for the observation that the apparently lower plaque burden in the thalamus of NT4X-167 injected animals did not reach significance.

Here, NT4X-167 was the only antibody whose administration decreased fibrillar and total Aβ deposits, especially N-truncated and pyroglutamate-modified Aβ in the cortex of 5XFAD mice. This indicates that passive immunization with NT4X-167 is efficacious in modulating the amyloid pathology, whereas treatment against total (antibody 1-57) or oligomeric $A\beta_{pE3-X}$ (antibody 9D5) alone did not reveal such an effect. However, this results are somehow controversial: It has been published before that the administration of antibodies specific for $A\beta_{pE3-X}$ had effects on either the amount of overall levels of Aβ measured by ELISA on brain lysates (PDAPP model, DeMattos et al. (2012)) or reduced $A\beta_{pE3-X}$-positive plaque load (APPswe/ΔE9 model, Frost et al. (2012)). In addition, Wirths et al. (2010c) reported that chronic passive administration of the antibody 9D5 to 5XFAD reduced overall plaque load for general Aβ, $A\beta_{X-42}$, $A\beta_{X-40}$ as well as for $A\beta_{pE3-X}$; furthermore the authors reported reduced levels of

$A\beta_{pE3-X}$ in the soluble and insoluble fraction of whole brain lysates and an ameliorated behavioral impairment after 6 weeks of treatment. Different aspects of these findings will be discussed in the following:

Lack of Plaque-lowering Effects in the 9D5 and 1-57 Groups

The results for the 9D5 group were strikingly deviant from Wirths et al. (2010c), who reported that treatment with 9D5 resulted in reduced plaque load in the treatment group compared to PBS-injected animals. Therefore, one could expect at least halting or a slow-down of amyloid deposition in the current study, in particular if oligomeric $A\beta_{pE3-X}$ promotes plaque deposition by a seeding mechanism (Wittnam et al., 2012). It might be that a considerably different protocol (prolongation of the treatment) compared to Wirths et al. (2010c) leads to the finding that effects of passive immunization are masked by an overall fast progression of the pathologic alterations. This would suggest that the treatment was capable of slowing down, but not of preventing the pathologic alterations in Wirths et al. (2010c), and treated animals catch up phenotypically with untreated controls during a prolonged immunization protocol. Considering that $A\beta_{4-X}$, which was not targeted in Wirths et al. (2010c), precedes $A\beta_{pE3-X}$ in 5XFAD (Antonios et al., 2013) and might substantially contribute to trigger the pathologic cascade, targeting $A\beta_{pE3-X}$ alone is probably not sufficient to cause persisting treatment effects.

Diverging methodologic procedures are another possible explanation for different study outcomes. The antibodies employed here for plaque load quantification were, except G2-10, others than those employed in Wirths et al. (2010c). Therefore, results of the current study allow for comparison between the treatment groups but comparison with previous studies is complicated due to methodologic divergence. However, the results obtained in both studies on 9D5 for the three analytical parameters, i.e. plaque load, levels of insoluble $A\beta$ in brain lysates and behavioral performance, were well in line with each other. This consistency within the individual studies indicates that phenotypical inter-animal variability needs to be taken into consideration, too. Both studies analyzed a relatively small number of animals (n = 4 per group in Wirths et al. (2010c); n = 7-8 here), therefore the statistics need to be interpreted with care.

These factors might to some extent account for the observed discrepancy between the two studies. However, it has been shown here that when acting on both major N-truncated Aβ isoforms, a treatment effect becomes visible, which further supports the importance of Aβ$_{4-X}$. NT4X-167 recognizes both Aβ$_{pE3-X}$ and Aβ$_{4-X}$ which probably makes it more capable of recognizing hetero-Aβ-assemblies containing N-truncated Aβ, improving its efficacy. NT4X-167 recognizes soluble oligomers and a subset of amyloid plaques and it shows a slight preference for the more soluble Aβ$_{4-40}$ (Antonios et al., 2013).

Whereas 1-57 strongly recognizes plaques in human and murine brain samples (Wirths et al., 2010a), NT4X-167 barely reacted with human AD plaques but with amyloid deposits in transgene mouse brains (Antonios et al., 2013). This points to important structural differences between plaques of human AD and to a preference of NT4X-167 for rather soluble or less-dense amyloid strucutures, probably promoted by the conformational properties of Aβ$_{4-X}$. Major structural differences between human and murine plaques have been described by Kuo et al. (2001), who reported that the human plaque cores were highly resistant to chemical and physical disruption whereas murine (APP23) plaques were completely soluble in SDS-containing buffers. In addition to the apparently different target engagement of NT4X-167 in human and murine samples, an apparent preference of Aβ$_{4-40}$ over Aβ$_{4-42}$ gives further indication that NT4X-167 might preferentially bind to more soluble Aβ assemblies (Antonios et al., 2013).

In vitro experiments suggested that intracellular Aβ aggregates released from the endosomal/lysosomal system are capable to induce Aβ fibrillization (Friedrich et al., 2010; Hu et al., 2009). It has further been demonstrated that PBS-soluble fractions from AD brains are efficiently inducing amyloid deposition when administered in murine brains (Fritschi et al., 2014b). The lower engagement of NT4X-167 with highly aggregated, more degradation-resistant amyloid deposits and on the contrary a better recognition of soluble oligomers might provide explanation for the efficacy of treatment with NT4X-167 compared to 1-57 treatment. Furthermore might differences in antibody binding capacity, the recognition of assemblies composed of more than one Aβ isoform (hetero-oligomers/fibrils) and the accessibility/abundance of epitopes and

neo-epitopes as well as the immunodetection protocol influence the outcome of quantitative measures.

However, the results found here for the 1-57 immunized group are somehow in line with the prevention trial reported in DeMattos et al. (2012) (antibody mE8). In both approaches, anti-Aβ_{pE3-X}-antibodies, both recognizing plaques, were employed, but mE8 detected only 0.6 % of all Aβ found in AD and PDAPP mouse brains. DeMattos et al. (2012) further claim that mE8 is plaque-specific, whereas 1-57 engages with soluble and deposited Aβ_{pE3-X} as shown by Western Blotting (see 3.1, page 57) and in Wirths et al. (2010a). Similar to the antibody mE8, 1-57 was not capable of altering plaque levels.

The treatment window chosen for the present study represents a stage of 5XFAD animals well in-between the onset and a possible plateau stage of plaque deposition. It has been shown that the levels of soluble Aβ is elevated in the vicinity of plaques (Koffie et al., 2009) and in PDAPP is in an equilibrium with the deposited Aβ (DeMattos et al., 2002). It has further been proposed that this cloud of soluble peptides surronding plaques acts as a barrier that prevent antibodies to engage with plaques, causing failure in modulationg plaque pathology. A small 0.1 % fraction of the antibodies in the periphery crosses the blood brain barrier (Giedraitis et al., 2007; Mehta et al., 2001) to encounter Aβ in the central nervous system, which is 20 to 67-fold more abundant in the central nervous system than in the periphery. Therefore, it has been previously proposed that antibodies can be overwhelmed by the amounts of accessible target. (Das et al., 2001).

It has been described previously that the efficacy of antibodies in amyloid removal is dose dependent DeMattos et al. (2012); Schroeter et al. (2008). Alhough the dosage seems generally well in line with the majority of other passive immunization studies that reported in vivo-efficacy (see also appendix, table 4.2, pages 115 ff), it might be, that the dosage was not sufficient for 1-57 to cause a significant effect. DeMattos et al. (2012) reported significant plaque removal only with 12.5 mg/kg body weight which is a 25 % higher dose than in the present study. However, a combination of all or some of these effects could have caused the failure of 1-57 to modulate the pathology.

No assumptions can be made, however, if 1-57 would be capable of reducing pre-existing plaques in a trial on mice that reached a plateau stage of plaque deposition.

In contrast to these two studies, Frost et al. (2012) reported a significant plaque-lowering effect of anti-$A\beta_{pE3-X}$ passive immunization in both a preventative (starting before onset of plaque deposition) and a therapeutic trial. DeMattos et al. (2012); Frost et al. (2012); Wirths et al. (2010c) and the current study taken together do not allow to draw a profound conclusion. There is good indication that targeting N-truncated $A\beta$ peptides *in vivo* is possible and, given the right preconditions, might be capable of modulating $A\beta$ pathology. However, the considerable differences in the outcome of these attempts on passive immunization indicate that different approaches lead to divergent results, as these studies were conducted with different treatment strategies (initiation, end point, duration), antibodies (specificity, IgG-subtype), dosages, mouse models and analytical protocols.

Insoluble Amyloid-beta Levels in Brain of 5XFAD Mice after Passive Immunization

When assessing brains of passively immunized mice for insoluble $A\beta_{1-40/42}$ and $A\beta_{pE3-X}$ in SDS-fractions of brain lysates by ELISA, we did not observe any significant effect of the treatments (Data not shown; ELISA experiments were performed by Sandra Baches, Dept. of Neuropathology, Heinrich Heine Universität Düsseldorf, Germany). The results for $A\beta_{1-42}$ are well in line with the plaque load measures for $A\beta_{X-42}$ and $A\beta_{1-X}$ where we did not find significant differences among treatment groups. In contrast to ELISA experiments, the plaque load levels in the anterior motor cortex were significantly reduced for $A\beta_{pE3-X}$ and $A\beta_{X-40}$ in the NT4X-167 group. It is not clear, what led to the discrepancy observed between these analyses. One explanation might be that plaque load analysis focuses on distinct regions in thin sections of brain tissue, whereas the lysate fraction were representing an entire brain hemisphere. Both experimental approaches analyze different fractions of $A\beta$: A plaque load quantification focuses on a particular brain region in contrast to the analysis of whole brain lysates.

Moreover contains the SDS-fraction of brain lysates not only Aβ peptides from plaques but all amyloid aggreagates from the insoluble fractions of the brain tissue. Furthermore were the antibodies used for detection of Aβ in ELISA measurements different from those taken for plaque load quantification. This might account for important discrepancy as for instance the antibody IC16 was not suitable for plaque load analysis due to lower contrast observed in stainings compared to stainings with other antibodies such as Aβ[N], whereas it is well established in ELISA for detecting $Aβ_{1-X}$. Thus, the suitability of the antibody for a certain methodologic approach seems greatly important. Previously published studies that reported lowered Aβ levels in brain lysates followed different analytical protocols and were using other antibodies for detection than here (Bard et al., 2000; DeMattos et al., 2012; Wirths et al., 2010c).

The unequal methodology might, together with different sample sizes and models used, account for differential outcomes of measures and statistics. Nevertheless, the majority of passive immunization studies employed quantification of the amyloid plaque burden in brain sections of immunized mice as the main analytical parameter (Bard et al., 2000; DeMattos et al., 2001; Frost et al., 2012; Wilcock et al., 2004b,c, 2006; Wirths et al., 2010c). As ELISA data are lacking in some of these studies, this indicates that quantification of plaque burden is well-accepted and might be more robust to determine effects of passive immunization. The observation that the plaque load after immunization is lowered despite of ELISA measurements showing no significant difference between groups is, however, consistent with some previously published studies (Frost et al., 2012; Janus et al., 2000), of which the previous reported similar results in a trial on an antibody against N-truncated $Aβ_{pE3-X}$.

Behavioral Phenotype of 5XFAD Mice after Passive Immunization

Only a subset of studies addressed the question whether a rescue of behavioral or learning/memory deficits can be achieved by passive immunization against Aβ. Noticeably, such rescue or amelioration has been reported for different mouse models, PDAPP (Dodart et al., 2002), Tg2576 (Wilcock et al., 2004b,c, 2006) and 5XFAD (Wirths et al., 2010c).

Within the mentioned studies, different monoclonal antibodies were used, recognizing central Aβ epitopes (Dodart et al., 2002; Wilcock et al., 2004b,c, 2006), and a conformation-specific antibody (9D5, (Wirths et al., 2010c)) against $A\beta_{pE3-X}$, which has been investigated here as well. As mentioned previously, the outcome of Wirths et al. (2010c) was strikingly different from the results found here. This held also true for behavioral performance of treated mice, where, in contrast to the previous study, no rescue or amelioration of the 9D5 group was observed.

Here, no robust significant difference to the PBS-controls was observed for the NT4X-167, 1-57 or 9D5 groups in the Elevated Plus Maze and the Cross Maze paradigms but, however, a trend towards an amelioration of working memory impairment in the NT4X-167 group in the cross maze was observed.

However, it must be stated that the pathologic alterations in the 5XFAD model are still in progress at the age of 6 months (endpoint of treatment in Wirths et al. (2010c)), with the plaque burden increasing by approximately 2-fold between both 3-6 months and 6-12 months of age (Jawhar et al., 2012). Our experiments performed on $5XFAD^{hom}$ animals showed that even a 2-fold increase of the transgene dose would not lead to a plateau stage in plaque deposition before the age of 9 months (Richard et al., 2015). Robust spatial memory deficits are not present until the age of 7 months (Richard et al., 2015), but have been described as late as at the age of 12 months in $5XFAD^{hem}$ mice bred on a C57Bl6/J genetic background (Bouter et al., 2014). According to the modified amyloid cascade hypothesis, intracellullar Aβ peptides trigger a fatal cascade of secondary events that lead to behavioral and memory deficits. Intracellular Aβ is evident as early as at the age of 6 weeks in the 5XFAD model. Bouter et al. (2014) thoroughly investigated the molecular profile of plaques, memory decline and neuron loss in 5XFAD. The authors found 19 differently expressed genes in young (3-6-month-old) 5XFAD, which were mainly associated with inflammatory processes. Thus, the pathologically Aβ-triggered cascade is likely to be already ongoing at the starting point of the study, which probably interferes with reverting or halting a progressing development of behavioral symptoms.

Furthermore, it is likely that the pathological alterations in the mouse model do not exclusively rely on N-truncated Aβ. Aβ_{X-42} exerts similar neurotoxicity as Aβ_{pE3-42} and A$\beta_{4-40/42}$ *in vitro* (Bouter et al., 2013). Therefore it is conceivable that the major fraction of Aβ_{1-42} (and probably other species found in 5XFAD), which is not directly targeted, contributes significantly to induce behavioral alterations. Importantly, the Aβ pool in 5XFAD brain comprises much less N-truncated Aβ than in AD patients brain, where those represent a major fraction (Kawarabayashi et al., 2001; Portelius et al., 2010; Saido et al., 1995). 5XFAD accumulates predominantly N-terminally intact Aβ in neuronal cells that are prone to degenerate at 12 months (Antonios et al., 2013; Jawhar et al., 2012; Oakley et al., 2006).

Apparently in line with this hypothesis, various studies reported amelioration of behavioral and/or learning/memory deficits after administration of pan-Aβ antibodies recognizing central epitopes within the Aβ sequence (Dodart et al., 2002; Wilcock et al., 2004b,c, 2006). These antibodies bind well to the (in models) highly abundant N-terminally intact isoforms, which suggests that the observed treatment effects are not merely based on removal of N-truncated Aβ. Thus, given a key role for N-truncated Aβ, it can be hypothesized that immunotherapy targeting these isoforms would have better potential to alleviate or slow down the progression of cognitive deficits in patients or models that show higher levels of, or are exclusively expressing N-truncated Aβ isoforms.

The mean alternation rates of the WT and the NT4X-167 group were similar, but a comparison between the NT4X-167- and the PBS group did only reveal a positive trend that was overall not significant. This has to be interpreted with care into each direction, since the number of animals per group was relatively low. Inter-individual variation within small samples might therefore account for the observed discrepancy between the present study and Wirths et al. (2010c). It remains unclear if passive immunization with NT4X-167 can have effects on behavior/memory.

Nevertheless, comparison of the three treatment groups in the present studies indicates that, depending on the choice of the antibody/target for immunotherapy, there is a possibility to modify pathology in a mid-stage therapeutic approach. The lower plaque load measures in the NT4X-167 group, and the corresponding higher rate of correct alternations in the same group seem to support each other.

4.4.2 *Mechanism of Action of Anti-amyloid-beta Immunization*

Several hypotheses have been proposed for the mechanism of action of anti-Aβ antibodies in anti-Aβ-immunization. It has been shown that a small subset (0.1 %) of peripheral antibodies enter the central nervous system through the blood brain barrier (Pan et al., 2002), a finding that implies the possibility of antibody-mediated effects occuring by direct interaction with Aβ in the brain. Thus, one of three main hypotheses is that opsonization of antigens upon antibody recognition triggers phagocytosis by macrophages/microglia. This mechanism requires sufficient levels of antibodies in the brain after administration. Support for this hypothesis comes from studies that found abundant antibody-decorated plaques and increased microglial activity after immunization (Bard et al., 2000; DeMattos et al., 2012; Wilcock et al., 2004a,b, 2006). Clearance of pre-existing plaques after passive immunization has been credibly demonstrated in a murine model by Wang et al. (2011), in which the authors further support that microglial phagocytosis is involved in the observed plaque removal. DeMattos et al. (2012) discussed that antibodies might be hindered from altering plaques by saturation with soluble peptides in the vicinity of extracellular aggregates, thereby failing to trigger phagocytosis-dependent plaque removal.

However, it was earlier described that engagement of antibodies with soluble Aβ is not predictive of the antibodies´ *in vivo* efficacy (Bard et al., 2000) and others reported that the phagocytosis effector funciton is not essential to modulate Aβ pathology (Bacskai et al., 2002; Das et al., 2003). It was proposed that peripherally circulating antibodies might facilitate Aβ clearance from the brain through a so-called peripheral sink

mechanism, neutralizing circulating peptides and thereby shifting the Aβ equilibrium towards a higher efflux/reduced influx through the blood brain barrier (Bacskai et al., 2002; Das et al., 2003; DeMattos et al., 2001). Supporting this view, it has been shown that Aβ can be rapidly transported to the periphery (Ghersi-Egea et al., 1996; Shibata et al., 2000; Zlokovic et al., 1993, 1994, 1996).

A third mechanism possibly explaining a treatment effect of anti-Aβ antibodies is blocking of peptides by the mere molecular interaction, thereby preventing cytotoxicity, nucleation/seeding and/or conformational imprinting, mechanisms to which pathologic activity of Aβ has been attributed in numerous studies (Fritschi et al., 2014a,b; Nussbaum et al., 2012; Schlenzig et al., 2009). Catalytic activity of antibodies has been suggested by Solomon et al. (1996, 1997) and has further been supported by others (Adolfsson et al., 2012; Alcantar et al., 2010).

Of note, none of these proposed mechanisms are mutually exclusive. However, the present study focused on comparison of three antibodies in regarding their targets. Differential phagocytosis effector function was ruled out by the choice of antibodies of the same isotype (IgG2b) and the mid-stage treatment approach does not allow for discrimination between different mechanisms of action of the administered antibodies. To this end, additional experiments would be necessary.

4.4.3 *Therapeutic Advantage with NT4X-167?*

It is not clear to which extent the phenotypical alterations in 5XFAD can be attributed to N-truncated $A\beta_{pE3-X}$/ $A\beta_{4-X}$, although several recent *in vivo* studies from our laboratory have provided evidence that N-truncated Aβ isoforms are indeed connected with behavior deficits and memory impairment (Alexandru et al., 2011; Bouter et al., 2013; Wirths et al., 2009; Wittnam et al., 2012). There is further indication that a treatment effect can be achieved with antibodies targeting $A\beta_{pE3-X}$ (DeMattos et al., 2012; Frost et al., 2012). However, in the present study it was found that two anti-$A\beta_{pE3-X}$ antibody (1-57) had no significant treatment effects.

To rank the therapeutic potential of different antibodies/targets, it is of importance to conduct comparative approaches. The setup of the present comparative study rules out the bias of varying analytical methods, different models, and different IgG subtypes of antibodies. Therefore the different efficacy of treatments can be attributed to the antibodies´ target engagement and the results can in return give good indication if the addressed target is suitable for therapy.

The study conducted here offers the advantage of a scenario close to preclinical or early-stage AD. However, the obtained effetcs were less pronounced than in previous studies (DeMattos et al., 2012; Frost et al., 2012; Wirths et al., 2010c).

The observation that passive immunization against $A\beta_{pE3-x}$ alone was not capable of inducing treatment effects here indicates that $A\beta_{4-x}$ significantly contributes to the neuropathologic phenotype in the 5XFAD model. In contrast to the 1-57- and the 9D5 group, The treatment group that received NT4X-167 revealed significant plaque-lowering effects in an approach close to preclinical AD. Furthermore, the NT4X-167 treatment group was the only one that showed a positive trend in working memory performance. As pointed out above, comparison beetwen the available studies of a chronic passive immunization against N-truncated $A\beta$ is restricted due to varying setups of these studies.

Hence, the main conclusion must be drawn from the comparative approach conducted here. These results suggest that targeting a broader pool of N-terminally truncated $A\beta$, as with the antibody NT4X-167, might posess therapeutic advantage. In turn, this would rather qualify NT4X-167 than 1-57/9D5 as a therapeutic tool. This observation is, to date, unique and might give implications for developing a therapeutic strategy in AD .

Here, it was shown that passive immunization against $A\beta_{pE3-X}$ and $A\beta_{4-X}$, of which the latter is found intracellularly at early time points in the 5XFAD model, had significant effects on the plaque load of passively immunized mice. On the contrary, immunization against $A\beta_{pE3-X}$ alone did not have such an effect.

Importantly, effects reported in many passive immunization trials are mainly restricted to an amelioration of the $A\beta$-pathology assessed by means of plaque load and/or $A\beta$ quantification. Reports of behavioral improvement are few and several models frequently employed for such preclinical studies feature no neuron loss. Consequently, rescue of neuron loss upon passive immunization has not been described in these models. Other parameters such as behavior/memory perfomance of transgenic mice have not been commonly asessed, too. The present study has not aimed to determine a possible treatment effect on neuron loss and interpretation of behavioral data is restricted due to the relatively low animal number.

As pointed out, the mechanism of action of NT4X-167 *in vivo* can not be elucidated here. Although some effects of NT4X-167 on the amyloid plaque burden were observed, it remains unclear if passive immunization against N-truncated peptide isoforms can effectuate a robust and persisting improvement of $A\beta$-induced neurodegenerative alterations. Translation of preclinical anti-$A\beta$ immunization studies into clinics has been proven difficult (Lannfelt et al., 2014). Therefore no prediction for a clincal study on anti-$A\beta_{pE3-X}$/ $A\beta_{4-X}$ immunotherapy can be made.

In summary, the data obtained here have further validated the 5XFAD mouse model for analysis of N-truncated $A\beta$, behavior and memory. The passive immunization pilot study conducted provides a proof of the concept that $A\beta_{4-X}$ is accessible for passive immunotherapy *in vivo* and in turn indicates that NT4X-167 has therapeutic advantage over other antibodies targeting N-truncated $A\beta$. The suitability of the 5XFAD model for research on N-truncated $A\beta$ isoforms is further supported.

APPENDIX

Table 4.2

Parenteral Chronic Passive Immunization Approaches in the 5XFAD, PDAPP, TG2576, APP/PS1ΔE9 and APP23 Mouse Models. Abbreviations: m: months; d: days, h: hours; E: epitope; mab: monoclonal antibody, pab: polyclonal antibody, tg: transgenic; CNS: central nervous system. Note: Information regarding antibodies is inconsistent between certain publications.

Reference	Model	Trial	Antibodies, Adminstration, Dosage	Results
Bard et al. (2000)	PDAPP	Preventative, 8-10m to 14-16m	mab 10D5 (IgG1, E Aβ3−6, mab 3D6 (IgG2a, E Aβ1−5), mab 21F12 (IgG2a), pab Aβ1−42 (intraperitoneal, weekly)	Reduced plaque burden with pabAβ1−42 (−93 %), mab 10D5 (−81%), reduced ELISA total Aβ42 levels pab Aβ1−42: −55 %; mab 10D5: −64.5 %), no substantial effects of mab 21F12
	PDAPP	Preventative, 11.5-12mm to 17.5-18m	mab 10D5, mab 3D6, mab 16C11 (intraperitoneal, weekly)	Reduced Plaques with mab 10D5 (> −80 %), mab 3D6 (−86 %), no reduction of plaques with mab 11C16; no T-cell proliferative response; mab 10D5 & mab 3D6 entered CNS and labeled plaques
DeMattos et al. (2001)	PDAPP	Preventative, 4m to 9m	mab 266 (IgG1, E Aβ13−28) (weekly)	Prevention of plaque deposition in a subcohort
Dodart et al. (2002)	PDAPP	Therapeutic, 24m, 6w duration	mab 266 (IgG1, E Aβ13−28) (intraperitoneal, weekly, 360 μg/mouse)	Reversed recognition memory deficits, No reduction in plaque load, no correlation between behavior and plaque burden.
Pfeifer et al. (2002)	APP23	Therapeutic, 21m to 26m	mab β1 (E Aβ3−6) (intraperitoneal, weekly, 0.5 mg/mouse)	Significant reduction of diffuse plaques in neocortex, no increase in CAA but more frequent cerebral hemorrhages.
	APP23	Preventative, 5m to 11m	mab β1 (IgG2a, E Aβ3−6) (intraperitoneal, weekly, 0.5mg/mouse)	No hemorrhages found after immunization.
followed up in Burbach et al. (2007)	APP23	Therapeutic, 21m to 26m	mab β1 (E Aβ3−6) (intraperitoneal, weekly, 0.5 mg/mouse)	Number of macrophages in bleeding vessels are increased after passive immunization.
Bard et al. (2003)	PDAPP	Preventative, 12m to 18m	mab 10D5 (IgG1, E Aβ3−7), mab 3D6 (IgG2a, E Aβ3−7), mab 2C1 (IgG2a, E Aβ3−7), mab 6C6 (IgG1, E Aβ3−7), mab 12B4 (IgG2a, E Aβ3−7), mab 3A3 (IgG2b, E Aβ3−7), mab 12A11 (IgG2b, E Aβ3−7) (intraperitoneal, weekly, 10 mg/kg)	Significant reduction of plaque burden with IgG2a and IgG2b antibodies. IgG2a antibodies are more efficient in clearing plaques, support for importance of FC-Receptor mediated phagocytosis. Plaque clearance seemed independent of complement activation.
Bussiere et al. (2004)	PDAPP	Preventative, 12m to 18m	mab 10D5 (IgG1, E Aβ3−7), mab 12B4 (IgG2a, E Aβ3−7), mab 12A11 (IgG2b, E Aβ3−7) (intraperitoneal, weekly, 10 mg/kg)	IgG2a antibody (12B4) was most efficient in clearing fibrillar amyloid.

Table 4.3

Parenteral Chronic Passive Immunization Approaches in the 5XFAD, PDAPP, TG2576, APP/PS1ΔE9 and APP23 Mouse Models. Abbreviations: m: months; d: days, h: hours; E: epitope; mab: monoclonal antibody, pab: polyclonal antibody; tg: transgenic; CNS: central nervous system. Note: Information regarding antibodies is inconsistent between certain publications.

Reference	Model	Trial	Antibodies, Adminstration, Dosage	Results
Wilcock et al. (2004b)	Tg2576	Therapeutic, 19 to 20m; 19 to 21m and 19 to 22m	mab 2286 (IgG1, e: $A\beta_{28-40}$) (intraperitoneal, weekly, 10mg/kg)	3m administration of mab 2286 rescued reduced Y maze alternation rates, 2m and 3m treatment reduced congophilic plaque burden, mab 2286 entered brain an labeled plaques. Transiently increased FC-receptor expression in microglia indicated phagocytotic activation, elevated plasma $A\beta$ levels indicated peripheral sink mechanism.
Wilcock et al. (2004c)	Tg2576	Therapeutic, 19 to 20m; 19 to 21m, 19 to 22m and 23m to 28m	mab 2286 (IgG1, e: $A\beta_{28-40}$) (intraperitoneal, weekly)	Reversal of spatial learning/memory deficits after 3 and 5 months of treatment. Significant reduction of plaque load in Frontal Cortex and Hippocampus after 5 months of treatment. Treatment reduced total and parenchymal but increased vascular amyloid burden after 2m/3m treatment. Abundant and increasing occurence of microhemorrhages associated with vascular amyloid after 2m, 3m and 5m treatment.
Racke et al. (2005)	PDAPP	Therapeutic, 22-23m, 6w duration	mab 266 (IgG1, E $A\beta_{13-28}$), mab 3D6 (IgG2a, E $A\beta_{1-5}$) (intraperitoneal, weekly, 50 mg/kg)	3D6 increases mean occurrence of microhemorrhages, whereas mab 266 does not.
Wilcock et al. (2006)	Tg2576	Therapeutic, 20m to 24m	mab 2H6 (IgG2b, E $A\beta_{33-40}$), de-glycosylated mab 2H6 IgG2b (intraperitoneal, weekly, 10 mg/kg)	Both mab eliminated spatial learning deficits and elevate serum $A\beta$ levels (higher levels after treatment with the de-glycosylated antibody). Both mab variants reduce plaque burden in the frontal cortex and hippocampus, but increase vascular amyloid. De-glycosylated mab 2H6 lowers increase of vascular amyloid compared to mab 2H6. De-glycosylation rescues increased microhemorrhage occurence observed with mab 2H6, and does not lead to significantly increased microglia activation in the vicinity of plaques in contrast to mab 2H6.
Levites et al. (2006)	Tg2576	Preventative, 7m to 11m	mab 42.2 (IgG1, E $A\beta_{x-42}$), mab 40.1 (IgG1, E $A\beta_{x-40}$), mab 9 (IgG2a, E $A\beta_{1-16}$) (intraperitoneal, 500 μg/mouse, biweekly)	All antibodies equally effective in reducing plaque load and insoluble $A\beta$ ELISA measures, no difference observed for $A\beta_{40/42}$ ratio between mab 42.2 and mab 40.1 groups.
	Tg2576	Therapeutic 11m to 15m	mab 42.2, mab 40.1 , mab 9 (intraperitoneal, 500 μg/mouse, biweekly)	No significant plaque lowering effect in all groups.
Schroeter et al. (2008)	PDAPP	Mid-stage, 12m to 18m	mab 266 (IgG1, E $A\beta_{13-28}$), mab 3D6 (IgG2a, E $A\beta_{1-5}$) (intraperitoneal, weekly, 3 mg/kg)	mab 3D6 but not mab 266 cleared/prevented vascular amyloid, 3D6 treated animals with significantly more microhemorrhages
	PDAPP	Mid-stage, dose response study, 12m to 18m	mab 3D6 (intraperitoneal, weekly, 0.1, 0.3, 3 mg/kg)	Only high dose group 3D6 with significantly more microhemorrhages, partial clearance of vascular amyloid at lower dose (0.3 mg/kg)

Table 4.4
Parenteral Chronic Passive Immunization Approaches in the 5XFAD, PDAPP, TG2576, APP/PS1ΔE9 and APP23 Mouse Models. Abbreviations: m: months; d: days; h: hours; E: epitope; mab: monoclonal antibody; pab: polyclonal antibody; tg: transgenic; CNS: central nervous system. Note: Information regarding antibodies is inconsistent between certain publications.

Reference	Model	Trial	Antibodies, Adminstration, Dosage	Results
Wirths et al. (2010c)	5XFAD	Mid-stage, 4.5m to 6m	mab 9D5 (IgG2b, $Aβ_{pE3−x}$−oligomer-specific) (intraperitoneal, weekly, 250 μg/mouse)	Reduced $Aβ$, $Aβ_{x−42}$, $Aβ_{x−40}$ and $Aβ_{pE3−x}$-plaque burden, reduced soluble and insoluble $Aβ_{pE3−x}$ levels in ELISA, amelioration of reduced anxiety phenotype
DeMattos et al. (2012)	PDAPP	Therapeutic, 22-24m to 25-26m	mab mE8-IgG1 and mE8-IgG2a ($Aβ_{pE−x}$-plaque specific), mab 3D6 (IgG2a, E $Aβ_{1−5}$) (intraperitoneal, weekly, 12.5 mg/kg)	Lowered $Aβ_{1−42}$ levels in hippocampus and cortex with mab mE8 (ELISA), but not with mab 3D6. High phagocytosis effector function supports clearance of $Aβ_{1−42}$ Elevated plasma $Aβ_{x−40/42}$ levels in the mab 3D6 cohort. Increase in microhemorrhage in the mab 3D6 cohort. mE8-treated mice activates microglia indicating effects partly depending on phagocytosis effector function
	PDAPP	Preventative, 5.5m to 12.5m	mE8-IgG2a, mab 3D6 (intraperitoneal, weekly, 12.5 mg/kg)	mab 3D6 but not mE8-IgG2a lowered $Aβ_{1−42}$ levels in hippocampus and cortex (ELISA)
	PDAPP	Mid-stage dose-response study, 16m to 22m	mab mE8-IgG2a (subcutaneous, weekly, 1.5, 4, 12.5 mg/kg)	Reduction of $Aβ_{1−42}$ levels is dose-dependent
Frost et al. (2012)	APP/PS1ΔE9	Preventative,5.8m to 11m	mab 07/1 (IgG1, $Aβ_{pE3−x}$ specific) (intraperitoneal, 200 μg/mouse)	Treatment prevented deposition of fibrillar amyloid, general $Aβ$ and $Aβ_{pE3−x}$ in hippocamus and of the previous two in cerebellum. Vascular amyloid reduced in cerebellum. Microgliosis and Astrogliosis seemed attenuated. No microhemorrhages observed, no significant differences in ELISA on brain lysates.
	APP/PS1ΔE9	Therapeutic, 23m, 7w duration	mab 07/1 (intraperitoneal, weekly, 200 μg/mouse)	General and fibrillar amyloid plaque burden reduced in hippocampus, general and $Aβ_{pE3−x}$ plaque burden reduced in cerebellum, positive trend for fibrillar amyloid. No microhemorrhages observed, no significant differences in ELISA on brain lysates.
Here	5XFAD	Mid-stage, 4.5m to 7m	mab NT4X-167 (anti-$Aβ_{4−x}$ and $Aβ_{pE−x}$), mab 1-57 (anti-$Aβ_{pE−x}$), mab 9D5 ($Aβ_{pE3−x}$−oligomer-specific) (intraperitoneal, weekly, 10 mg/kg)	Significant reduction of fibrillar amyloid deposits, $Aβ_{pE−x}$- and $Aβ_{40}$-positive plaques and trend towards amelioration of working memory impairment in the mab NT4X-167 group. Levels of $Aβ$ in ELISA unaltered. No microhemorrhages in all groups, no treatment effects for mab 1-57 and mab 9D5

REFERENCES

O. Adolfsson, M. Pihlgren, N. Toni, Y. Varisco, A. L. Buccarello, K. Antoniello, S. Lohmann, K. Piorkowska, V. Gafner, J. K. Atwal, J. Maloney, M. Chen, A. Gogineni, R. M. Weimer, D. L. Mortensen, M. Friesen-hahn, C. Ho, R. Paul, A. Pfeifer, A. Muhs, and R. J. Watts. An effector-reduced anti-beta-amyloid (Abeta)) antibody with unique Abeta binding properties promotes neuroprotection and glial engulf-ment of Abeta. *J. Neurosci.*, 32(28):9677–9689, Jul 2012.

M. S. Albert, S. T. DeKosky, D. Dickson, B. Dubois, H. H. Feldman, N. C. Fox, A. Gamst, D. M. Holtzman, W. J. Jagust, R. C. Petersen, P. J. Snyder, M. C. Carrillo, B. Thies, and C. H. Phelps. The diagnosis of mild cognitive impairment due to Alzheimer's disease: recommendations from the National Insti-tute on Aging-Alzheimer's Association workgroups on diagnostic guidelines for Alzheimer's disease. *Alzheimers Dement*, 7(3):270–279, May 2011.

N.A. Alcantar, J. Jimenez, and D. Morgan. Direct observation of the kinetic mechanisms for abeta peptide aggregation: Towards elucidating alzheimer plaque dissolution. *Alzheimer's & Dementia: The Journal of the Alzheimer's Association*, 6:S247, 2010.

A. Alexandru, W. Jagla, S. Graubner, A. Becker, C. Bauscher, S. Kohlmann, R. Sedlmeier, K. A. Raber, H. Cynis, R. Ronicke, K. G. Reymann, E. Petrasch-Parwez, M. Hartlage-Rubsamen, A. Waniek, S. Ross-ner, S. Schilling, A. P. Osmand, H. U. Demuth, and S. von Horsten. Selective hippocampal neurodegen-eration in transgenic mice expressing small amounts of truncated Abeta is induced by pyroglutamate-Abeta formation. *J. Neurosci.*, 31(36):12790–12801, Sep 2011.

A. C. Alonso, I. Grundke-Iqbal, and K. Iqbal. Alzheimer's disease hyperphosphorylated tau sequesters normal tau into tangles of filaments and disassembles microtubules. *Nat. Med.*, 2(7):783–787, Jul 1996.

A. Alzheimer. Über Eine Eigenartige Erkrankung der Hirnrinde. *Allg. Z. Psychiatr.*, 64:146–148, 1907.

W. Annaert and B. De Strooper. A cell biological perspective on Alzheimer's disease. *Annu. Rev. Cell Dev. Biol.*, 18:25–51, 2002.

G. Antonios, N. Saiepour, Y. Bouter, B. C. Richard, A. Paetau, A. Verkkoniemi-Ahola, L. Lannfelt, M. In-gelsson, G. G. Kovacs, T. Pillot, O. Wirths, and T. A. Bayer. N-truncated Abeta starting with position four: early intraneuronal accumulation and rescue of toxicity using NT4X-167, a novel monoclonal antibody. *Acta Neuropathol Commun*, 1(1):56, 2013.

I. Aprahamian, J. E. Martinelli, A. L. Neri, and M. S. Yassuda. The accuracy of the Clock Drawing Test compared to that of standard screening tests for Alzheimer's disease: results from a study of Brazilian elderly with heterogeneous educational backgrounds. *Int Psychogeriatr*, 22(1):64–71, Feb 2010.

G. W. Arendash, M. N. Gordon, D. M. Diamond, L. A. Austin, J. M. Hatcher, P. Jantzen, G. DiCarlo, D. Wilcock, and D. Morgan. Behavioral assessment of Alzheimer's transgenic mice following long-term Abeta vaccination: task specificity and correlations between Abeta deposition and spatial memory. *DNA Cell Biol.*, 20(11):737–744, Nov 2001a.

G. W. Arendash, D. L. King, M. N. Gordon, D. Morgan, J. M. Hatcher, C. E. Hope, and D. M. Diamond. Progressive, age-related behavioral impairments in transgenic mice carrying both mutant amyloid pre-cursor protein and presenilin-1 transgenes. *Brain Res.*, 891(1-2):42–53, Feb 2001b.

G. W. Arendash, J. Lewis, R. E. Leighty, E. McGowan, J. R. Cracchiolo, M. Hutton, and M. F. Garcia. Multi-metric behavioral comparison of APPsw and P301L models for Alzheimer's disease: linkage of poorer cognitive performance to tau pathology in forebrain. *Brain Res.*, 1012(1-2):29–41, Jun 2004.

S. E. Arnold, B. T. Hyman, J. Flory, A. R. Damasio, and G. W. Van Hoesen. The topographical and neuroanatomical distribution of neurofibrillary tangles and neuritic plaques in the cerebral cortex of patients with Alzheimer's disease. *Cereb. Cortex*, 1(1):103–116, 1991.

P. V. Arriagada, J. H. Growdon, E. T. Hedley-Whyte, and B. T. Hyman. Neurofibrillary tangles but not senile plaques parallel duration and severity of Alzheimer's disease. *Neurology*, 42(3 Pt 1):631–639, Mar 1992.

N. Aytan, J. K. Choi, I. Carreras, N. W. Kowall, B. G. Jenkins, and A. Dedeoglu. Combination therapy in a transgenic model of Alzheimer's disease. *Exp. Neurol.*, 250:228–238, Dec 2013.

B. J. Bacskai, S. T. Kajdasz, M. E. McLellan, D. Games, P. Seubert, D. Schenk, and B. T. Hyman. Non-Fc-mediated mechanisms are involved in clearance of amyloid-beta in vivo by immunotherapy. *J. Neurosci.*, 22(18):7873–7878, Sep 2002.

C. Ballard, S. Gauthier, A. Corbett, C. Brayne, D. Aarsland, and E. Jones. Alzheimer's disease. *Lancet*, 377 (9770):1019–1031, Mar 2011.

F. Bard, C. Cannon, R. Barbour, R. L. Burke, D. Games, H. Grajeda, T. Guido, K. Hu, J. Huang, K. Johnson-Wood, K. Khan, D. Kholodenko, M. Lee, I. Lieberburg, R. Motter, M. Nguyen, F. Soriano, N. Vasquez, K. Weiss, B. Welch, P. Seubert, D. Schenk, and T. Yednock. Peripherally administered antibodies against amyloid beta-peptide enter the central nervous system and reduce pathology in a mouse model of Alzheimer disease. *Nat. Med.*, 6(8):916–919, Aug 2000.

F. Bard, R. Barbour, C. Cannon, R. Carretto, M. Fox, D. Games, T. Guido, K. Hoenow, K. Hu, K. Johnson-Wood, K. Khan, D. Kholodenko, C. Lee, M. Lee, R. Motter, M. Nguyen, A. Reed, D. Schenk, P. Tang, N. Vasquez, P. Seubert, and T. Yednock. Epitope and isotype specificities of antibodies to beta -amyloid peptide for protection against Alzheimer's disease-like neuropathology. *Proc. Natl. Acad. Sci. U.S.A.*, 100(4):2023–2028, Feb 2003.

T. A. Bayer and O. Wirths. Intracellular accumulation of amyloid-Beta - a predictor for synaptic dysfunction and neuron loss in Alzheimer's disease. *Front Aging Neurosci*, 2:8, 2010.

T. A. Bayer and O. Wirths. Focusing the amyloid cascade hypothesis on N-truncated Abeta peptides as drug targets against Alzheimer's disease. *Acta Neuropathol.*, 127(6):787–801, Jun 2014.

L. Bertram, C. M. Lill, and R. E. Tanzi. The genetics of Alzheimer disease: back to the future. *Neuron*, 68 (2):270–281, Oct 2010.

S. Bhattacharya, C. Haertel, A. Maelicke, and D. Montag. Galantamine slows down plaque formation and behavioral decline in the 5XFAD mouse model of Alzheimer's disease. *PLoS ONE*, 9(2):e89454, 2014.

H. Bickeboller, D. Campion, A. Brice, P. Amouyel, D. Hannequin, O. Didierjean, C. Penet, C. Martin, J. Perez-Tur, A. Michon, B. Dubois, F. Ledoze, C. Thomas-Anterion, F. Pasquier, M. Puel, J. F. Demonet, O. Moreaud, M. C. Babron, D. Meulien, D. Guez, M. C. Chartier-Harlin, T. Frebourg, Y. Agid, M. Martinez, and F. Clerget-Darpoux. Apolipoprotein E and Alzheimer disease: genotype-specific risks by age and sex. *Am. J. Hum. Genet.*, 60(2):439–446, Feb 1997.

J. Bien, T. Jefferson, M. Causevi?, T. Jumpertz, L. Munter, G. Multhaup, S. Weggen, C. Becker-Pauly, and C. U. Pietrzik. The metalloprotease meprin beta generates amino terminal-truncated amyloid beta peptide species. *J. Biol. Chem.*, 287(40):33304–33313, Sep 2012.

K. Blennow, M. J. de Leon, and H. Zetterberg. Alzheimer's disease. *Lancet*, 368(9533):387–403, Jul 2006.

D. R. Borchelt, T. Ratovitski, J. van Lare, M. K. Lee, V. Gonzales, N. A. Jenkins, N. G. Copeland, D. L. Price, and S. S. Sisodia. Accelerated amyloid deposition in the brains of transgenic mice coexpressing mutant presenilin 1 and amyloid precursor proteins. *Neuron*, 19(4):939–945, Oct 1997.

Y. Bouter, K. Dietrich, J. L. Wittnam, N. Rezaei-Ghaleh, T. Pillot, S. Papot-Couturier, T. Lefebvre, F. Sprenger, O. Wirths, M. Zweckstetter, and T. A. Bayer. N-truncated amyloid-beta4-42 forms stable aggregates and induces acute and long-lasting behavioral deficits. *Acta Neuropathol.*, 126(2):189–205, Aug 2013.

Y. Bouter, T. Kacprowski, R. Weissmann, K. Dietrich, H. Borgers, A. Brauss, C. Sperling, O. Wirths, M. Albrecht, L. R. Jensen, A. W. Kuss, and T. A. Bayer. Deciphering the molecular profile of plaques, memory decline and neuron loss in two mouse models for Alzheimer's disease by deep sequencing. *Front Aging Neurosci*, 6:75, 2014.

H. Braak and E. Braak. Neuropathological stageing of Alzheimer-related changes. *Acta Neuropathol.*, 82 (4):239–259, 1991.

R. Bullock and A. Dengiz. Cognitive performance in patients with Alzheimer's disease receiving cholinesterase inhibitors for up to 5 years. *Int. J. Clin. Pract.*, 59(7):817–822, Jul 2005.

R. Bullock, J. Touchon, H. Bergman, G. Gambina, Y. He, G. Rapatz, J. Nagel, and R. Lane. Rivastigmine and donepezil treatment in moderate to moderately-severe Alzheimer's disease over a 2-year period. *Curr Med Res Opin*, 21(8):1317–1327, Aug 2005.

G. J. Burbach, A. Vlachos, E. Ghebremedhin, D. Del Turco, J. Coomaraswamy, M. Staufenbiel, M. Jucker, and T. Deller. Vessel ultrastructure in APP23 transgenic mice after passive anti-Abeta immunotherapy and subsequent intracerebral hemorrhage. *Neurobiol. Aging*, 28(2):202–212, Feb 2007.

T. Bussiere, F. Bard, R. Barbour, H. Grajeda, T. Guido, K. Khan, D. Schenk, D. Games, P. Seubert, and M. Buttini. Morphological characterization of Thioflavin-S-positive amyloid plaques in transgenic Alzheimer mice and effect of passive Abeta immunotherapy on their clearance. *Am. J. Pathol.*, 165 (3):987–995, Sep 2004.

M. E. Calhoun, K. H. Wiederhold, D. Abramowski, A. L. Phinney, A. Probst, C. Sturchler-Pierrat, M. Staufenbiel, B. Sommer, and M. Jucker. Neuron loss in APP transgenic mice. *Nature*, 395(6704): 755–756, Oct 1998.

P. Carrillo-Mora, R. Luna, and L. Colin-Barenque. Amyloid beta: multiple mechanisms of toxicity and only some protective effects? *Oxid Med Cell Longev*, 2014:795375, 2014.

C. Casas, N. Sergeant, J. M. Itier, V. Blanchard, O. Wirths, N. van der Kolk, V. Vingtdeux, E. van de Steeg, G. Ret, T. Canton, H. Drobecq, A. Clark, B. Bonici, A. Delacourte, J. Benavides, C. Schmitz, G. Tremp, T. A. Bayer, P. Benoit, and L. Pradier. Massive CA1/2 neuronal loss with intraneuronal and N-terminal truncated Abeta42 accumulation in a novel Alzheimer transgenic model. *Am. J. Pathol.*, 165(4):1289–1300, Oct 2004.

J. M. Castellano, J. Kim, F. R. Stewart, H. Jiang, R. B. DeMattos, B. W. Patterson, A. M. Fagan, J. C. Morris, K. G. Mawuenyega, C. Cruchaga, A. M. Goate, K. R. Bales, S. M. Paul, R. J. Bateman, and D. M. Holtzman. Human apoE isoforms differentially regulate brain amyloid-beta peptide clearance. *Sci Transl Med*, 3(89):89ra57, Jun 2011.

P. F. Chapman, G. L. White, M. W. Jones, D. Cooper-Blacketer, V. J. Marshall, M. Irizarry, L. Younkin, M. A. Good, T. V. Bliss, B. T. Hyman, S. G. Younkin, and K. K. Hsiao. Impaired synaptic plasticity and learning in aged amyloid precursor protein transgenic mice. *Nat. Neurosci.*, 2(3):271–276, Mar 1999.

G. Chen, K. S. Chen, J. Knox, J. Inglis, A. Bernard, S. J. Martin, A. Justice, L. McConlogue, D. Games, S. B. Freedman, and R. G. Morris. A learning deficit related to age and beta-amyloid plaques in a mouse model of Alzheimer's disease. *Nature*, 408(6815):975–979, 2000.

Y. Chen, Z. Tian, Z. Liang, S. Sun, C. L. Dai, M. H. Lee, F. M. LaFerla, I. Grundke-Iqbal, K. Iqbal, F. Liu, and C. X. Gong. Brain gene expression of a sporadic (icv-STZ Mouse) and a familial mouse model (3xTg-AD mouse) of Alzheimer's disease. *PLoS ONE*, 7(12):e51432, 2012.

Y. Chen, Z. Liang, J. Blanchard, C. L. Dai, S. Sun, M. H. Lee, I. Grundke-Iqbal, K. Iqbal, F. Liu, and C. X. Gong. A non-transgenic mouse model (icv-STZ mouse) of Alzheimer's disease: similarities to and differences from the transgenic model (3xTg-AD mouse). *Mol. Neurobiol.*, 47(2):711–725, Apr 2013.

W. H. Cho, J. C. Park, D. H. Kim, M. S. Kim, S. Y. Lee, H. Park, J. H. Kang, S. W. Yeon, and J. S. Han. ID1201, the ethanolic extract of the fruit of Melia toosendan ameliorates impairments in spatial learning and reduces levels of amyloid beta in 5XFAD mice. *Neurosci. Lett.*, 583:170–175, Nov 2014.

V. W. Chow, M. P. Mattson, P. C. Wong, and M. Gleichmann. An overview of APP processing enzymes and products. *Neuromolecular Med.*, 12(1):1–12, Mar 2010.

D. Z. Christensen. *Pathological Alterations Induced by Intraneuronal Abeta in Alzheimers Disease*. PhD thesis, Georg-August University Gttingen, Faculty of Medicine, 2009.

D. Z. Christensen, S. L. Kraus, A. Flohr, M. C. Cotel, O. Wirths, and T. A. Bayer. Transient intraneuronal A beta rather than extracellular plaque pathology correlates with neuron loss in the frontal cortex of APP/PS1KI mice. *Acta Neuropathol.*, 116(6):647–655, Dec 2008.

D. Z. Christensen, T. A. Bayer, and O. Wirths. Intracellular Ariggers neuron loss in the cholinergic system of the APP/PS1KI mouse model of Alzheimer's disease. *Neurobiol. Aging*, 31(7):1153–1163, Jul 2010a.

D. Z. Christensen, T. Schneider-Axmann, P. J. Lucassen, T. A. Bayer, and O. Wirths. Accumulation of intraneuronal Abeta correlates with ApoE4 genotype. *Acta Neuropathol.*, 119(5):555–566, May 2010b.

D. Z. Christensen, M. Huettenrauch, M. Mitkovski, L. Pradier, and O. Wirths. Axonal degeneration in an Alzheimer mouse model is PS1 gene dose dependent and linked to intraneuronal Abeta accumulation. *Front Aging Neurosci*, 6:139, 2014.

E. H. Corder, A. M. Saunders, W. J. Strittmatter, D. E. Schmechel, P. C. Gaskell, G. W. Small, A. D. Roses, J. L. Haines, and M. A. Pericak-Vance. Gene dose of apolipoprotein E type 4 allele and the risk of Alzheimer's disease in late onset families. *Science*, 261(5123):921–923, Aug 1993.

M. R. D'Andrea, R. G. Nagele, H. Y. Wang, P. A. Peterson, and D. H. Lee. Evidence that neurones accumulating amyloid can undergo lysis to form amyloid plaques in Alzheimer's disease. *Histopathology*, 38(2):120–134, Feb 2001.

M. R. D'Andrea, R. G. Nagele, N. A. Gumula, P. A. Reiser, D. A. Polkovitch, B. M. Hertzog, and P. Andrade-Gordon. Lipofuscin and Abeta42 exhibit distinct distribution patterns in normal and Alzheimer's disease brains. *Neurosci. Lett.*, 323(1):45–49, Apr 2002.

P. Das, M. P. Murphy, L. H. Younkin, S. G. Younkin, and T. E. Golde. Reduced effectiveness of Abeta1-42 immunization in APP transgenic mice with significant amyloid deposition. *Neurobiol. Aging*, 22(5): 721–727, 2001.

P. Das, V. Howard, N. Loosbrock, D. Dickson, M. P. Murphy, and T. E. Golde. Amyloid-beta immunization effectively reduces amyloid deposition in FcRgamma-/- knock-out mice. *J. Neurosci.*, 23(24):8532–8538, Sep 2003.

S. M. de la Monte and J. R. Wands. Alzheimer's disease is type 3 diabetes-evidence reviewed. *J Diabetes Sci Technol*, 2(6):1101–1113, Nov 2008.

V. J. De-Paula, M. Radanovic, B. S. Diniz, and O. V. Forlenza. Alzheimer's disease. *Subcell. Biochem.*, 65: 329–352, 2012.

R. B. DeMattos, K. R. Bales, D. J. Cummins, J. C. Dodart, S. M. Paul, and D. M. Holtzman. Peripheral anti-A beta antibody alters CNS and plasma A beta clearance and decreases brain A beta burden in a mouse model of Alzheimer's disease. *Proc. Natl. Acad. Sci. U.S.A.*, 98(15):8850–8855, Jul 2001.

R. B. DeMattos, K. R. Bales, M. Parsadanian, M. A. O'Dell, E. M. Foss, S. M. Paul, and D. M. Holtzman. Plaque-associated disruption of CSF and plasma amyloid-beta (Abeta) equilibrium in a mouse model of Alzheimer's disease. *J. Neurochem.*, 81(2):229–236, Apr 2002.

R. B. DeMattos, J. Lu, Y. Tang, M. M. Racke, C. A. Delong, J. A. Tzaferis, J. T. Hole, B. M. Forster, P. C. McDonnell, F. Liu, R. D. Kinley, W. H. Jordan, and M. L. Hutton. A plaque-specific antibody clears existing beta-amyloid plaques in Alzheimer's disease mice. *Neuron*, 76(5):908–920, Dec 2012.

D. W. Dickson, H. A. Crystal, L. A. Mattiace, D. M. Masur, A. D. Blau, P. Davies, S. H. Yen, and M. K. Aronson. Identification of normal and pathological aging in prospectively studied nondemented elderly humans. *Neurobiol. Aging*, 13(1):179–189, 1992.

K. T. Dineley, X. Xia, D. Bui, J. D. Sweatt, and H. Zheng. Accelerated plaque accumulation, associative learning deficits, and up-regulation of alpha 7 nicotinic receptor protein in transgenic mice co-expressing mutant human presenilin 1 and amyloid precursor proteins. *J. Biol. Chem.*, 277(25):22768–22780, Jun 2002.

J. C. Dodart, H. Meziane, C. Mathis, K. R. Bales, S. M. Paul, and A. Ungerer. Behavioral disturbances in transgenic mice overexpressing the V717F beta-amyloid precursor protein. *Behav. Neurosci.*, 113(5): 982–990, Oct 1999.

J. C. Dodart, C. Mathis, J. Saura, K. R. Bales, S. M. Paul, and A. Ungerer. Neuroanatomical abnormalities in behaviorally characterized APP(V717F) transgenic mice. *Neurobiol. Dis.*, 7(2):71–85, Apr 2000.

J. C. Dodart, K. R. Bales, K. S. Gannon, S. J. Greene, R. B. DeMattos, C. Mathis, C. A. DeLong, S. Wu, X. Wu, D. M. Holtzman, and S. M. Paul. Immunization reverses memory deficits without reducing brain Abeta burden in Alzheimer's disease model. *Nat. Neurosci.*, 5(5):452–457, May 2002.

D. N. Drechsel, A. A. Hyman, M. H. Cobb, and M. W. Kirschner. Modulation of the dynamic instability of tubulin assembly by the microtubule-associated protein tau. *Mol. Biol. Cell*, 3(10):1141–1154, Oct 1992.

C. Duyckaerts, M. C. Potier, and B. Delatour. Alzheimer disease models and human neuropathology: similarities and differences. *Acta Neuropathol.*, 115(1):5–38, Jan 2008.

C. Duyckaerts, B. Delatour, and M. C. Potier. Classification and basic pathology of Alzheimer disease. *Acta Neuropathol.*, 118(1):5–36, Jul 2009.

W. A. Eimer and R. Vassar. Neuron loss in the 5XFAD mouse model of Alzheimer's disease correlates with intraneuronal Abeta42 accumulation and Caspase-3 activation. *Mol Neurodegener*, 8:2, 2013.

G. A. Elder, M. A. Gama Sosa, and R. De Gasperi. Transgenic mouse models of Alzheimer's disease. *Mt. Sinai J. Med.*, 77(1):69–81, 2010.

F. S. Esch, P. S. Keim, E. C. Beattie, R. W. Blacher, A. R. Culwell, T. Oltersdorf, D. McClure, and P. J. Ward. Cleavage of amyloid beta peptide during constitutive processing of its precursor. *Science*, 248(4959): 1122–1124, Jun 1990.

C. Esh, L. Patton, W. Kalback, T. A. Kokjohn, J. Lopez, D. Brune, A. J. Newell, T. Beach, D. Schenk, D. Games, S. Paul, K. Bales, B. Ghetti, E. M. Castano, and A. E. Roher. Altered APP processing in PDAPP (Val717 –> Phe) transgenic mice yields extended-length Abeta peptides. *Biochemistry*, 44(42): 13807–13819, Oct 2005.

P. Fernandez-Vizarra, A. P. Fernandez, S. Castro-Blanco, J. Serrano, M. L. Bentura, R. Martinez-Murillo, A. Martinez, and J. Rodrigo. Intra- and extracellular Abeta and PHF in clinically evaluated cases of Alzheimer's disease. *Histol. Histopathol.*, 19(3):823–844, Jul 2004.

I. Ferrer, M. Boada Rovira, M. L. Sanchez Guerra, M. J. Rey, and F. Costa-Jussa. Neuropathology and pathogenesis of encephalitis following amyloid-beta immunization in Alzheimer's disease. *Brain Pathol.*, 14 (1):11–20, Jan 2004.

M. S. Fiandaca, M. E. Mapstone, A. K. Cheema, and H. J. Federoff. The critical need for defining preclinical biomarkers in Alzheimer's disease. *Alzheimers Dement*, 10(3 Suppl):196–212, Jun 2014.

M. A. Fiol-deRoque, R. Gutierrez-Lanza, S. Teres, M. Torres, P. Barcelo, R. V. Rial, A. Verkhratsky, P. V. Escriba, X. Busquets, and J. J. Rodriguez. Cognitive recovery and restoration of cell proliferation in the dentate gyrus in the 5XFAD transgenic mice model of Alzheimer's disease following 2-hydroxy-DHA treatment. *Biogerontology*, 14(6):763–775, Dec 2013.

M. F. Folstein, S. E. Folstein, and P. R. McHugh. "Mini-mental state". A practical method for grading the cognitive state of patients for the clinician. *J Psychiatr Res*, 12(3):189–198, Nov 1975.

L. Fratiglioni, S. Paillard-Borg, and B. Winblad. An active and socially integrated lifestyle in late life might protect against dementia. *Lancet Neurol*, 3(6):343–353, Jun 2004.

R. P. Friedrich, K. Tepper, R. Ronicke, M. Soom, M. Westermann, K. Reymann, C. Kaether, and M. Fandrich. Mechanism of amyloid plaque formation suggests an intracellular basis of Abeta pathogenicity. *Proc. Natl. Acad. Sci. U.S.A.*, 107(5):1942–1947, Feb 2010.

S. K. Fritschi, A. Cintron, L. Ye, J. Mahler, A. Buhler, F. Baumann, M. Neumann, K. P. Nilsson, P. Hammarstrom, L. C. Walker, and M. Jucker. Abeta seeds resist inactivation by formaldehyde. *Acta Neuropathol.*, 128(4):477–484, Oct 2014a.

S. K. Fritschi, F. Langer, S. A. Kaeser, L. F. Maia, E. Portelius, D. Pinotsi, C. F. Kaminski, D. T. Winkler, W. Maetzler, K. Keyvani, P. Spitzer, J. Wiltfang, G. S. Kaminski Schierle, H. Zetterberg, M. Staufenbiel, and M. Jucker. Highly potent soluble amyloid-beta seeds in human Alzheimer brain but not cerebrospinal fluid. *Brain*, 137(Pt 11):2909–2915, Nov 2014b.

J. L. Frost, B. Liu, M. Kleinschmidt, S. Schilling, H. U. Demuth, and C. A. Lemere. Passive immunization against pyroglutamate-3 amyloid-beta reduces plaque burden in Alzheimer-like transgenic mice: a pilot study. *Neurodegener Dis*, 10(1-4):265–270, 2012.

J. L. Frost, K. X. Le, H. Cynis, E. Ekpo, M. Kleinschmidt, R. M. Palmour, F. R. Ervin, S. Snigdha, C. W. Cotman, T. C. Saido, R. J. Vassar, P. St George-Hyslop, T. Ikezu, S. Schilling, H. U. Demuth, and C. A. Lemere. Pyroglutamate-3 amyloid-beta deposition in the brains of humans, non-human primates, canines, and Alzheimer disease-like transgenic mouse models. *Am. J. Pathol.*, 183(2):369–381, Aug 2013.

J. D. Fryer, J. W. Taylor, R. B. DeMattos, K. R. Bales, S. M. Paul, M. Parsadanian, and D. M. Holtzman. Apolipoprotein E markedly facilitates age-dependent cerebral amyloid angiopathy and spontaneous hemorrhage in amyloid precursor protein transgenic mice. *J. Neurosci.*, 23(21):7889–7896, Aug 2003.

K. Furukawa, B. L. Sopher, R. E. Rydel, J. G. Begley, D. G. Pham, G. M. Martin, M. Fox, and M. P. Mattson. Increased activity-regulating and neuroprotective efficacy of alpha-secretase-derived secreted amyloid precursor protein conferred by a C-terminal heparin-binding domain. *J. Neurochem.*, 67(5):1882–1896, Nov 1996.

D. Galimberti and E. Scarpini. Progress in Alzheimer's disease. *J. Neurol.*, 259(2):201–211, Feb 2012.

D. Games, D. Adams, R. Alessandrini, R. Barbour, P. Berthelette, C. Blackwell, T. Carr, J. Clemens, T. Donaldson, and F. Gillespie. Alzheimer-type neuropathology in transgenic mice overexpressing V717F beta-amyloid precursor protein. *Nature*, 373(6514):523–527, Feb 1995.

M. Garcia-Alloza, E. M. Robbins, S. X. Zhang-Nunes, S. M. Purcell, R. A. Betensky, S. Raju, C. Prada, S. M. Greenberg, B. J. Bacskai, and M. P. Frosch. Characterization of amyloid deposition in the APPswe/PS1dE9 mouse model of Alzheimer disease. *Neurobiol. Dis.*, 24(3):516–524, Dec 2006.

D. C. German, U. Yazdani, S. G. Speciale, P. Pasbakhsh, D. Games, and C. L. Liang. Cholinergic neuropathology in a mouse model of Alzheimer's disease. *J. Comp. Neurol.*, 462(4):371–381, Aug 2003.

J. F. Ghersi-Egea, P. D. Gorevic, J. Ghiso, B. Frangione, C. S. Patlak, and J. D. Fenstermacher. Fate of cerebrospinal fluid-borne amyloid beta-peptide: rapid clearance into blood and appreciable accumulation by cerebral arteries. *J. Neurochem.*, 67(2):880–883, Aug 1996.

P. Giannakopoulos, F. R. Herrmann, T. Bussiere, C. Bouras, E. Kovari, D. P. Perl, J. H. Morrison, G. Gold, and P. R. Hof. Tangle and neuron numbers, but not amyloid load, predict cognitive status in Alzheimer's disease. *Neurology*, 60(9):1495–1500, May 2003.

V. Giedraitis, J. Sundelof, M. C. Irizarry, N. Garevik, B. T. Hyman, L. O. Wahlund, M. Ingelsson, and L. Lannfelt. The normal equilibrium between CSF and plasma amyloid beta levels is disrupted in Alzheimer's disease. *Neurosci. Lett.*, 427(3):127–131, Nov 2007.

G. G. Glenner and C. W. Wong. Alzheimer's disease: initial report of the purification and characterization of a novel cerebrovascular amyloid protein. *Biochem. Biophys. Res. Commun.*, 120(3):885–890, May 1984.

M. Goedert and R. Jakes. Mutations causing neurodegenerative tauopathies. *Biochim. Biophys. Acta*, 1739 (2-3):240–250, Jan 2005.

T. Gomez-Isla, R. Hollister, H. West, S. Mui, J. H. Growdon, R. C. Petersen, J. E. Parisi, and B. T. Hyman. Neuronal loss correlates with but exceeds neurofibrillary tangles in Alzheimer's disease. *Ann. Neurol.*, 41(1):17–24, Jan 1997.

G. K. Gouras, J. Tsai, J. Naslund, B. Vincent, M. Edgar, F. Checler, J. P. Greenfield, V. Haroutunian, J. D. Buxbaum, H. Xu, P. Greengard, and N. R. Relkin. Intraneuronal Abeta42 accumulation in human brain. *Am. J. Pathol.*, 156(1):15–20, Jan 2000.

G. K. Gouras, D. Tampellini, R. H. Takahashi, and E. Capetillo-Zarate. Intraneuronal beta-amyloid accumulation and synapse pathology in Alzheimer's disease. *Acta Neuropathol.*, 119(5):523–541, May 2010.

I. Grundke-Iqbal, K. Iqbal, Y. C. Tung, M. Quinlan, H. M. Wisniewski, and L. I. Binder. Abnormal phosphorylation of the microtubule-associated protein tau (tau) in Alzheimer cytoskeletal pathology. *Proc. Natl. Acad. Sci. U.S.A.*, 83(13):4913–4917, Jul 1986.

Y. Gu, J. W. Nieves, Y. Stern, J. A. Luchsinger, and N. Scarmeas. Food combination and Alzheimer disease risk: a protective diet. *Arch. Neurol.*, 67(6):699–706, Jun 2010.

N. Gustke, B. Trinczek, J. Biernat, E. M. Mandelkow, and E. Mandelkow. Domains of tau protein and interactions with microtubules. *Biochemistry*, 33(32):9511–9522, Aug 1994.

E. A. Guzman, Y. Bouter, B. C. Richard, L. Lannfelt, M. Ingelsson, A. Paetau, A. Verkkoniemi-Ahola, O. Wirths, and T. A. Bayer. Abundance of Abeta5-X like immunoreactivity in transgenic 5XFAD, APP/PS1KI and 3xTG mice, sporadic and familial Alzheimer's disease. *Mol Neurodegener*, 9:13, 2014.

K. A. Gyure, R. Durham, W. F. Stewart, J. E. Smialek, and J. C. Troncoso. Intraneuronal abeta-amyloid precedes development of amyloid plaques in Down syndrome. *Arch. Pathol. Lab. Med.*, 125(4):489–492, Apr 2001.

C. Haass. Take five–BACE and the gamma-secretase quartet conduct Alzheimer's amyloid beta-peptide generation. *EMBO J.*, 23(3):483–488, Feb 2004.

C. Haass and D. J. Selkoe. Soluble protein oligomers in neurodegeneration: lessons from the Alzheimer's amyloid beta-peptide. *Nat. Rev. Mol. Cell Biol.*, 8(2):101–112, Feb 2007.

C. Haass, C. Kaether, G. Thinakaran, and S. Sisodia. Trafficking and proteolytic processing of APP. *Cold Spring Harb Perspect Med*, 2(5):a006270, May 2012.

C. B. Hall, R. B. Lipton, M. Sliwinski, M. J. Katz, C. A. Derby, and J. Verghese. Cognitive activities delay onset of memory decline in persons who develop dementia. *Neurology*, 73(5):356–361, Aug 2009.

G. M. Halliday, K. L. Double, V. Macdonald, and J. J. Kril. Identifying severely atrophic cortical subregions in Alzheimer's disease. *Neurobiol. Aging*, 24(6):797–806, Oct 2003.

J. Hardy and D. Allsop. Amyloid deposition as the central event in the aetiology of Alzheimer's disease. *Trends Pharmacol. Sci.*, 12(10):383–388, Oct 1991.

W. Härtig, S. Goldhammer, U. Bauer, F. Wegner, O. Wirths, T. A. Bayer, and J. Grosche. Concomitant detection of beta-amyloid peptides with N-terminal truncation and different C-terminal endings in cortical plaques from cases with Alzheimer's disease, senile monkeys and triple transgenic mice. *J. Chem. Neuroanat.*, 40(1):82–92, Sep 2010.

R. E. Hartman, Y. Izumi, K. R. Bales, S. M. Paul, D. F. Wozniak, and D. M. Holtzman. Treatment with an amyloid-beta antibody ameliorates plaque load, learning deficits, and hippocampal long-term potentiation in a mouse model of Alzheimer's disease. *J. Neurosci.*, 25(26):6213–6220, Jun 2005.

J. Hau and S.J. Schapiro. *Handbook of Laboratory Animal Science, Second Edition: Essential Principles and Practices*. Taylor & Francis, 2002.

A. Hillmann, S. Hahn, S. Schilling, T. Hoffmann, H. U. Demuth, B. Bulic, T. Schneider-Axmann, T. A. Bayer, S. Weggen, and O. Wirths. No improvement after chronic ibuprofen treatment in the 5XFAD mouse model of Alzheimer's disease. *Neurobiol. Aging*, 33(4):39–50, Apr 2012.

C. Hock, U. Konietzko, A. Papassotiropoulos, A. Wollmer, J. Streffer, R. C. von Rotz, G. Davey, E. Moritz, and R. M. Nitsch. Generation of antibodies specific for beta-amyloid by vaccination of patients with Alzheimer disease. *Nat. Med.*, 8(11):1270–1275, Nov 2002.

D. M. Holtzman, J. C. Morris, and A. M. Goate. Alzheimer's disease: the challenge of the second century. *Sci Transl Med*, 3(77):77sr1, Apr 2011.

S. Hong, O. Quintero-Monzon, B. L. Ostaszewski, D. R. Podlisny, W. T. Cavanaugh, T. Yang, D. M. Holtzman, J. R. Cirrito, and D. J. Selkoe. Dynamic analysis of amyloid beta-protein in behaving mice reveals opposing changes in ISF versus parenchymal Abeta during age-related plaque formation. *J. Neurosci.*, 31(44):15861–15869, Nov 2011.

S. Howell, J. Nalbantoglu, and P. Crine. Neutral endopeptidase can hydrolyze beta-amyloid(1-40) but shows no effect on beta-amyloid precursor protein metabolism. *Peptides*, 16(4):647–652, 1995.

K. Hsiao, P. Chapman, S. Nilsen, C. Eckman, Y. Harigaya, S. Younkin, F. Yang, and G. Cole. Correlative memory deficits, Abeta elevation, and amyloid plaques in transgenic mice. *Science*, 274(5284):99–102, Oct 1996.

X. Hu, S. L. Crick, G. Bu, C. Frieden, R. V. Pappu, and J. M. Lee. Amyloid seeds formed by cellular uptake, concentration, and aggregation of the amyloid-beta peptide. *Proc. Natl. Acad. Sci. U.S.A.*, 106 (48):20324–20329, Dec 2009.

M. Hullmann. *Evaluation of the effects of inhaled nanoparticles on the central nervous system of mice.* PhD thesis, Heinrich Heine Universität Düsseldorf, 2012.

M. Hutton, C. L. Lendon, P. Rizzu, M. Baker, S. Froelich, H. Houlden, S. Pickering-Brown, S. Chakraverty, A. Isaacs, A. Grover, J. Hackett, J. Adamson, S. Lincoln, D. Dickson, P. Davies, R. C. Petersen, M. Stevens, E. de Graaff, E. Wauters, J. van Baren, M. Hillebrand, M. Joosse, J. M. Kwon, P. Nowotny, L. K. Che, J. Norton, J. C. Morris, L. A. Reed, J. Trojanowski, H. Basun, L. Lannfelt, M. Neystat, S. Fahn, F. Dark, T. Tannenberg, P. R. Dodd, N. Hayward, J. B. Kwok, P. R. Schofield, A. Andreadis, J. Snowden, D. Craufurd, D. Neary, F. Owen, B. A. Oostra, J. Hardy, A. Goate, J. van Swieten, D. Mann, T. Lynch, and P. Heutink. Association of missense and 5'-splice-site mutations in tau with the inherited dementia FTDP-17. *Nature*, 393(6686):702–705, Jun 1998.

K. Iqbal, C. Alonso, Adel, S. Chen, M. O. Chohan, E. El-Akkad, C. X. Gong, S. Khatoon, B. Li, F. Liu, A. Rahman, H. Tanimukai, and I. Grundke-Iqbal. Tau pathology in Alzheimer disease and other tauopathies. *Biochim. Biophys. Acta*, 1739(2-3):198–210, Jan 2005.

S. Itagaki, P. L. McGeer, H. Akiyama, S. Zhu, and D. Selkoe. Relationship of microglia and astrocytes to amyloid deposits of Alzheimer disease. *J. Neuroimmunol.*, 24(3):173–182, Oct 1989.

N. Iwata, S. Tsubuki, Y. Takaki, K. Shirotani, B. Lu, N. P. Gerard, C. Gerard, E. Hama, H. J. Lee, and T. C. Saido. Metabolic regulation of brain Abeta by neprilysin. *Science*, 292(5521):1550–1552, May 2001.

T. Iwatsubo, A. Odaka, N. Suzuki, H. Mizusawa, N. Nukina, and Y. Ihara. Visualization of Abeta 42(43) and Abeta 40 in senile plaques with end-specific A beta monoclonals: evidence that an initially deposited species is Abeta 42(43). *Neuron*, 13(1):45–53, Jul 1994.

C. R. Jack, M. M. Shiung, S. D. Weigand, P. C. O'Brien, J. L. Gunter, B. F. Boeve, D. S. Knopman, G. E. Smith, R. J. Ivnik, E. G. Tangalos, and R. C. Petersen. Brain atrophy rates predict subsequent clinical conversion in normal elderly and amnestic MCI. *Neurology*, 65(8):1227–1231, Oct 2005.

C. R. Jack, D. S. Knopman, W. J. Jagust, L. M. Shaw, P. S. Aisen, M. W. Weiner, R. C. Petersen, and J. Q. Trojanowski. Hypothetical model of dynamic biomarkers of the Alzheimer's pathological cascade. *Lancet Neurol*, 9(1):119–128, Jan 2010.

C. R. Jack, M. S. Albert, D. S. Knopman, G. M. McKhann, R. A. Sperling, M. C. Carrillo, B. Thies, and C. H. Phelps. Introduction to the recommendations from the National Institute on Aging-Alzheimer's Association workgroups on diagnostic guidelines for Alzheimer's disease. *Alzheimers Dement*, 7(3): 257–262, May 2011.

C. R. Jack, H. J. Wiste, T. G. Lesnick, S. D. Weigand, D. S. Knopman, P. Vemuri, V. S. Pankratz, M. L. Senjem, J. L. Gunter, M. M. Mielke, V. J. Lowe, B. F. Boeve, and R. C. Petersen. Brain Beta-amyloid load approaches a plateau. *Neurology*, 80(10):890–896, Mar 2013.

W. Jagust. Positron emission tomography and magnetic resonance imaging in the diagnosis and prediction of dementia. *Alzheimers Dement*, 2(1):36–42, Jan 2006.

A. Jan, O. Gokce, R. Luthi-Carter, and H. A. Lashuel. The ratio of monomeric to aggregated forms of Abeta40 and Abeta42 is an important determinant of amyloid-beta aggregation, fibrillogenesis, and toxicity. *J. Biol. Chem.*, 283(42):28176–28189, Oct 2008.

C. Janus, J. Pearson, J. McLaurin, P. M. Mathews, Y. Jiang, S. D. Schmidt, M. A. Chishti, P. Horne, D. Heslin, J. French, H. T. Mount, R. A. Nixon, M. Mercken, C. Bergeron, P. E. Fraser, P. St George-Hyslop, and D. Westaway. A beta peptide immunization reduces behavioural impairment and plaques in a model of Alzheimer's disease. *Nature*, 408(6815):979–982, 2000.

J. T. Jarrett, E. P. Berger, and P. T. Lansbury. The carboxy terminus of the beta amyloid protein is critical for the seeding of amyloid formation: implications for the pathogenesis of Alzheimer's disease. *Biochemistry*, 32(18):4693–4697, May 1993.

S. Jawhar, O. Wirths, S. Schilling, S. Graubner, H. U. Demuth, and T. A. Bayer. Overexpression of glutaminyl cyclase, the enzyme responsible for pyroglutamate Abeta formation, induces behavioral deficits, and glutaminyl cyclase knock-out rescues the behavioral phenotype in 5XFAD mice. *J. Biol. Chem.*, 286 (6):4454–4460, Feb 2011.

S. Jawhar, A. Trawicka, C. Jenneckens, T. A. Bayer, and O. Wirths. Motor deficits, neuron loss, and reduced anxiety coinciding with axonal degeneration and intraneuronal Abeta aggregation in the 5XFAD mouse model of Alzheimer's disease. *Neurobiol. Aging*, 33(1):29–40, Jan 2012.

T. Jonsson, J. K. Atwal, S. Steinberg, J. Snaedal, P. V. Jonsson, S. Bjornsson, H. Stefansson, P. Sulem, D. Gudbjartsson, J. Maloney, K. Hoyte, A. Gustafson, Y. Liu, Y. Lu, T. Bhangale, R. R. Graham, J. Huttenlocher, G. Bjornsdottir, O. A. Andreassen, E. G. Jonsson, A. Palotie, T. W. Behrens, O. T. Magnusson, A. Kong, U. Thorsteinsdottir, R. J. Watts, and K. Stefansson. A mutation in APP protects against Alzheimer's disease and age-related cognitive decline. *Nature*, 488(7409):96–99, Aug 2012.

C. Kaether, C. Haass, and H. Steiner. Assembly, trafficking and function of gamma-secretase. *Neurodegener Dis*, 3(4-5):275–283, 2006.

W. Kalback, M. D. Watson, T. A. Kokjohn, Y. M. Kuo, N. Weiss, D. C. Luehrs, J. Lopez, D. Brune, S. S. Sisodia, M. Staufenbiel, M. Emmerling, and A. E. Roher. APP transgenic mice Tg2576 accumulate Abeta peptides that are distinct from the chemically modified and insoluble peptides deposited in Alzheimer's disease senile plaques. *Biochemistry*, 41(3):922–928, Jan 2002.

N. Kaneko, R. Yamamoto, T. A. Sato, and K. Tanaka. Identification and quantification of amyloid beta-related peptides in human plasma using matrix-assisted laser desorption/ionization time-of-flight mass spectrometry. *Proc. Jpn. Acad., Ser. B, Phys. Biol. Sci.*, 90(3):104–117, 2014.

J. Kang, H. G. Lemaire, A. Unterbeck, J. M. Salbaum, C. L. Masters, K. H. Grzeschik, G. Multhaup, K. Beyreuther, and B. Muller-Hill. The precursor of Alzheimer's disease amyloid A4 protein resembles a cell-surface receptor. *Nature*, 325(6106):733–736, 1987.

T. Karl, R. Pabst, and S. von Horsten. Behavioral phenotyping of mice in pharmacological and toxicological research. *Exp. Toxicol. Pathol.*, 55(1):69–83, Jul 2003.

R. A. Karlnoski, A. Rosenthal, J. Alamed, V. Ronan, M. N. Gordon, P. E. Gottschall, J. Grimm, J. Pons, and D. Morgan. Deglycosylated anti-Abeta antibody dose-response effects on pathology and memory in APP transgenic mice. *J Neuroimmune Pharmacol*, 3(3):187–197, Sep 2008.

E. Karran, M. Mercken, and B. De Strooper. The amyloid cascade hypothesis for Alzheimer's disease: an appraisal for the development of therapeutics. *Nat Rev Drug Discov*, 10(9):698–712, Sep 2011.

T. Kawarabayashi, L. H. Younkin, T. C. Saido, M. Shoji, K. H. Ashe, and S. G. Younkin. Age-dependent changes in brain, CSF, and plasma amyloid (beta) protein in the Tg2576 transgenic mouse model of Alzheimer's disease. *J. Neurosci.*, 21(2):372–381, Jan 2001.

P. H. Kelly, L. Bondolfi, D. Hunziker, H. P. Schlecht, K. Carver, E. Maguire, D. Abramowski, K. H. Wiederhold, C. Sturchler-Pierrat, M. Jucker, R. Bergmann, M. Staufenbiel, and B. Sommer. Progressive age-related impairment of cognitive behavior in APP23 transgenic mice. *Neurobiol. Aging*, 24(2):365–378, 2003.

M. Kidd. Paired helical filaments in electron microscopy of Alzheimer's disease. *Nature*, 197:192–193, Jan 1963.

M. Kivipelto, E. L. Helkala, M. P. Laakso, T. Hanninen, M. Hallikainen, K. Alhainen, H. Soininen, J. Tuomilehto, and A. Nissinen. Midlife vascular risk factors and Alzheimer's disease in later life: longitudinal, population based study. *BMJ*, 322(7300):1447–1451, Jun 2001.

M. Kivipelto, T. Ngandu, L. Fratiglioni, M. Viitanen, I. Kareholt, B. Winblad, E. L. Helkala, J. Tuomilehto, H. Soininen, and A. Nissinen. Obesity and vascular risk factors at midlife and the risk of dementia and Alzheimer disease. *Arch. Neurol.*, 62(10):1556–1560, Oct 2005.

D. S. Knopman, J. E. Parisi, A. Salviati, M. Floriach-Robert, B. F. Boeve, R. J. Ivnik, G. E. Smith, D. W. Dickson, K. A. Johnson, L. E. Petersen, W. C. McDonald, H. Braak, and R. C. Petersen. Neuropathology of cognitively normal elderly. *J. Neuropathol. Exp. Neurol.*, 62(11):1087–1095, Nov 2003.

J. Koenigsknecht-Talboo, M. Meyer-Luehmann, M. Parsadanian, M. Garcia-Alloza, M. B. Finn, B. T. Hyman, B. J. Bacskai, and D. M. Holtzman. Rapid microglial response around amyloid pathology after systemic anti-Abeta antibody administration in PDAPP mice. *J. Neurosci.*, 28(52):14156–14164, Dec 2008.

R. M. Koffie, M. Meyer-Luehmann, T. Hashimoto, K. W. Adams, M. L. Mielke, M. Garcia-Alloza, K. D. Micheva, S. J. Smith, M. L. Kim, V. M. Lee, B. T. Hyman, and T. L. Spires-Jones. Oligomeric amyloid beta associates with postsynaptic densities and correlates with excitatory synapse loss near senile plaques. *Proc. Natl. Acad. Sci. U.S.A.*, 106(10):4012–4017, Mar 2009.

J. R. Korenberg, S. M. Pulst, R. L. Neve, and R. West. The Alzheimer amyloid precursor protein maps to human chromosome 21 bands q21.105-q21.05. *Genomics*, 5(1):124–127, Jul 1989.

L. A. Kotilinek, B. Bacskai, M. Westerman, T. Kawarabayashi, L. Younkin, B. T. Hyman, S. Younkin, and K. H. Ashe. Reversible memory loss in a mouse transgenic model of Alzheimer's disease. *J. Neurosci.*, 22(15):6331–6335, Aug 2002.

D. L. Krause and N. Muller. Neuroinflammation, microglia and implications for anti-inflammatory treatment in Alzheimer's disease. *Int J Alzheimers Dis*, 2010, 2010.

J. J. Kril, J. Hodges, and G. Halliday. Relationship between hippocampal volume and CA1 neuron loss in brains of humans with and without Alzheimer's disease. *Neurosci. Lett.*, 361(1-3):9–12, May 2004.

Y. M. Kuo, M. R. Emmerling, A. S. Woods, R. J. Cotter, and A. E. Roher. Isolation, chemical characterization, and quantitation of A beta 3-pyroglutamyl peptide from neuritic plaques and vascular amyloid deposits. *Biochem. Biophys. Res. Commun.*, 237(1):188–191, Aug 1997.

Y. M. Kuo, T. A. Kokjohn, T. G. Beach, L. I. Sue, D. Brune, J. C. Lopez, W. M. Kalback, D. Abramowski, C. Sturchler-Pierrat, M. Staufenbiel, and A. E. Roher. Comparative analysis of amyloid-beta chemical structure and amyloid plaque morphology of transgenic mouse and Alzheimer's disease brains. *J. Biol. Chem.*, 276(16):12991–12998, Apr 2001.

L. Lannfelt, N. R. Relkin, and E. R. Siemers. Amyloid-directed immunotherapy for Alzheimer's disease. *J. Intern. Med.*, 275(3):284–295, Mar 2014.

E. B. Lee, L. Z. Leng, V. M. Lee, and J. Q. Trojanowski. Meningoencephalitis associated with passive immunization of a transgenic murine model of Alzheimer's amyloidosis. *FEBS Lett.*, 579(12):2564–2568, May 2005.

V. M. Lee, B. J. Balin, L. Otvos, and J. Q. Trojanowski. A68: a major subunit of paired helical filaments and derivatized forms of normal Tau. *Science*, 251(4994):675–678, Feb 1991.

C. L. Leibson, W. A. Rocca, V. A. Hanson, R. Cha, E. Kokmen, P. C. O'Brien, and P. J. Palumbo. Risk of dementia among persons with diabetes mellitus: a population-based cohort study. *Am. J. Epidemiol.*, 145(4):301–308, Feb 1997.

M. B. Lenders, M. C. Peers, G. Tramu, A. Delacourte, A. Defossez, H. Petit, and M. Mazzuca. Dystrophic peptidergic neurites in senile plaques of Alzheimer's disease hippocampus precede formation of paired helical filaments. *Brain Res.*, 481(2):344–349, Mar 1989.

Y. Levites, P. Das, R. W. Price, M. J. Rochette, L. A. Kostura, E. M. McGowan, M. P. Murphy, and T. E. Golde. Anti-Abeta42- and anti-Abeta40-specific mAbs attenuate amyloid deposition in an Alzheimer disease mouse model. *J. Clin. Invest.*, 116(1):193–201, Jan 2006.

H. Lewis, D. Beher, N. Cookson, A. Oakley, M. Piggott, C. M. Morris, E. Jaros, R. Perry, P. Ince, R. A. Kenny, C. G. Ballard, M. S. Shearman, and R. N. Kalaria. Quantification of Alzheimer pathology in ageing and dementia: age-related accumulation of amyloid-beta(42) peptide in vascular dementia. *Neuropathol. Appl. Neurobiol.*, 32(2):103–118, Apr 2006.

M. C. Liao, M. Ahmed, S. O. Smith, and W. E. Van Nostrand. Degradation of amyloid beta protein by purified myelin basic protein. *J. Biol. Chem.*, 284(42):28917–28925, Oct 2009.

A. Lord, H. Englund, L. Soderberg, S. Tucker, F. Clausen, L. Hillered, M. Gordon, D. Morgan, L. Lannfelt, F. E. Pettersson, and L. N. Nilsson. Amyloid-beta protofibril levels correlate with spatial learning in Arctic Alzheimer's disease transgenic mice. *FEBS J.*, 276(4):995–1006, Feb 2009a.

A. Lord, A. Gumucio, H. Englund, D. Sehlin, V. S. Sundquist, L. Soderberg, C. Moller, P. Gellerfors, L. Lannfelt, F. E. Pettersson, and L. N. Nilsson. An amyloid-beta protofibril-selective antibody prevents amyloid formation in a mouse model of Alzheimer's disease. *Neurobiol. Dis.*, 36(3):425–434, Dec 2009b.

O. H. Lowry, N. J. Rosebrough, A. L. Farr, and R. J. Randall. Protein measurement with the Folin phenol reagent. *J. Biol. Chem.*, 193(1):265–275, Nov 1951.

T. N. Luong, H. J. Carlisle, A. Southwell, and P. H. Patterson. Assessment of motor balance and coordination in mice using the balance beam. *J Vis Exp*, (49), 2011.

J. Maeda, B. Ji, T. Irie, T. Tomiyama, M. Maruyama, T. Okauchi, M. Staufenbiel, N. Iwata, M. Ono, T. C. Saido, K. Suzuki, H. Mori, M. Higuchi, and T. Suhara. Longitudinal, quantitative assessment of amyloid, neuroinflammation, and anti-amyloid treatment in a living mouse model of Alzheimer's disease enabled by positron emission tomography. *J. Neurosci.*, 27(41):10957–10968, Oct 2007.

A. Majumdar, D. Cruz, N. Asamoah, A. Buxbaum, I. Sohar, P. Lobel, and F. R. Maxfield. Activation of microglia acidifies lysosomes and leads to degradation of Alzheimer amyloid fibrils. *Mol. Biol. Cell*, 18 (4):1490–1496, Apr 2007.

A. Marcello, O. Wirths, T. Schneider-Axmann, M. Degerman-Gunnarsson, L. Lannfelt, and T. A. Bayer. Reduced levels of IgM autoantibodies against N-truncated pyroglutamate Abeta in plasma of patients with Alzheimer's disease. *Neurobiol. Aging*, 32(8):1379–1387, Aug 2011.

J. E. Martinelli, J. F. Cecato, D. Bartholomeu, and J. M. Montiel. Comparison of the diagnostic accuracy of neuropsychological tests in differentiating Alzheimer's disease from mild cognitive impairment: can the montreal cognitive assessment be better than the cambridge cognitive examination? *Dement Geriatr Cogn Dis Extra*, 4(2):113–121, May 2014.

I. C. Martins, I. Kuperstein, H. Wilkinson, E. Maes, M. Vanbrabant, W. Jonckheere, P. Van Gelder, D. Hartmann, R. D'Hooge, B. De Strooper, J. Schymkowitz, and F. Rousseau. Lipids revert inert Abeta amyloid fibrils to neurotoxic protofibrils that affect learning in mice. *EMBO J.*, 27(1):224–233, Jan 2008.

E. Masliah, R. D. Terry, M. Mallory, M. Alford, and L. A. Hansen. Diffuse plaques do not accentuate synapse loss in Alzheimer's disease. *Am. J. Pathol.*, 137(6):1293–1297, Dec 1990.

E. Masliah, A. Sisk, M. Mallory, L. Mucke, D. Schenk, and D. Games. Comparison of neurodegenerative pathology in transgenic mice overexpressing V717F beta-amyloid precursor protein and Alzheimer's disease. *J. Neurosci.*, 16(18):5795–5811, Sep 1996.

C. L. Masters, G. Simms, N. A. Weinman, G. Multhaup, B. L. McDonald, and K. Beyreuther. Amyloid plaque core protein in Alzheimer disease and Down syndrome. *Proc. Natl. Acad. Sci. U.S.A.*, 82(12): 4245–4249, Jun 1985.

M. P. Mattson. Cellular actions of beta-amyloid precursor protein and its soluble and fibrillogenic derivatives. *Physiol. Rev.*, 77(4):1081–1132, Oct 1997.

N. Mattsson, K. Blennow, and H. Zetterberg. CSF biomarkers: pinpointing Alzheimer pathogenesis. *Ann. N. Y. Acad. Sci.*, 1180:28–35, Oct 2009.

C.D. McCullagh, D. Craig, S.P. McIlroy, and A.P. Passmore. Risk factors for dementia. *Advances in Psychiatric Treatment*, 7:24–31, 2001.

G. McKhann, D. Drachman, M. Folstein, R. Katzman, D. Price, and E. M. Stadlan. Clinical diagnosis of Alzheimer's disease: report of the NINCDS-ADRDA Work Group under the auspices of Department of Health and Human Services Task Force on Alzheimer's Disease. *Neurology*, 34(7):939–944, Jul 1984.

G. M. McKhann, D. S. Knopman, H. Chertkow, B. T. Hyman, C. R. Jack, C. H. Kawas, W. E. Klunk, W. J. Koroshetz, J. J. Manly, R. Mayeux, R. C. Mohs, J. C. Morris, M. N. Rossor, P. Scheltens, M. C. Carrillo, B. Thies, S. Weintraub, and C. H. Phelps. The diagnosis of dementia due to Alzheimer's disease: recommendations from the National Institute on Aging-Alzheimer's Association workgroups on diagnostic guidelines for Alzheimer's disease. *Alzheimers Dement*, 7(3):263–269, May 2011.

J. McLaurin, R. Cecal, M. E. Kierstead, X. Tian, A. L. Phinney, M. Manea, J. E. French, M. H. Lambermon, A. A. Darabie, M. E. Brown, C. Janus, M. A. Chishti, P. Horne, D. Westaway, P. E. Fraser, H. T. Mount, M. Przybylski, and P. St George-Hyslop. Therapeutically effective antibodies against amyloid-beta peptide target amyloid-beta residues 4-10 and inhibit cytotoxicity and fibrillogenesis. *Nat. Med.*, 8(11): 1263–1269, Nov 2002.

P. D. Mehta, T. Pirttila, B. A. Patrick, M. Barshatzky, and S. P. Mehta. Amyloid beta protein 1-40 and 1-42 levels in matched cerebrospinal fluid and plasma from patients with Alzheimer disease. *Neurosci. Lett.*, 304(1-2):102–106, May 2001.

J. N. Meissner, Y. Bouter, and T. A. Bayer. Neuron Loss and Behavioral Deficits in the TBA42 Mouse Model Expressing N-Truncated Pyroglutamate Amyloid-3-42. *J. Alzheimers Dis.*, Dec 2014.

M. Meyer-Luehmann, T. L. Spires-Jones, C. Prada, M. Garcia-Alloza, A. de Calignon, A. Rozkalne, J. Koenigsknecht-Talboo, D. M. Holtzman, B. J. Bacskai, and B. T. Hyman. Rapid appearance and local toxicity of amyloid-beta plaques in a mouse model of Alzheimer's disease. *Nature*, 451(7179): 720–724, Feb 2008.

L. A. Miles, G. A. Crespi, L. Doughty, and M. W. Parker. Bapineuzumab captures the N-terminus of the Alzheimer's disease amyloid-beta peptide in a helical conformation. *Sci Rep*, 3:1302, 2013.

B. R. Miller, J. L. Dorner, M. Shou, Y. Sari, S. J. Barton, D. R. Sengelaub, R. T. Kennedy, and G. V. Rebec. Up-regulation of GLT1 expression increases glutamate uptake and attenuates the Huntington's disease phenotype in the R6/2 mouse. *Neuroscience*, 153(1):329–337, Apr 2008.

D. L. Miller, I. A. Papayannopoulos, J. Styles, S. A. Bobin, Y. Y. Lin, K. Biemann, and K. Iqbal. Peptide compositions of the cerebrovascular and senile plaque core amyloid deposits of Alzheimer's disease. *Arch. Biochem. Biophys.*, 301(1):41–52, Feb 1993.

L. Miravalle, M. Calero, M. Takao, A. E. Roher, B. Ghetti, and R. Vidal. Amino-terminally truncated Abeta peptide species are the main component of cotton wool plaques. *Biochemistry*, 44(32):10810–10821, Aug 2005.

A. Mochizuki, A. Tamaoka, A. Shimohata, Y. Komatsuzaki, and S. Shoji. Abeta42-positive non-pyramidal neurons around amyloid plaques in Alzheimer's disease. *Lancet*, 355(9197):42–43, Jan 2000.

D. Moechars, K. Lorent, B. De Strooper, I. Dewachter, and F. Van Leuven. Expression in brain of amyloid precursor protein mutated in the alpha-secretase site causes disturbed behavior, neuronal degeneration and premature death in transgenic mice. *EMBO J.*, 15(6):1265–1274, Mar 1996.

D. Moechars, I. Dewachter, K. Lorent, D. Reverse, V. Baekelandt, A. Naidu, I. Tesseur, K. Spittaels, C. V. Haute, F. Checler, E. Godaux, B. Cordell, and F. Van Leuven. Early phenotypic changes in transgenic mice that overexpress different mutants of amyloid precursor protein in brain. *J. Biol. Chem.*, 274(10): 6483–6492, Mar 1999.

P. M. Moran, L. S. Higgins, B. Cordell, and P. C. Moser. Age-related learning deficits in transgenic mice expressing the 751-amino acid isoform of human beta-amyloid precursor protein. *Proc. Natl. Acad. Sci. U.S.A.*, 92(12):5341–5345, Jun 1995.

D. Morgan, D. M. Diamond, P. E. Gottschall, K. E. Ugen, C. Dickey, J. Hardy, K. Duff, P. Jantzen, G. DiCarlo, D. Wilcock, K. Connor, J. Hatcher, C. Hope, M. Gordon, and G. W. Arendash. A beta peptide vaccination prevents memory loss in an animal model of Alzheimer's disease. *Nature*, 408(6815):982–985, 2000.

C. Mori, E. T. Spooner, K. E. Wisniewsk, T. M. Wisniewski, H. Yamaguch, T. C. Saido, D. R. Tolan, D. J. Selkoe, and C. A. Lemere. Intraneuronal Abeta42 accumulation in Down syndrome brain. *Amyloid*, 9 (2):88–102, Jun 2002.

H. Mori, K. Takio, M. Ogawara, and D. J. Selkoe. Mass spectrometry of purified amyloid beta protein in Alzheimer's disease. *J. Biol. Chem.*, 267(24):17082–17086, Aug 1992.

M. L. Moro, G. Giaccone, R. Lombardi, A. Indaco, A. Uggetti, M. Morbin, S. Saccucci, G. Di Fede, M. Catania, D. M. Walsh, A. Demarchi, A. Rozemuller, N. Bogdanovic, O. Bugiani, B. Ghetti, and F. Tagliavini. APP mutations in the Abeta coding region are associated with abundant cerebral deposition of Abeta38. *Acta Neuropathol.*, 124(6):809–821, Dec 2012.

J. C. Morris and J. L. Price. Pathologic correlates of nondemented aging, mild cognitive impairment, and early-stage Alzheimer's disease. *J. Mol. Neurosci.*, 17(2):101–118, Oct 2001.

R. Morris. Developments of a water-maze procedure for studying spatial learning in the rat. *J. Neurosci. Methods*, 11(1):47–60, May 1984.

K. S. Murayama, F. Kametani, T. Tabira, and W. Araki. A novel monoclonal antibody specific for the amino-truncated beta-amyloid Abeta5-40/42 produced from caspase-cleaved amyloid precursor protein. *J. Neurosci. Methods*, 161(2):244–249, Apr 2007.

J. Näslund, A. Schierhorn, U. Hellman, L. Lannfelt, A. D. Roses, L. O. Tjernberg, J. Silberring, S. E. Gandy, B. Winblad, and P. Greengard. Relative abundance of Alzheimer A beta amyloid peptide variants in Alzheimer disease and normal aging. *Proc. Natl. Acad. Sci. U.S.A.*, 91(18):8378–8382, Aug 1994.

J. A. Nicoll, D. Wilkinson, C. Holmes, P. Steart, H. Markham, and R. O. Weller. Neuropathology of human Alzheimer disease after immunization with amyloid-beta peptide: a case report. *Nat. Med.*, 9(4):448–452, Apr 2003.

L. N. Nilsson, G. W. Arendash, R. E. Leighty, D. A. Costa, M. A. Low, M. F. Garcia, J. R. Cracciolo, A. Rojiani, X. Wu, K. R. Bales, S. M. Paul, and H. Potter. Cognitive impairment in PDAPP mice depends on ApoE and ACT-catalyzed amyloid formation. *Neurobiol. Aging*, 25(9):1153–1167, Oct 2004.

P. Nilsson, T. Saito, and T. C. Saido. New mouse model of Alzheimer's. *ACS Chem Neurosci*, 5(7):499–502, Jul 2014.

R. M. Nitsch, B. E. Slack, R. J. Wurtman, and J. H. Growdon. Release of Alzheimer amyloid precursor derivatives stimulated by activation of muscarinic acetylcholine receptors. *Science*, 258(5080):304–307, Oct 1992.

J. M. Nussbaum, S. Schilling, H. Cynis, A. Silva, E. Swanson, T. Wangsanut, K. Tayler, B. Wiltgen, A. Hatami, R. Ronicke, K. Reymann, B. Hutter-Paier, A. Alexandru, W. Jagla, S. Graubner, C. G. Glabe, H. U. Demuth, and G. S. Bloom. Prion-like behaviour and tau-dependent cytotoxicity of pyroglutamylated amyloid-beta. *Nature*, 485(7400):651–655, May 2012.

H. Oakley, S. L. Cole, S. Logan, E. Maus, P. Shao, J. Craft, A. Guillozet-Bongaarts, M. Ohno, J. Disterhoft, L. Van Eldik, R. Berry, and R. Vassar. Intraneuronal beta-amyloid aggregates, neurodegeneration, and neuron loss in transgenic mice with five familial Alzheimer's disease mutations: potential factors in amyloid plaque formation. *J. Neurosci.*, 26(40):10129–10140, Oct 2006.

S. Oddo, A. Caccamo, J. D. Shepherd, M. P. Murphy, T. E. Golde, R. Kayed, R. Metherate, M. P. Mattson, Y. Akbari, and F. M. LaFerla. Triple-transgenic model of Alzheimer's disease with plaques and tangles: intracellular Abeta and synaptic dysfunction. *Neuron*, 39(3):409–421, Jul 2003.

J. M. Orgogozo, S. Gilman, J. F. Dartigues, B. Laurent, M. Puel, L. C. Kirby, P. Jouanny, B. Dubois, L. Eisner, S. Flitman, B. F. Michel, M. Boada, A. Frank, and C. Hock. Subacute meningoencephalitis in a subset of patients with AD after Abeta42 immunization. *Neurology*, 61(1):46–54, Jul 2003.

W. Pan, B. Solomon, L. M. Maness, and A. J. Kastin. Antibodies to beta-amyloid decrease the blood-to-brain transfer of beta-amyloid peptide. *Exp. Biol. Med. (Maywood)*, 227(8):609–615, Sep 2002.

D. M. Paresce, H. Chung, and F. R. Maxfield. Slow degradation of aggregates of the Alzheimer's disease amyloid beta-protein by microglial cells. *J. Biol. Chem.*, 272(46):29390–29397, Nov 1997.

R. J. Perrin, A. M. Fagan, and D. M. Holtzman. Multimodal techniques for diagnosis and prognosis of Alzheimer's disease. *Nature*, 461(7266):916–922, Oct 2009.

R. C. Petersen. Mild cognitive impairment as a diagnostic entity. *J. Intern. Med.*, 256(3):183–194, Sep 2004.

M. Pfeifer, S. Boncristiano, L. Bondolfi, A. Stalder, T. Deller, M. Staufenbiel, P. M. Mathews, and M. Jucker. Cerebral hemorrhage after passive anti-Abeta immunotherapy. *Science*, 298(5597):1379, Nov 2002.

C. J. Pike, B. J. Cummings, and C. W. Cotman. Early association of reactive astrocytes with senile plaques in Alzheimer's disease. *Exp. Neurol.*, 132(2):172–179, Apr 1995a.

C. J. Pike, M. J. Overman, and C. W. Cotman. Amino-terminal deletions enhance aggregation of beta-amyloid peptides in vitro. *J. Biol. Chem.*, 270(41):23895–23898, Oct 1995b.

S. W. Pimplikar. Reassessing the amyloid cascade hypothesis of Alzheimer's disease. *Int. J. Biochem. Cell Biol.*, 41(6):1261–1268, Jun 2009.

B. L. Plassman, R. J. Havlik, D. C. Steffens, M. J. Helms, T. N. Newman, D. Drosdick, C. Phillips, B. A. Gau, K. A. Welsh-Bohmer, J. R. Burke, J. M. Guralnik, and J. C. Breitner. Documented head injury in early adulthood and risk of Alzheimer's disease and other dementias. *Neurology*, 55(8):1158–1166, Oct 2000.

E. Portelius, N. Bogdanovic, M. K. Gustavsson, I. Volkmann, G. Brinkmalm, H. Zetterberg, B. Winblad, and K. Blennow. Mass spectrometric characterization of brain amyloid beta isoform signatures in familial and sporadic Alzheimer's disease. *Acta Neuropathol.*, 120(2):185–193, Aug 2010.

E. Portelius, H. Zetterberg, R. A. Dean, A. Marcil, P. Bourgeois, M. Nutu, U. Andreasson, E. Siemers, K. G. Mawuenyega, W. C. Sigurdson, P. C. May, S. M. Paul, D. M. Holtzman, K. Blennow, and R. J. Bateman. Amyloid-beta(1-15/16) as a marker for beta-secretase inhibition in Alzheimer's disease. *J. Alzheimers Dis.*, 31(2):335–341, 2012.

R. Postina, A. Schroeder, I. Dewachter, J. Bohl, U. Schmitt, E. Kojro, C. Prinzen, K. Endres, C. Hiemke, M. Blessing, P. Flamez, A. Dequenne, E. Godaux, F. van Leuven, and F. Fahrenholz. A disintegrin-metalloproteinase prevents amyloid plaque formation and hippocampal defects in an Alzheimer disease mouse model. *J. Clin. Invest.*, 113(10):1456–1464, May 2004.

J. L. Price and J. C. Morris. Tangles and plaques in nondemented aging and "preclinical" Alzheimer's disease. *Ann. Neurol.*, 45(3):358–368, Mar 1999.

J. L. Price, D. W. McKeel, V. D. Buckles, C. M. Roe, C. Xiong, M. Grundman, L. A. Hansen, R. C. Petersen, J. E. Parisi, D. W. Dickson, C. D. Smith, D. G. Davis, F. A. Schmitt, W. R. Markesbery, J. Kaye, R. Kurlan, C. Hulette, B. F. Kurland, R. Higdon, W. Kukull, and J. C. Morris. Neuropathology of nondemented aging: presumptive evidence for preclinical Alzheimer disease. *Neurobiol. Aging*, 30(7):1026–1036, Jul 2009.

M. Prince, M. Cullen, and A. Mann. Risk factors for Alzheimer's disease and dementia: a case-control study based on the MRC elderly hypertension trial. *Neurology*, 44(1):97–104, Jan 1994.

D. Puzzo, L. Lee, A. Palmeri, G. Calabrese, and O. Arancio. Behavioral assays with mouse models of Alzheimer's disease: practical considerations and guidelines. *Biochem. Pharmacol.*, 88(4):450–467, Apr 2014.

C. Qiu, B. Winblad, A. Marengoni, I. Klarin, J. Fastbom, and L. Fratiglioni. Heart failure and risk of dementia and Alzheimer disease: a population-based cohort study. *Arch. Intern. Med.*, 166(9):1003–1008, May 2006.

H. W. Querfurth and F. M. LaFerla. Alzheimer's disease. *N. Engl. J. Med.*, 362(4):329–344, Jan 2010.

M. M. Racke, L. I. Boone, D. L. Hepburn, M. Parsadainian, M. T. Bryan, D. K. Ness, K. S. Piroozi, W. H. Jordan, D. D. Brown, W. P. Hoffman, D. M. Holtzman, K. R. Bales, B. D. Gitter, P. C. May, S. M. Paul, and R. B. DeMattos. Exacerbation of cerebral amyloid angiopathy-associated microhemorrhage in amyloid precursor protein transgenic mice by immunotherapy is dependent on antibody recognition of deposited forms of amyloid beta. *J. Neurosci.*, 25(3):629–636, Jan 2005.

J. F. Reilly, D. Games, R. E. Rydel, S. Freedman, D. Schenk, W. G. Young, J. H. Morrison, and F. E. Bloom. Amyloid deposition in the hippocampus and entorhinal cortex: quantitative analysis of a transgenic mouse model. *Proc. Natl. Acad. Sci. U.S.A.*, 100(8):4837–4842, Apr 2003.

J. Reinert, H. Martens, M. Huettenrauch, T. Kolbow, L. Lannfelt, M. Ingelsson, A. Paetau, A. Verkkoniemi-Ahola, T. A. Bayer, and O. Wirths. Abeta38 in the brains of patients with sporadic and familial Alzheimer's disease and transgenic mouse models. *J. Alzheimers Dis.*, 39(4):871–881, 2014.

B. C. Richard, A. Kurdakova, S. Baches, T. A. Bayer, S. Weggen, and O. Wirths. Gene Dosage Dependent Aggravation of the Neurological Phenotype in the 5XFAD Mouse Model of Alzheimer's Disease. *J. Alzheimers Dis.*, 45(4):1223–1236, Jan 2015.

A. Rijal Upadhaya, F. Scheibe, I. Kosterin, D. Abramowski, J. Gerth, S. Kumar, S. Liebau, H. Yamaguchi, J. Walter, M. Staufenbiel, and D. R. Thal. The type of Abeta-related neuronal degeneration differs between amyloid precursor protein (APP23) and amyloid beta-peptide (APP48) transgenic mice. *Acta Neuropathol Commun*, 1(1):77, 2013.

E. M. Rockenstein, L. McConlogue, H. Tan, M. Power, E. Masliah, and L. Mucke. Levels and alternative splicing of amyloid beta protein precursor (APP) transcripts in brains of APP transgenic mice and humans with Alzheimer's disease. *J. Biol. Chem.*, 270(47):28257–28267, Nov 1995.

S. L. Rogers, R. S. Doody, R. C. Mohs, and L. T. Friedhoff. Donepezil improves cognition and global function in Alzheimer disease: a 15-week, double-blind, placebo-controlled study. Donepezil Study Group. *Arch. Intern. Med.*, 158(9):1021–1031, May 1998.

J. M. Rubio-Perez and J. M. Morillas-Ruiz. A review: inflammatory process in Alzheimer's disease, role of cytokines. *ScientificWorldJournal*, 2012:756357, 2012.

P. Rüfenacht, A. Guntert, B. Bohrmann, A. Ducret, and H. Dobeli. Quantification of the A beta peptide in Alzheimer's plaques by laser dissection microscopy combined with mass spectrometry. *J Mass Spectrom*, 40(2):193–201, Feb 2005.

B. Rumble, R. Retallack, C. Hilbich, G. Simms, G. Multhaup, R. Martins, A. Hockey, P. Montgomery, K. Beyreuther, and C. L. Masters. Amyloid A4 protein and its precursor in Down's syndrome and Alzheimer's disease. *N. Engl. J. Med.*, 320(22):1446–1452, Jun 1989.

C. Russo, E. Violani, S. Salis, V. Venezia, V. Dolcini, G. Damonte, U. Benatti, C. D'Arrigo, E. Patrone, P. Carlo, and G. Schettini. Pyroglutamate-modified amyloid beta-peptides–AbetaN3(pE)–strongly affect cultured neuron and astrocyte survival. *J. Neurochem.*, 82(6):1480–1489, Sep 2002.

T. C. Saido, T. Iwatsubo, D. M. Mann, H. Shimada, Y. Ihara, and S. Kawashima. Dominant and differential deposition of distinct beta-amyloid peptide species, A beta N3(pE), in senile plaques. *Neuron*, 14(2): 457–466, Feb 1995.

M. Salkovic-Petrisic, F. Tribl, M. Schmidt, S. Hoyer, and P. Riederer. Alzheimer-like changes in protein kinase B and glycogen synthase kinase-3 in rat frontal cortex and hippocampus after damage to the insulin signalling pathway. *J. Neurochem.*, 96(4):1005–1015, Feb 2006.

A. Sasaki, M. Shoji, Y. Harigaya, T. Kawarabayashi, M. Ikeda, M. Naito, E. Matsubara, K. Abe, and Y. Nakazato. Amyloid cored plaques in Tg2576 transgenic mice are characterized by giant plaques, slightly activated microglia, and the lack of paired helical filament-typed, dystrophic neurites. *Virchows Arch.*, 441(4):358–367, Oct 2002.

A. Saul, F. Sprenger, T. A. Bayer, and O. Wirths. Accelerated tau pathology with synaptic and neuronal loss in a novel triple transgenic mouse model of Alzheimer's disease. *Neurobiol. Aging*, 34(11):2564–2573, Nov 2013.

D. Schenk. Amyloid-beta immunotherapy for Alzheimer's disease: the end of the beginning. *Nat. Rev. Neurosci.*, 3(10):824–828, Oct 2002.

D. Schenk, R. Barbour, W. Dunn, G. Gordon, H. Grajeda, T. Guido, K. Hu, J. Huang, K. Johnson-Wood, K. Khan, D. Kholodenko, M. Lee, Z. Liao, I. Lieberburg, R. Motter, L. Mutter, F. Soriano, G. Shopp, N. Vasquez, C. Vandevert, S. Walker, M. Wogulis, T. Yednock, D. Games, and P. Seubert. Immunization with amyloid-beta attenuates Alzheimer-disease-like pathology in the PDAPP mouse. *Nature*, 400(6740): 173–177, Jul 1999.

H. Schieb, H. Kratzin, O. Jahn, W. Mobius, S. Rabe, M. Staufenbiel, J. Wiltfang, and H. W. Klafki. Beta-amyloid peptide variants in brains and cerebrospinal fluid from amyloid precursor protein (APP) transgenic mice: comparison with human Alzheimer amyloid. *J. Biol. Chem.*, 286(39):33747–33758, Sep 2011.

D. Schlenzig, S. Manhart, Y. Cinar, M. Kleinschmidt, G. Hause, D. Willbold, S. A. Funke, S. Schilling, and H. U. Demuth. Pyroglutamate formation influences solubility and amyloidogenicity of amyloid peptides. *Biochemistry*, 48(29):7072–7078, Jul 2009.

B. Schmand, G. Walstra, J. Lindeboom, S. Teunisse, and C. Jonker. Early detection of Alzheimer's disease using the Cambridge Cognitive Examination (CAMCOG). *Psychol Med*, 30(3):619–627, May 2000.

T. D. Schmittgen and K. J. Livak. Analyzing real-time PCR data by the comparative C(T) method. *Nat Protoc*, 3(6):1101–1108, 2008.

C. Schmitz, B. P. Rutten, A. Pielen, S. Schafer, O. Wirths, G. Tremp, C. Czech, V. Blanchard, G. Multhaup, P. Rezaie, H. Korr, H. W. Steinbusch, L. Pradier, and T. A. Bayer. Hippocampal neuron loss exceeds amyloid plaque load in a transgenic mouse model of Alzheimer's disease. *Am. J. Pathol.*, 164(4):1495–1502, Apr 2004.

M. L. Schroeter, T. Stein, N. Maslowski, and J. Neumann. Neural correlates of Alzheimer's disease and mild cognitive impairment: a systematic and quantitative meta-analysis involving 1351 patients. *Neuroimage*, 47(4):1196–1206, Oct 2009.

S. Schroeter, K. Khan, R. Barbour, M. Doan, M. Chen, T. Guido, D. Gill, G. Basi, D. Schenk, P. Seubert, and D. Games. Immunotherapy reduces vascular amyloid-beta in PDAPP mice. *J. Neurosci.*, 28(27): 6787–6793, Jul 2008.

N. Schupf and G. H. Sergievsky. Genetic and host factors for dementia in Down's syndrome. *Br J Psychiatry*, 180:405–410, May 2002.

D. J. Selkoe. The molecular pathology of Alzheimer's disease. *Neuron*, 6(4):487–498, Apr 1991.

D. J. Selkoe. Alzheimer's disease: genes, proteins, and therapy. *Physiol. Rev.*, 81(2):741–766, Apr 2001.

D. J. Selkoe. *Alzheimer's disease*. Cold Spring Harb Perspect Biol 3, 2011.

D. J. Selkoe, C. R. Abraham, M. B. Podlisny, and L. K. Duffy. Isolation of low-molecular-weight proteins from amyloid plaque fibers in Alzheimer's disease. *J. Neurochem.*, 46(6):1820–1834, Jun 1986.

J. S. Seo, Y. H. Leem, K. W. Lee, S. W. Kim, J. K. Lee, and P. L. Han. Severe motor neuron degeneration in the spinal cord of the Tg2576 mouse model of Alzheimer disease. *J. Alzheimers Dis.*, 21(1):263–276, 2010.

N. Sergeant, S. Bombois, A. Ghestem, H. Drobecq, V. Kostanjevecki, C. Missiaen, A. Wattez, J. P. David, E. Vanmechelen, C. Sergheraert, and A. Delacourte. Truncated beta-amyloid peptide species in preclinical Alzheimer's disease as new targets for the vaccination approach. *J. Neurochem.*, 85(6):1581–1591, Jun 2003.

A. Serrano-Pozo, M. P. Frosch, E. Masliah, and B. T. Hyman. Neuropathological alterations in Alzheimer disease. *Cold Spring Harb Perspect Med*, 1(1):a006189, Sep 2011.

M. Shibata, S. Yamada, S. R. Kumar, M. Calero, J. Bading, B. Frangione, D. M. Holtzman, C. A. Miller, D. K. Strickland, J. Ghiso, and B. V. Zlokovic. Clearance of Alzheimer's amyloid-ss(1-40) peptide from brain by LDL receptor-related protein-1 at the blood-brain barrier. *J. Clin. Invest.*, 106(12):1489–1499, Dec 2000.

S. S. Sisodia, E. H. Koo, K. Beyreuther, A. Unterbeck, and D. L. Price. Evidence that beta-amyloid protein in Alzheimer's disease is not derived by normal processing. *Science*, 248(4954):492–495, Apr 1990.

T. M. Sivanandam and M. K. Thakur. Traumatic brain injury: a risk factor for Alzheimer's disease. *Neurosci Biobehav Rev*, 36(5):1376–1381, May 2012.

B. Solomon, R. Koppel, E. Hanan, and T. Katzav. Monoclonal antibodies inhibit in vitro fibrillar aggregation of the Alzheimer beta-amyloid peptide. *Proc. Natl. Acad. Sci. U.S.A.*, 93(1):452–455, Jan 1996.

B. Solomon, R. Koppel, D. Frankel, and E. Hanan-Aharon. Disaggregation of Alzheimer beta-amyloid by site-directed mAb. *Proc. Natl. Acad. Sci. U.S.A.*, 94(8):4109–4112, Apr 1997.

C. Soto, E. M. Castano, B. Frangione, and N. C. Inestrosa. The alpha-helical to beta-strand transition in the amino-terminal fragment of the amyloid beta-peptide modulates amyloid formation. *J. Biol. Chem.*, 270(7):3063–3067, Feb 1995.

R. A. Sperling, P. S. Aisen, L. A. Beckett, D. A. Bennett, S. Craft, A. M. Fagan, T. Iwatsubo, C. R. Jack, J. Kaye, T. J. Montine, D. C. Park, E. M. Reiman, C. C. Rowe, E. Siemers, Y. Stern, K. Yaffe, M. C. Carrillo, B. Thies, M. Morrison-Bogorad, M. V. Wagster, and C. H. Phelps. Toward defining the preclinical stages of Alzheimer's disease: recommendations from the National Institute on Aging-Alzheimer's Association workgroups on diagnostic guidelines for Alzheimer's disease. *Alzheimers Dement*, 7(3): 280–292, May 2011.

C. Sturchler-Pierrat, D. Abramowski, M. Duke, K. H. Wiederhold, C. Mistl, S. Rothacher, B. Ledermann, K. Burki, P. Frey, P. A. Paganetti, C. Waridel, M. E. Calhoun, M. Jucker, A. Probst, M. Staufenbiel, and B. Sommer. Two amyloid precursor protein transgenic mouse models with Alzheimer disease-like pathology. *Proc. Natl. Acad. Sci. U.S.A.*, 94(24):13287–13292, Nov 1997.

T. Sunderland, J. L. Hill, A. M. Mellow, B. A. Lawlor, J. Gundersheimer, P. A. Newhouse, and J. H. Grafman. Clock drawing in Alzheimer's disease. A novel measure of dementia severity. *J Am Geriatr Soc*, 37(8): 725–729, Aug 1989.

N. Suzuki, T. Iwatsubo, A. Odaka, Y. Ishibashi, C. Kitada, and Y. Ihara. High tissue content of soluble Abeta 1-40 is linked to cerebral amyloid angiopathy. *Am. J. Pathol.*, 145(2):452–460, Aug 1994.

R. H. Takahashi, T. A. Milner, F. Li, E. E. Nam, M. A. Edgar, H. Yamaguchi, M. F. Beal, H. Xu, P. Greengard, and G. K. Gouras. Intraneuronal Alzheimer abeta42 accumulates in multivesicular bodies and is associated with synaptic pathology. *Am. J. Pathol.*, 161(5):1869–1879, Nov 2002.

K. Takeda, W. Araki, H. Akiyama, and T. Tabira. Amino-truncated amyloid beta-peptide (Abeta5-40/42) produced from caspase-cleaved amyloid precursor protein is deposited in Alzheimer's disease brain. *FASEB J.*, 18(14):1755–1757, Nov 2004.

D. R. Thal, U. Rub, M. Orantes, and H. Braak. Phases of Abeta-deposition in the human brain and its relevance for the development of AD. *Neurology*, 58(12):1791–1800, Jun 2002.

G. Thinakaran and E. H. Koo. Amyloid precursor protein trafficking, processing, and function. *J. Biol. Chem.*, 283(44):29615–29619, Oct 2008.

H. M. Tucker, M. Kihiko, J. N. Caldwell, S. Wright, T. Kawarabayashi, D. Price, D. Walker, S. Scheff, J. P. McGillis, R. E. Rydel, and S. Estus. The plasmin system is induced by and degrades amyloid-beta aggregates. *J. Neurosci.*, 20(11):3937–3946, Jun 2000.

S. M. Tucker, D. R. Borchelt, and J. C. Troncoso. Limited clearance of pre-existing amyloid plaques after intracerebral injection of Abeta antibodies in two mouse models of Alzheimer disease. *J. Neuropathol. Exp. Neurol.*, 67(1):30–40, Jan 2008.

E. E. Tuppo and H. R. Arias. The role of inflammation in Alzheimer's disease. *Int. J. Biochem. Cell Biol.*, 37 (2):289–305, Feb 2005.

B. Urbanc, L. Cruz, R. Le, J. Sanders, K. H. Ashe, K. Duff, H. E. Stanley, M. C. Irizarry, and B. T. Hyman. Neurotoxic effects of thioflavin S-positive amyloid deposits in transgenic mice and Alzheimer's disease. *Proc. Natl. Acad. Sci. U.S.A.*, 99(22):13990–13995, Oct 2002.

D. Van Dam, R. D'Hooge, M. Staufenbiel, C. Van Ginneken, F. Van Meir, and P. P. De Deyn. Age-dependent cognitive decline in the APP23 model precedes amyloid deposition. *Eur. J. Neurosci.*, 17(2):388–396, Jan 2003.

W. E. Van Nostrand and M. Porter. Plasmin cleavage of the amyloid beta-protein: alteration of secondary structure and stimulation of tissue plasminogen activator activity. *Biochemistry*, 38(35):11570–11576, Aug 1999.

G. D. Van Vickle, C. L. Esh, T. A. Kokjohn, R. L. Patton, W. M. Kalback, D. C. Luehrs, T. G. Beach, A. J. Newel, F. Lopera, B. Ghetti, R. Vidal, E. M. Castano, and A. E. Roher. Presenilin-1 280Glu–>Ala mutation alters C-terminal APP processing yielding longer abeta peptides: implications for Alzheimer's disease. *Mol. Med.*, 14(3-4):184–194, 2008.

R. Vassar, B. D. Bennett, S. Babu-Khan, S. Kahn, E. A. Mendiaz, P. Denis, D. B. Teplow, S. Ross, P. Amarante, R. Loeloff, Y. Luo, S. Fisher, J. Fuller, S. Edenson, J. Lile, M. A. Jarosinski, A. L. Biere, E. Curran, T. Burgess, J. C. Louis, F. Collins, J. Treanor, G. Rogers, and M. Citron. Beta-secretase cleavage of Alzheimer's amyloid precursor protein by the transmembrane aspartic protease BACE. *Science*, 286 (5440):735–741, Oct 1999.

M. Vidal, R. Morris, F. Grosveld, and E. Spanopoulou. Tissue-specific control elements of the Thy-1 gene. *EMBO J.*, 9(3):833–840, Mar 1990.

V. L. Villemagne, K. E. Pike, G. Chetelat, K. A. Ellis, R. S. Mulligan, P. Bourgeat, U. Ackermann, G. Jones, C. Szoeke, O. Salvado, R. Martins, G. O'Keefe, C. A. Mathis, W. E. Klunk, D. Ames, C. L. Masters, and C. C. Rowe. Longitudinal assessment of Abeta and cognition in aging and Alzheimer disease. *Ann. Neurol.*, 69(1):181–192, Jan 2011.

P. J. Visser, P. Scheltens, and F. R. Verhey. Do MCI criteria in drug trials accurately identify subjects with predementia Alzheimer's disease? *J. Neurol. Neurosurg. Psychiatr.*, 76(10):1348–1354, Oct 2005.

A. G. Vlassenko, M. A. Mintun, C. Xiong, Y. I. Sheline, A. M. Goate, T. L. Benzinger, and J. C. Morris. Amyloid-beta plaque growth in cognitively normal adults: longitudinal [11C]Pittsburgh compound B data. *Ann. Neurol.*, 70(5):857–861, Nov 2011.

C. V. Vorhees and M. T. Williams. Morris water maze: procedures for assessing spatial and related forms of learning and memory. *Nat Protoc*, 1(2):848–858, 2006.

H. Wada, K. Nakajoh, T. Satoh-Nakagawa, T. Suzuki, T. Ohrui, H. Arai, and H. Sasaki. Risk factors of aspiration pneumonia in Alzheimer's disease patients. *Gerontology*, 47(5):271–276, 2001.

G. Waldemar, B. Dubois, M. Emre, J. Georges, I. G. McKeith, M. Rossor, P. Scheltens, P. Tariska, and B. Winblad. Recommendations for the diagnosis and management of Alzheimer's disease and other disorders associated with dementia: EFNS guideline. *Eur. J. Neurol.*, 14(1):1–26, Jan 2007.

A. K. Wallin, C. Wattmo, and L. Minthon. Galantamine treatment in Alzheimer's disease: response and long-term outcome in a routine clinical setting. *Neuropsychiatr Dis Treat*, 7:565–576, 2011.

A. Wang, P. Das, R. C. Switzer, T. E. Golde, and J. L. Jankowsky. Robust amyloid clearance in a mouse model of Alzheimer's disease provides novel insights into the mechanism of amyloid-beta immuno-therapy. *J. Neurosci.*, 31(11):4124–4136, Mar 2011.

A. D. Watt, G. A. Crespi, R. A. Down, D. B. Ascher, A. Gunn, K. A. Perez, C. A. McLean, V. L. Ville-magne, M. W. Parker, K. J. Barnham, and L. A. Miles. Do current therapeutic anti-Abeta antibodies for Alzheimer's disease engage the target? *Acta Neuropathol.*, 127(6):803–810, Jun 2014.

M. D. Weingarten, A. H. Lockwood, S. Y. Hwo, and M. W. Kirschner. A protein factor essential for microtubule assembly. *Proc. Natl. Acad. Sci. U.S.A.*, 72(5):1858–1862, May 1975.

H. Welander, J. Franberg, C. Graff, E. Sundstrom, B. Winblad, and L. O. Tjernberg. Abeta43 is more frequent than Abeta40 in amyloid plaque cores from Alzheimer disease brains. *J. Neurochem.*, 110(2): 697–706, Jul 2009.

S. C. Weninger and B. A. Yankner. Inflammation and Alzheimer disease: the good, the bad, and the ugly. *Nat. Med.*, 7(5):527–528, May 2001.

M. Wietrzych, H. Meziane, A. Sutter, N. Ghyselinck, P. F. Chapman, P. Chambon, and W. Krezel. Working memory deficits in retinoid X receptor gamma-deficient mice. *Learn. Mem.*, 12(3):318–326, 2005.

D. M. Wilcock, G. DiCarlo, D. Henderson, J. Jackson, K. Clarke, K. E. Ugen, M. N. Gordon, and D. Morgan. Intracranially administered anti-Abeta antibodies reduce beta-amyloid deposition by mechanisms both independent of and associated with microglial activation. *J. Neurosci.*, 23(9):3745–3751, May 2003.

D. M. Wilcock, S. K. Munireddy, A. Rosenthal, K. E. Ugen, M. N. Gordon, and D. Morgan. Microglial activation facilitates Abeta plaque removal following intracranial anti-Abeta antibody administration. *Neurobiol. Dis.*, 15(1):11–20, Feb 2004a.

D. M. Wilcock, A. Rojiani, A. Rosenthal, G. Levkowitz, S. Subbarao, J. Alamed, D. Wilson, N. Wilson, M. J. Freeman, M. N. Gordon, and D. Morgan. Passive amyloid immunotherapy clears amyloid and transiently activates microglia in a transgenic mouse model of amyloid deposition. *J. Neurosci.*, 24(27): 6144–6151, Jul 2004b.

D. M. Wilcock, A. Rojiani, A. Rosenthal, S. Subbarao, M. J. Freeman, M. N. Gordon, and D. Morgan. Passive immunotherapy against Abeta in aged APP-transgenic mice reverses cognitive deficits and depletes parenchymal amyloid deposits in spite of increased vascular amyloid and microhemorrhage. *J Neuroinflammation*, 1(1):24, Dec 2004c.

D. M. Wilcock, J. Alamed, P. E. Gottschall, J. Grimm, A. Rosenthal, J. Pons, V. Ronan, K. Symmonds, M. N. Gordon, and D. Morgan. Deglycosylated anti-amyloid-beta antibodies eliminate cognitive deficits and reduce parenchymal amyloid with minimal vascular consequences in aged amyloid precursor protein transgenic mice. *J. Neurosci.*, 26(20):5340–5346, May 2006.

A. Willuweit, J. Velden, R. Godemann, A. Manook, F. Jetzek, H. Tintrup, G. Kauselmann, B. Zevnik, G. Henriksen, A. Drzezga, J. Pohlner, M. Schoor, J. A. Kemp, and H. von der Kammer. Early-onset and robust amyloid pathology in a new homozygous mouse model of Alzheimer's disease. *PLoS ONE*, 4 (11):e7931, 2009.

J. Wiltfang, H. Esselmann, M. Bibl, A. Smirnov, M. Otto, S. Paul, B. Schmidt, H. W. Klafki, M. Maler, T. Dyrks, M. Bienert, M. Beyermann, E. Ruther, and J. Kornhuber. Highly conserved and disease-specific patterns of carboxyterminally truncated Abeta peptides 1-37/38/39 in addition to 1-40/42 in Alzheimer's disease and in patients with chronic neuroinflammation. *J. Neurochem.*, 81(3):481–496, May 2002.

O. Wirths and T. A. Bayer. Neuron loss in transgenic mouse models of Alzheimer's disease. *Int J Alzheimers Dis*, 2010, 2010.

O. Wirths and T. A. Bayer. Intraneuronal Abeta accumulation and neurodegeneration: lessons from transgenic models. *Life Sci.*, 91(23-24):1148–1152, Dec 2012.

O. Wirths, G. Multhaup, C. Czech, V. Blanchard, S. Moussaoui, G. Tremp, L. Pradier, K. Beyreuther, and T. A. Bayer. Intraneuronal Abeta accumulation precedes plaque formation in beta-amyloid precursor protein and presenilin-1 double-transgenic mice. *Neurosci. Lett.*, 306(1-2):116–120, Jun 2001.

O. Wirths, G. Multhaup, C. Czech, N. Feldmann, V. Blanchard, G. Tremp, K. Beyreuther, L. Pradier, and T. A. Bayer. Intraneuronal APP/A beta trafficking and plaque formation in beta-amyloid precursor protein and presenilin-1 transgenic mice. *Brain Pathol.*, 12(3):275–286, Jul 2002.

O. Wirths, G. Multhaup, and T. A. Bayer. A modified beta-amyloid hypothesis: intraneuronal accumulation of the beta-amyloid peptide–the first step of a fatal cascade. *J. Neurochem.*, 91(3):513–520, Nov 2004.

O. Wirths, J. Weis, J. Szczygielski, G. Multhaup, and T. A. Bayer. Axonopathy in an APP/PS1 transgenic mouse model of Alzheimer's disease. *Acta Neuropathol.*, 111(4):312–319, Apr 2006.

O. Wirths, J. Weis, R. Kayed, T. C. Saido, and T. A. Bayer. Age-dependent axonal degeneration in an Alzheimer mouse model. *Neurobiol. Aging*, 28(11):1689–1699, Nov 2007.

O. Wirths, H. Breyhan, H. Cynis, S. Schilling, H. U. Demuth, and T. A. Bayer. Intraneuronal pyroglutamate-Abeta 3-42 triggers neurodegeneration and lethal neurological deficits in a transgenic mouse model. *Acta Neuropathol.*, 118(4):487–496, Oct 2009.

O. Wirths, T. Bethge, A. Marcello, A. Harmeier, S. Jawhar, P. J. Lucassen, G. Multhaup, D. L. Brody, T. Esparza, M. Ingelsson, H. Kalimo, L. Lannfelt, and T. A. Bayer. Pyroglutamate Abeta pathology in APP/PS1KI mice, sporadic and familial Alzheimer's disease cases. *J Neural Transm*, 117(1):85–96, Jan 2010a.

O. Wirths, H. Breyhan, A. Marcello, M. C. Cotel, W. Bruck, and T. A. Bayer. Inflammatory changes are tightly associated with neurodegeneration in the brain and spinal cord of the APP/PS1KI mouse model of Alzheimer's disease. *Neurobiol. Aging*, 31(5):747–757, May 2010b.

O. Wirths, C. Erck, H. Martens, A. Harmeier, C. Geumann, S. Jawhar, S. Kumar, G. Multhaup, J. Walter, M. Ingelsson, M. Degerman-Gunnarsson, H. Kalimo, I. Huitinga, L. Lannfelt, and T. A. Bayer. Identification of low molecular weight pyroglutamate Abeta oligomers in Alzheimer disease: a novel tool for therapy and diagnosis. *J. Biol. Chem.*, 285(53):41517–41524, Dec 2010c.

G. B. Witman, D. W. Cleveland, M. D. Weingarten, and M. W. Kirschner. Tubulin requires tau for growth onto microtubule initiating sites. *Proc. Natl. Acad. Sci. U.S.A.*, 73(11):4070–4074, Nov 1976.

J. L. Wittnam, E. Portelius, H. Zetterberg, M. K. Gustavsson, S. Schilling, B. Koch, H. U. Demuth, K. Blennow, O. Wirths, and T. A. Bayer. Pyroglutamate amyloid beta aggravates behavioral deficits in transgenic amyloid mouse model for Alzheimer disease. *J. Biol. Chem.*, 287(11):8154–8162, Mar 2012.

World Health Organzation. *Dementia A public health priority*. WHO Library, 2012.

H. Xiong, D. Callaghan, J. Wodzinska, J. Xu, M. Premyslova, Q. Y. Liu, J. Connelly, and W. Zhang. Biochemical and behavioral characterization of the double transgenic mouse model (APPswe/PS1dE9) of Alzheimer's disease. *Neurosci Bull*, 27(4):221–232, Aug 2011.

Q. Yuan, H. Su, Y. Zhang, W. H. Chau, C. T. Ng, Y. Q. Song, J. D. Huang, W. Wu, and Z. X. Lin. Amyloid pathology in spinal cord of the transgenic Alzheimer's disease mice is correlated to the corticospinal tract pathway. *J. Alzheimers Dis.*, 35(4):675–685, 2013.

H. Zetterberg and N. Mattsson. Understanding the cause of sporadic Alzheimer's disease. *Expert Rev Neurother*, 14(6):621–630, Jun 2014.

S. Zhou, H. Zhou, P. J. Walian, and B. K. Jap. The discovery and role of CD147 as a subunit of gammasecretase complex. *Drug News Perspect.*, 19(3):133–138, Apr 2006.

B. V. Zlokovic, J. Ghiso, J. B. Mackic, J. G. McComb, M. H. Weiss, and B. Frangione. Blood-brain barrier transport of circulating Alzheimer's amyloid beta. *Biochem. Biophys. Res. Commun.*, 197(3):1034–1040, Dec 1993.

B. V. Zlokovic, C. L. Martel, J. B. Mackic, E. Matsubara, T. Wisniewski, J. G. McComb, B. Frangione, and J. Ghiso. Brain uptake of circulating apolipoproteins J and E complexed to Alzheimer's amyloid beta. *Biochem. Biophys. Res. Commun.*, 205(2):1431–1437, Dec 1994.

B. V. Zlokovic, C. L. Martel, E. Matsubara, J. G. McComb, G. Zheng, R. T. McCluskey, B. Frangione, and J. Ghiso. Glycoprotein 330/megalin: probable role in receptor-mediated transport of apolipoprotein J alone and in a complex with Alzheimer disease amyloid beta at the blood-brain and bloodcerebrospinal fluid barriers. *Proc. Natl. Acad. Sci. U.S.A.*, 93(9):4229–4234, Apr 1996.

LIST OF ABBREVIATIONS

Please note: Metric prefixes and units described in the International System of Units (SI) are not listed here.

Aβ	Amyloid-beta peptide
Aβ_{X1-X2}	Amyloid-beta peptide ranging from N-terminal amino acid X1 to C-teminal amino acid X2
AD	Alzheimer´s disease
ANOVA	Analysis of Variance
APP	Amyloid-Precursor-Protein
BSA	Bovine serum albumin
CAA	Cerebral Amyloid Angiopathy
IP	Immuno-Precipitation
MALDI-TOF	Matrix-Assisted Laser Desoption/Ionisation - Time of Flight
NaOH	Sodium hydroxide
Na$_2$HPO$_4$	Sodium hydrogen phosphate
NFT	Neuro-fibrillary Tangles
PBS	Phosphate-buffered saline
PCR	Polymerase-chain-reaction
PGDF	Platelet-derived groth factor-β
PrP	Prion Protein
PS	Presenilin
RT	Room Temperature
SDS	Sodium dodecyl sulfate
TBS	Tris-buffered saline
TBS-T	Tris-buffered saline supplemented with Tween-20
Tris	Tris(hydroxymethyl)-aminomethane
WT	wild-type C57B6/J
5XFAD	Transgenic mice (Tg6799) expressing five familial AD mutations
5XFAD^{hem}	hemizygous 5XFAD
5XFAD^{hom}	homozygous 5XFAD

LIST OF TABLES

145

CURRICULUM VITAE

BERNHARD CLEMENS RICHARD

PERSONAL INFORMATION

Born in Münster, Germany, 8. April 1985

email bernhard.richard@med.uni-goettingen.de

phone (Mobile) +49 (176) 6177 4700

WORK EXPERIENCE

	since 2012	Doctoral Studies — GÖTTINGEN

University Medicine Göttingen

Doctoral Thesis: In Vitro and In Vivo Studies on Antibodies - N-terminally Truncated Abeta in the 5XFAD Mouse Model
Description: Within this project, N-terminally truncated Amyloid-beta was investigated in the 5XFAD Alzheimers disease model. A therapeutic pilot study with several specific antbodies was conducted.

Uppsala University (2014)

Mass-Spectrometric Analysis of Abeta in Murine Brains

Methodological and Technical Knowledge

Immunohistochemistry, Behavioral Testing, RT-PCR, PCR/Cloning, Immunoblotting, Gel Electrophoresis, Immunoprecipitation, Mass Spectrometry, Transgenic Animal Models, HPLC, Culture of Pro- and Eukaryotic Cells, Affinity Chromatography, Prep. Ultracentrifugation, FRET, Fluorescence/CD-Spectroscopy, Immunoprecipitation, Mass Spectrometry, Transgenic Animal Models, MS Office, Digital Image Processing, Statistics Software: Graph Pad Prism 6, Statistica

	2009-2012	Freelance Work — MAINZ

DJK Moguntia Bretzenheim e.V.

Head Coach in Table Tennis, responsible for conceptuation, organization and realization of training and exercises for children and young people.

TSV Schott Mainz e.V.

Coach in Table Tennis, responsible for methodology, scheduling and realization of training and exercises for children and young people.

	2008-2009	Part-Time Teaching Employment — MAINZ

University Mainz

Scientific Assistant, Dept. of Special Botany, Johannes Gutenberg-University Mainz

	2004-2005	Civilian Service — MÜNSTER

Herz-Jesu Hospital Hiltrup GmbH

Medical Care at the Neurology Division

NABU Münster e.V.

Nature and Landscape Conservancy

EDUCATION

	2005-2011	Diploma Studies (Biology) — Mainz

University Mainz, Diploma in Biology

Overall Grade 1.3 (very good)
Thesis: *Labeling Recombinant Light-Harvesting Complex II by Means of a New, Sequence-Specific and Membrane-Soluble Fluorescent Dye*
Description: Within this thesis the idea of using a new fluorescent dye to label lipophilic proteins during processing/trafficking *in vitro* and *in vivo* was explored.
Advisor: Prof. Harald PAULSEN, Dept. of General Plant Physiology

PUBLICATIONS

Journal of Alzheimers Disease, 2015

GENE DOSAGE DEPENDENT AGGRAVATION OF THE NEUROLOGICAL PHENOTYPE IN THE 5XFAD MOUSE MODEL OF ALZHEIMERS DISEASE.
Authors: **Bernhard C. Richard**, Anastasiia KURDAKOVA, Sandra BACHES, Sascha WEGGEN, Thomas A. BAYER, Oliver WIRTHS

Analytical and Bioanalytical Chemistry, 2015 Feb;407(4):1041-57

MICELLAR EXTRACTION POSSESSES A NEW ADVANTAGE FOR THE ANALYSIS OF ALZHEIMER'S DISEASE BRAIN PROTEOME.
Authors: Sravani MUSUNURI, Kim KULTIMA, **Bernhard C. Richard**, Martin INGELSSON, Lars LANNFELT, Jonas BERGQUIST, Ganna SHEVCHENKO

Molecular Neurodegeneration, 2014 Apr 2;9:13

ABUNDANCE OF A-X LIKE IMMUNOREACTIVITY IN TRANSGENIC 5XFAD, APP/PS1KI AND 3XTG MICE, SPORADIC AND FAMILIAL ALZHEIMER'S DISEASE.
Authors: Erika AVENDANO GUZMAN, Yvonne BOUTER, **Bernhard C. Richard**, Lars LANNFELT, Martin INGELSSON, Anders PAETAU, Auli VERKKONIEMI-AHOLA, Oliver WIRTHS, Thomas A. BAYER

Acta Neuropathologica Communications, 2013 Sep 6;1(1):56

N-TRUNCATED ABETA STARTING WITH POSITION FOUR: EARLY INTRANEURONAL ACCUMULATION AND RESCUE OF TOXICITY USING NT4X-167, A NOVEL MONOCLONAL ANTIBODY.
Authors: Gregory ANTONIOS*, Nasrin SAIEPOUR*, Yvonne BOUTER*, **Bernhard C. Richard***, Anders PAETAU, Auli VERKKONIEMI-AHOLA, Lars LANNFELT, Martin INGELSSON, Gabor G. KOVACS, Thierry PILLOT, Oliver WIRTHS, Thomas A. BAYER   *equal contribution*

STIPENDS AND MEMBERSHIPS

Stipends

2012-2015 · Göttingen University, U4 Doctoral Studies Stipend

2014 · Mobility within the U4: Long-Time Research Travel Grant funded by the German Academic Exchange Service (DAAD)

Graduate School

2012-2015 · Enrolled in the Göttingen Graduate School for Neurosciences, Biophysics and Molecular Biosciences (GGNB), Molecular Physiology of the Brain (CMPB)

Graduate School

2012-2015 · Enrolled in the U4 Graduate School The Ageing Brain, Ghent, Göttingen, Groningen, Uppsala

Communication Skills

2014 · Poster at the Alzheimers Association International Conference (AAIC) in Copenhagen

ADDITIONAL SKILLS AND ABILITIES

Language Abilities

Fluent in written and spoken English · German (Mothertongue) · Swedish (Intermediate: Daily and basic scientific conversation) · Qualification in Latin

March 10, 2015